ADDIS ABABA UNIVERSITY

ADDIS ABABA INSTITUTE OF TECHNOLOGY

SCHOOL OF MECHANICAL AND INDUSTRIAL ENGINEERING

Design and Thermal Energy Analysis of Sugarcane Bagasse Dryer to Improve Thermal Efficiency of Boiler for Ethiopian Sugar Factory. (A Case for Wonji/Shoa Sugar Factory)

A Thesis Submitted to the School of Graduate Studies of Addis Ababa University in Partial Fulfillment of the Requirements for the Degree of Masters of Science in Mechanical Engineering (With Specialization in Thermal Engineering)

By:

Belachew Girma

Advisor:

Dr. Yilma Taddese

November, 2018

Addis Ababa, Ethiopia

Addis Ababa University

Addis Ababa Institute of Technology

School of Mechanical and Industrial Engineering

Thermal Engineering Stream

Design and Thermal Energy Analysis of Sugarcane Bagasse Dryer to Improve Thermal Efficiency of Boiler for Ethiopian Sugar Factory. (A Case for Wonji/Shoa Sugar Factory)

By:

Belachew Girma

Approved by Board of Examiners:

Dr. Yilma Taddese		
Advisor	Date	Signature
Dr. Ing. Eddessa Dribsa		
Internal Examiner	Date	Signature
Dr.Ing. Wondwossen Bogale		
External Examiner	Date	Signature
Dr. Yilma Taddese		
Chairman of SMIE	Date	Signature
Dr. Ermias Tesfaye		
Director of Post Graduate	Date	Signature

Declaration

I, the undersigned, declare that this thesis entitled ***"Design and Thermal Energy Analysis of Sugarcane Bagasse Dryer to Improve Thermal Efficiency of Boiler for Ethiopian Sugar Factory. (A Case for Wonji/Shoa Sugar Factory)"*** is my original work under School of Mechanical and Industrial Engineering, AAiT, and has not been submitted by any other person for an award of a degree in this or any other University, and that all resources of materials used for this thesis have been duly acknowledged and a list of references is given.

Name:

Belachew Girma Tesemma _____

Signature

This thesis has been submitted to the Addis Ababa University with my approval as the University Advisor.

Advisor:

Dr. Yilma Taddese _____

Signature

TABLE OF CONTENTS

LIST OF FIGURES

LIST OF TABLES

LIST OF ACRONYM AND ABBREVIATIONS

SYMBOL	DESCRIPTIONS	UNITS
AAiT	Addis Ababa Institute of Technology	-
SMIE	School of Mechanical and Industrial Engineering	-
FBD	Fluidized Bed Dryer	-
SFBD	Static Fluidized Bed Dryer	-
VFBD	Vibrating Fluidized Bed Dryer	-
TCD	Tons of Cane a Day	-
CAD	Computer Aided Design	-
I.D Fan	Induced Draft Fan	-
F.D Fan	Forced Draft Fan	-
i.e.	that is	-
GCV	Gross Calorific Value	kJ/kg
NCV	Net Calorific Value	kJ/kg
P	Total Weight Of Flue Gases	Kg
M	Excess Air Factor	%
W	Moisture Content	%
Q	Sensible Heat Losses In The Flue Gases	kJ/kg
HHV	Higher Heating Value	kJ/kg
LHV	Lower Heating Value	kJ/kg
H	Efficiency	%
A_c	Cross-sectional Area	m^2
D_i	Internal Diameter	M
D_o	Outer Diameter	M
V	Volume	m^3
P	Density	kg/m^3
T	Temperature	^oC
P	Pressure	Pa
H	Height	M
V	Velocity	m/s
h_i	Internal Heat Transfer Coefficient	$W/m^2.K$
h_o	External Heat Transfer Coefficient	$W/m^2.K$
$h_{c,o}$	Outside Convective Heat Transfer Coefficient	$W/m^2.K$
Re	Reynolds number	-

Nu	Nusselt number	-
Pr	Prandl number	-
K	Thermal Conductivity	W/m.K
ν	Kinematic Viscosity	m^2/s
U	Overall Heat Transfer Coefficient	W/m^2 .K
$\dot{Q}$	Heat Transfer Rate	J/s
C_{pf}	Specific Heat Capacity of Flue Gas	kJ/kg.K
C_{pb}	Specific Heat Capacity of Bagasse	kJ/kg.K
m_f	Mass Flow Rate of Flue Gas	kg/s
m_b	Mass Flow Rate of Bagasse	kg/s
$T_{b,out}$	Outlet Temperature Of Bagasse	K
$T_{f,out}$	Outlet Temperature Of Flue Gas	K
$T_{b,in}$	Inlet Temperature Of Bagasse	K
$T_{f,in}$	Inlet Temperature Of Flue Gas	K
ε	Effectiveness	-
NTU	Number of Transfer Units	-
ΔH	Enthalpy Change	J/s
M_i	Initial Moisture Content	%
M_f	Final Moisture Content	%
$\dot{m}_i$	Mass Flow Rate at Inlet	Kg/s
$\dot{m}_o$	Mass Flow Rate at Outlet	Kg/s
E_{in}	Energy at Inlet	J
E_{out}	Energy at Outlet	J
ΔS	Entropy Change	kJ/kg.K
S_{gen}	Entropy Generation	kJ/kg.K
$\dot{E}_b$	Exergy Transfer Rate of The Bagasse	kJ/kg
$\dot{E}_{dfg}$	Exergy Transfer Rate of The Drying Flue Gas	kJ/kg
$\dot{E}_{evap}$	Exergy Evaporation Rate	kJ/kg
$\dot{E}_{loss}$	Rate of Exergy Loss	kJ/kg
η_{th}	Thermal Efficiency	%
η_e	Energy Efficiency	%
η_{ex}	Exergy Efficiency	%
TPH	Ton Per Hour	-
ETB	Ethiopian Birr	-

ACKNOWLEDGMENTS

I take this opportunity to express my profound gratitude and deep regards to my advisor Dr. Yilma Taddese for his exemplary guidance, monitoring and consistent encouragement throughout the course of this thesis, as well as for providing necessary information regarding the project.

I also take this opportunity to thank the Wonji Sugar Factory for giving the valuable data that I need for the accomplishment of this paper. Additionally, I would like to express my gratitude to Mizan-Tepi University for sponsoring me to have my graduate study in Addis Ababa University and the Ministry of Education for supporting me the necessary allowances in the course of the work.

At last but not least, I would like to thank Mr. Minale, Wonji Sugar Factory worker for giving me the valuable information and supplying the necessary data by sacrificing his working time.

ABSTRACT

Sugarcane Bagasse is the fibrous residue of sugar cane stalk coming from the mills after crushing and extraction of juice. It is used as a fuel for boiler to generate energy. In Wonji/Shoa sugar factory a sugarcane bagasse of 52% moisture content which is very high moisture content in history of the sugar factory is used as a fuel for boilers to generate steam. If the moisture content of bagasse is high its heat generation capacity or calorific value is lower; indirectly that means the boiler efficiency become low, because it's heating value is reduced and it cause the largest loss in the boilers due to the moisture carries the latent heat of vaporization up the stack.

This study is aimed to reduce this moisture content of sugarcane bagasse and so increase the thermal efficiency of boiler for Wonji/Shoa sugar factory. To do that, a Fluidized Bed Bagasse Dryer has been designed and the thermal analysis of the system was also carried out by ANSYS Fluent.

The Fluidized Bed Bagasse Dryer uses the hot flue gases that comes from boiler to chimney which is optimum solution to enhance thermal efficiency of boiler. In other way, re-using this flue gases for bagasse drying improves the environmental pollution. The bagasse and the hot flue gases mixed in the drying chamber of Fluidized Bed Bagasse Dryer to evaporate the water contained in the bagasse. Finally, this designed Fluidized Bed Bagasse Dryer enables to reduce bagasse moisture content from 52% to 41% and also increases the efficiency of boiler by 5.5% from 70 to 75.5% according to the analysis done analytically and using ANSYS Fluent. Both analysis gives almost the same result. In addition, the total cost of the dryer was estimated to be 1,310,136.146 Ethiopian birr. By installing this bagasse dryer, the factory can increases its income by 17,364 Ethiopian birr per day and recover this cost within 3.14months.

CHAPTER ONE: INTRODUCTION

1.1 Background of Ethiopian Sugar Factories

As the Ethiopian Sugar Industry Profile indicates, modern sugar industry started in Ethiopia at Wonji some 110 km east of the capital Addis Ababa in 1951, as a share company by foreign private investors & Ethiopian government. The Netherland's H.V.A. Company had entered into the sector as a foreign share holder. When the factory started production in 1954 its initial production was 1400 quintals of sugar per year. At the start, the share company had five thousand hectares of land for its sugarcane cultivation. As its location is one of the most suitable areas of the world to the sector it opened a door to Wonji Candy Factory to come forward.

Then, Shoa Sugar Factory followed in 1962 with 1,700 quintals of sugar production capacity per day. The two factories known by the name Wonji Shoa Sugar Factory altogether had the capacity of producing 750,000 quintals of sugar per annum till recent time i.e. prior to the completion of the new Wonji Shoa Sugar Factory. Serving for more than half a century and getting obsolete, these two Wonji and Shoa sugar factories were closed in 2011 and 2012 respectively. Replacing these pioneer factories, the new and modern factory had started production in 2013 with higher production capacity.

The second factory Metehara Sugar Factory is established as a share company between same Netherlands Company and the Ethiopian government in 1965 and started production in 1969 at a location known as Merti some 200 km from Addis Ababa. Currently, the factory with a total 10,235 hectares of sugarcane cultivation land has a capacity of producing more than 1.3 million quintals sugar and 12.5 million liters ethanol per year on average.

Five years after the establishment of Metehara Sugar Factory i.e. in 1974 following the dawn fall of the emperor's regime all sugar factories were made to be administered under the ownership of the government and started operating under the Ethiopian Sugar Corporation. The corporation had also been made to administer the Addis Ketema and Asmara Candy Factories together with the above mentioned three sugar factories.

Later in 1992 when the Corporation which had administered all sugar factories was dissolved by statute; all the above factories were reestablished as separate public enterprises. Following this the Ethiopian Sugar Industry Support Center came into existence in 1998 to provide support to the factories. The center was established as a share company of the Development Bank of Ethiopia,

Ethiopian Insurance Corporation and the three sugar factories.

Fincha Sugar Factory as the third sugarcane crushing mill to the nation came into existence in late 1998 though its establishment process and other activities dated back to 1975. The gap between the establishment and commencement of production of the factory is mainly occurred due to the political change the nation had undergone. Its finance sources were African Development Bank and Development Fund; Governments of Australia and Spain as well as domestic banks of the nation. Its initial sugar production was 500,000 quintals per annum. More modern than the former factories, the factory's construction job including its ethanol plant was executed by American company known as F.C. Shefer and associates Netherland's company called Dewetto International while many domestic construction companies had also played their part in the process.

In 2006 Tendaho Sugar Development Project was established as a fourth two-phased project in the country. Construction of the first phase of the factory has started production in 2015. The two-phased project, reaching its maximum crushing capacity, eventually enables the factory produce 3 Million quintals of sugar and 30 million Litters ethanol per year. The factory will in total have 50,000 hectares of sugarcane cultivation land. It was during the inception of Tendaho Sugar Factory that the Ethiopian Sugar Development Agency came into existence replacing the support center to assist the sugar factories in project development, research and training.

Now, the Government, to ensure equitable share of the nation's resource among its peoples, has started broadening the sugar development sector which had been limited in Oromia around Wonji Shoa, Metehara and Fincha Sugar Factories for long years to Afar, Amhara, Tigray and Southern Nations, Nationalities and Peoples regional states. Accordingly, various activities are being carried out to build two sugar factories each with a capacity of crushing 12 thousand tons of cane per day (TCD) at Tana-Beles Sugar Development Project in both Amhara and Benishangul-Gumuz regions and these two factories all together have 50 thousand hectares of sugarcane cultivation land.

Likewise, activities are being carried out at Omo-Kuraz Sugar Development Project of South Omo, Bench-Maji and Kaffa zones of Southern Nations, Nationalities and Peoples Regional State where four sugar factories are at different levels of construction owning 100 thousand hectares of sugarcane plantation land. Among them three are each with a crushing capacity of 12 thousand TCD while one with 24 thousand TCD. Omo-Kuraz factory one is almost start production in early 2017. Similarly, the construction of one sugar factory with 24 thousand TCD using 50 thousand hectares of cane plantation field is underway at Wolkayit Sugar Development Project of Tigray Regional State.

1.2 What is Sugarcane Bagasse?

Sugarcane Bagasse is the fibrous residue of the sugar cane stalk coming from the mills after crushing and extraction of juice. Its composition varies with the variety of cane, its maturity, the method of harvesting and the efficiency of the milling plant. It consists of woody fiber, water, soluble solids and ash in varying percentages. The percentage of chemical compounds of sugarcane bagasse is Fiber 14%, Cellulose 44.43%, Hemi cellulose 22.9%, Lignin 17.52% and Water soluble materials 14.18%[1-2]. The sugarcane bagasse fiber bundles are usually coarse and stiff.

When sugarcane bagasse burned in quantity, it provides sufficient heat and electrical energy which supplied to all Sugar mills and other machines those needs energy. In comparison to other agricultural residues, sugarcane bagasse is considered as a rich solar energy reservoir due to its very high yields[3]. It offers the advantage of being a cheap, plentiful and low polluting fuel. In addition, chemical energy harvesting from sugarcane bagasse is attractive since it is a renewable source of energy, and the combustion of sugarcane bagasse produces the same amount of CO_2 as it consumes during its growth so it has a neutral carbon[4]. In other word the resulting CO_2 emissions are equal to the amount of CO_2 that the Sugarcane plant absorbed from the atmosphere during its growing phase, which makes the process of cogeneration greenhouse gas-neutral.

Cogeneration of sugarcane bagasse is one of the most attractive and successful energy projects that have already been demonstrated in many Sugarcane producing countries such as Mauritius, Reunion Island, India and Brazil[5]. Combined heat and power from Sugarcane in the form of power generation offers renewable energy options that promote sustainable development, take advantage of domestic resources, increase profitability and competitiveness in the industry, and cost-effectively address climate mitigation and other environmental goals.

The moisture content in bagasse varies considerably with the degree of extraction. The average value of the moisture content in bagasse reaches 52 % in almost all the sugarcane factories[3]. Moisture content is the main determinant of calorific value i.e. the lower the moisture content, the higher the calorific value. The higher the moisture content, the lower is the amount of combustible material per unit weight of bagasse and the total available heat. According to *Toolseeram Ramjeawon* study, the bagasse has a gross calorific value of 19,250 kJ/kg at zero moisture and 9950 kJ/kg at 48% moisture content[6]. Therefore, calorific value varies inversely with the moisture content (for low moisture content high calorific value obtained & for high moisture content low calorific value gained). Furthermore, the portion of heat which is used to evaporate the bagasse

moisture and to superheat the resulting steam to the temperature of the flue gases must be deducted from the total available heat.

As *Ali K. Abdel-Rahman* study indicates, each kg of water in bagasse requires 418 kJ (100 kcal) to reach its boiling point and 2,259 kJ (540 kcal) to convert it into steam[3]. The increase in moisture content of bagasse is not only increasing the heat loss but also lowers the combustion temperature in the furnace. At present day all of the Ethiopian sugar cane factories including Wonji sugar factory consume their entire production of bagasse as fuel for boilers and still have to purchase considerable amount of oil fuel. The reason why is, because they use moist bagasse as it is. If they use dried bagasse for boiler a large amount of bagasse left as surplus because small amount of dried bagasse yield high calorific value that needed for factory so they not consume entire bagasse. This surplus bagasse used for additional purpose as a raw material for the production of different products such as paper, board, charcoal & etc. Therefore, it becomes necessary to search for a means to utilize bagasse efficiently. This is the role of bagasse drying.

1.3 Sugarcane Bagasse Drying

Sugarcane bagasse drying is a crucial and vital component for the sugar factory to generate more energy. It is an old idea only to concentrate on producing sugar alone from sugar cane, the byproduct bagasse today attract as much attention as the conventional main product, sugar. Bagasse which is considered as a waste material in past years, today become a valuable material which can be used as a raw material for the production of paper, particle board, furfural, and other products, but it is most commonly used as fuel for the production of steam and electric energy through cogeneration systems in sugar factories[5], [7].

It is also currently used to produce bioethanol[1], [8]. Furthermore sugarcane bagasse ash is used for ceramic tile making[9]. According to *E. Hugot & Peter Rein* statement, for every 100 tons of sugarcane crushed, a sugar factory produces nearly 30 up to 33 tons of wet bagasse[10-11]. That means bagasse represents 30-33% of the total sugarcane mass. Some studies are conducted on bagasse drying in some countries like America, Brazil, Philippines, China, Cuba and India based on their own context and they use bagasse drier which made them more profitable[11]. But in our country there is a gap. No contextual or related studies are conducted on bagasse drying and no bagasse dryers used to improve boiler efficiency. As much as possible, this study is going to fill this gap.

Wonji the eldest sugar factory in Ethiopia, uses a bagasse with 52% moisture content which is poor in calorific value. The factory mills crushes 6250 tons of sugarcane stalk per hour. There are two

boilers with a capacity of each burning 55.55tons of bagasse per hour. The temperature of flue gases released from the boiler is 425^{o}C before entering the Economizer and after Economizer it will be reduced to 270^{o}C. This temperature is optimum to evaporate the moisture contained in sugarcane bagasse because it is above the boiling point of water 100^{o}C. The thermal efficiency of this factories boiler is poor because a bagasse dryer has not been used. Lesser moisture content in bagasse would simply mean higher energy density and better combustion quality resulting in the improved thermal efficiencies of the boilers.

1.4 Problem Statement

Wonji Sugar Factory uses the byproduct bagasse directly as a primary fuel for boiler which is a good way to change its byproducts into valuable energy. But there is a problem while using the bagasse directly as it is. The moisture content of the bagasse comes from the sugar mill of this factory is 52% which is very high moisture content when compared to others modern factory, 47.5% to 50%[3]. So during the combustion process in a boiler considerable amount of furnace energy is wasted in evaporating the water contained in this bagasse. If the moisture content of bagasse is high its heat generation capacity or calorific value is lower; indirectly that means the boiler efficiency become poor because its heating value is reduced and it cause the largest loss in the boilers because the moisture carries the latent heat of vaporization up the stack.

Also, wet bagasse makes incomplete and bad combustion processes that release dangerous pollutant gases which affect environmental conditions. In addition to this, the life span of the boiler and boiler part is exposed for danger due to this high moisture content. The high moisture content causes corrosion & fouling on boiler parts and reduces both its efficiency and life time. In general, due to this high moisture content the profitability of the factory becomes less. Surely if the moisture content of this bagasse is lowered as much as possible, the factories profitability increased more and more. The present boiler efficiency of Wonji Sugar Factory is around 70$\pm$1%. This is increased if the dried bagasse with low moisture content is used.

As most studies indicate 1% moisture content reduction, increases the thermal efficiency of boiler by half(that means if moisture content is reduced by 4 points, the thermal efficiency of boiler is increased by 2%) [3], [12]. Countries like Brazil and India improve their boiler efficiency by using dried bagasse[1]. In our country Ethiopia still nothing is done on bagasse moisture reduction to overcome the above mentioned problems. So in order to alleviate these problems a bagasse dryer equipment which reduce the bagasse moisture content is very crucial. So this study is going to solve these mentioned problems by utilizing the waste flue gases released from furnace to dry the bagasse

and this dried bagasse enhances thermal efficiency of a boiler and also help to elongates boilers life span or time. Due to this, a complete combustion will occur and no more toxic gases are released to the ambient. Therefore, bagasse drying is a necessity to improve boiler efficiency, as well as environmental disaster conditions and also to reduce the bagasse consumption or quantities used as a fuel.

1.5 Objective

1.5.1 General objective

The general objective of this research paper is: Designing and analyzing thermal energy of sugarcane bagasse dryer which is used to improve thermal efficiency of boiler.

1.5.2 Specific objectives

- Analytical design of bagasse dryer.
- Develop the model of sugarcane bagasse dryer using CAD software's.
- Simulate the model of bagasse dryer using analysis software ANSYS Fluent.
- Analyzing thermal energy transfer in bagasse dryer.
- Determine the relationship between bagasse moisture content and boiler efficiency.
- Calculate benefit expected while using bagasse dryer.
- Indicate where this bagasse dryer is installed

1.6 Scope of the Study

This research paper was intended to design and analyze thermal energy of sugarcane bagasse dryer which is used to reduce bagasse moisture content with the objective of improving boiler efficiency. At the same time while boiler efficiency improved, combustion efficiency is also improved and the amount of pollutant gases released to the environment will be decreased. But the combustion and pollutant gases analysis is not done in this research paper. Also, due to financial constraint the dryer device is not manufactured presently by the researcher, it is left as future work. However, all the detail necessary design variables and information's used for manufacturing of the device is given in below methodology parts.

1.7 Thesis Organization

This thesis organized into five chapters.

Chapter 1: This chapter gives the details about the studies introduction with elaborating the problems. In addition, it also lays down the objectives of the thesis and its relevance.

Chapter 2: Introduces previous research studies related to bagasse drying and other necessary background information for the current study.

Chapter 3: Presents the methodologies and detail design of bagasse dryer

Chapter 4: Presents the result and discusses the graphs generated from analytical and ANSYS Fluent analysis.

Chapter 5: Provides the conclusion and recommendation for future works.

CHAPTER TWO: LITERATURE REVIEW

The first interest shown in bagasse drying with boiler flue gases dates back to 1910, when *Kerr* showed that it was possible in some Louisiana mills[3]. At that time *Kerr* try to cover the sugar mill's energy demand from bagasse owing high moisture content ranging from 44.45 to 54.47%. His dryer was a square tower with bagasse descending and flue gas rising in a countercurrent manner. The tower is equipped with deflectors to promote better gas-solid contact. According to a report *Kerr* made of his work, the dryer was not used commercially. However, the first commercial installation on bagasse drying using the flue gases was carried out in Atlantic Sugar Association by Vincent Processes INC in 1970s.

Between 1910 and 1970, only a small number of papers were published on bagasse drying and even few industrial applications were reported. The reason for the lack of interest in bagasse drying during this period was the low cost of fossil fuel. From techniques of bagasse drying, Fluidized bed drying is considered to be one of the most successful drying techniques in the recent past. The first commercial unit was installed in the United States in 1948 to dry dolomite[13]. Now, hundreds of fluidized bed dryers are in operation worldwide primarily for particulate materials that can be easily fluidized, (e.g., sand, grains, ion exchange resins, chemical crystals, granular fertilizers, and so on)[13].

According to *Wade A. Amous* report, bone dried bagasse presents a gross calorific value of 17632kJ/kg and because of the moisture content, the net calorific value at 50% moisture is only about 8816kJ/kg[14-15]. In addition to increasing the gross calorific value, the reduction of moisture content in the bagasse also reduces the volume of the flue gases. Furthermore, the specific heat of water vapor is almost twice that of the other gases. Hence, the reduction of water vapor in the combustion gases will result in a higher combustion temperature, thus improving boiler efficiency. *Bailliet*, found an increase of 8.9% in boiler efficiency when fired with bagasse reduced from 52 to 32% moisture [3]. So bagasse drying is a concept which deserves additional attention and development efforts.

Due to the energy crisis in the 1970`s, efforts have been concentrated in further reducing the bagasse moisture by drying with waste heat from flue gases, with the advantages of increased boiler efficiency from about 65% to 70%, decreasing stack particulate and CO_2 emission and bagasse saved for other uses[8]. Now at present time some countries like Brazil, India, and Australia are using bagasse drying technology. They use the hot flue gases from boiler or furnaces to dry the bagasse without any cost increment. But in Ethiopia no one tried to use bagasse drying technology & also no more

studies conducted on bagasse drying mechanism and so there is a high gap which need great attention.

2.1 Why bagasse drying is needed?

During the combustion process in a boiler considerable amount of furnace energy is wasted in evaporating the water contained in the fresh bagasse. The basic principle of bagasse dryer is to dry this fresh bagasse by utilizing the waste heat in flue gases. Lesser moisture content in bagasse would simply mean higher energy density and better combustion quality resulting in the improved thermal efficiencies of the boilers. *Ali K. Abdel-Rahman*, 2015 and *Wade A. Amos*, 1998, states the main advantages of bagasse drying as follows:

1) ***Increasing the calorific values****:* Calorific value is the quantity of heat produced per unit weight of fuel. The higher or gross calorific value (GCV) of a fuel is the amount of heat energy released by the complete combustion per unit mass of that fuel taking into consideration that all the products being cooled down to the original temperature of 20^{o}C. A lower or net calorific value (NCV) is also used. The difference between the two values being the latent heat of the water vapor which is not included in the NCV because the boiler plant cannot recover it due to the high temperature value of flue gases leaving the boiler. The bagasse drying process increases the gross calorific value (GCV) and net calorific value (NCV) of bagasse with the respective decrease in moisture content. Many formula have been proposed to determine the calorific values of wet bagasse; among these the better known formula is the *Hugot* formula. According to *Hugot* formulas[3], [10]:-

$$GCV = 4.1839[4{,}600 - 12s - 46w], \text{ in kcal/kg} \quad (1)$$

$$NCV = 4.1839[4{,}250 - 12s - 48.5w], \text{ in kcal/kg} \quad (2)$$

Where, w - is the moisture content (%) of the bagasse.

s - is the sugar content (%) of bagasse.

According to *Ali K. Abdel-Rahman* statement, when bagasse flows out of the mills, it has a moisture content (w) of the order of 47.5 to 50%, and a sugar content (s) which of the order of 1.5 to 2 % by weight. But the moisture content of that Wonji is 52%, this is due to inefficient extraction of juice by mill. It is a known fact that GCV of bagasse is largely dependent upon its moisture content. Higher moisture content in bagasse reduce its GCV and also results in higher energy loss because the fuel moisture carries that latent heat of vaporization up the stack.

2) **Increasing the furnace temperature:** When the moisture content in bagasse is in the range of 47 to 56 %, it will have a difficult time in reaching the ignition temperature, having expended much of its heat of combustion in evaporating the bagasse contained moisture. The vapor generated from the evaporation of bagasse moisture tends to shield the air from the surface of the bagasse and the flame suffocates from lack of oxygen. To maintain combustion, more excess air is blown into the furnace, with the net result that the combustion temperature is again lowered. Dry bagasse will increase the furnace temperature by about 20.5 to 30%[16-17]. Careful monitoring of the excess air is necessary to ensure a maximum furnace temperature to enable the flue gases to carry enough heat for the proper operation of heat recovery devices such as air heaters, economizers and bagasse dryers.
3) **Increasing the energy production**: As the combustion gas temperature is increased due to dryness of bagasse, the heat absorbed by the water walls of the boiler is increased which results in raising the amount of transferred heat for generating steam. Hence, as a result of bagasse drying, the steam-to-bagasse ratio will improve considerably, leading to increased energy production
4) **Increasing the vaporization coefficient**: Vaporization coefficient is the weight of steam generated per kg of burnt bagasse. Bagasse drying increases the vaporization coefficient considering the feeding water is at a temperature of 90^{o}C, and discounting the loss of weight due to the bagasse drying.
5) **Increasing the stability of boiler's operation**: Drying increases the burn ability of bagasse which increases the stability of boiler's operation due to the low moisture content of the supplied bagasse. The boiler could tolerate moisture contents up to 56 % with deteriorating performance, but combustion will probably be unstable above that point. The improvements found in operating with dry fuel are: increased stability and decreased fuel requirements per unit of steam generated[3].
6) **Increasing the combustion velocity**: The dry bagasse introduced to the furnace is at high temperature, which facilitates combustion and rapid ignition. Velocity of combustion is definitely increased with a better heat absorption in water walls, resulting in a higher heat transfer rate. More heat transmitted to boiler-water means an efficiency increase in the boiler[16].
7) **Increasing the speed of boiler's response to load changes**: One of the very important improvements found in operating boilers with dry fuel is the faster boiler response to load changes.

This is due to the increase in the net calorific value (NCV) and furnace temperature of the dried bagasse.

8) **Reduction of the losses**: This is due to the losses by incomplete combustion of wet bagasse while the dried bagasse burns completely leaving almost no residues.
9) **Increasing steam production**: Drying of bagasse theoretically increases the steam production to about 15.03 % or, saving about 12.7 % of bagasse for same steam production. Moreover, steam generation increases from 2.25 to 2.59 kg-steam/kg-bagasse due to bagasse drying.
10) **Decreasing the flue gases volume**: This is due to the fact that dry bagasse is using a lower excess air for combustion. The amount of flue gases may be calculated by *Hugot* formula[10]:

$$P = 5.76\ (1 - w)\ m + 1 \quad kg/kg \tag{3}$$

Where P is weight of flue gas, m is excess air factor and w is moisture content. Pollution is diminished due to the smaller gases volume and the smaller amount of sots. Bagasse drying reduces air pollution from 10,000 mg/$Nm^3$of ash to less than 300 mg/Nm^3[3].

11) **Reducing the losses of sensible heat**: An increase in furnace temperature is noted, but at the same time there is an important decrease of heat losses in flue gases, because the dried bagasse needs lesser excess air in furnace (m = 1.2 as compared to m = 1.5 for wet bagasse) and also 50 % of the flue gases are diverted towards bagasse dryer and leave the dryer at 100^{o}C (instead of 220^{o}C or 300^{o}C). Sensible heat losses in the flue gases after they have been utilized in the bagasse drying process (kJ/kg) calculated according to *Hugot* formula[10]:

$$q = 4.1839\ [(1.0 - w)\ (1.4\ m - 0.13) + 0.5]\ T \quad kJ/kg \tag{4}$$

Where T is temperature of flue gas.

All this advantages are very important for sugar factories to enhance their profitability. But in our country no one sugar factories try to dry the bagasse, this is the reason why the factories efficiency is not reach the maximum possible efficiency.

2.2 Bagasse Drying Methods

There are different methods for drying the bagasse. These methods can be classified according to the drying medium as follows:

(a) Bagasse drying by using flue gases from boilers,

(b) Bagasse drying by using heated air,

(c) Bagasse drying by using solar energy and

(d) Bagasse drying by using high pressure superheated steam.

The cheapest and most efficient method is drying bagasse in direct contact with the flue gases from boilers and this can be done without setting the bagasse on fire in the dryer. Theoretically the wasted heat in stack is more than sufficient to evaporate all the moisture from the bagasse[18]. The drying process requires approximately 60 % of the hot gases generated in the furnace[3]. These 60 % of the gases after drying the bagasse are relatively cooler and attain a higher degree of humidity. These are then mixed with rest of 40 % of hot gases. The resulting mixture has an average temperature between 130 to 140^{o}C, which is well above the low corrosion point of carbon steel.

The advantages of using the flue gas in drying of bagasse is not only limited to drying the bagasse, rather it has crucial advantage for the following reasons:

1) Reduction of the air pollution from values of about 10,000 mg/Nm^3 of ash to less than 300 mg/Nm^3[3]; and
2) Reduction of the heat losses in the flue gases due to decreasing the exit temperature of gases. (The bagasse dryer allows cooling of the gases to 90^{o}C, the only limit being imposed by the necessity to avoid cooling to the dew point of 60 - 70^{o}C.)[3]

2.3 Types of Bagasse Dryers

Bagasse dryers are classified in several ways. They can be classified according to the method of operation and method of heat supply. According to the method of operation bagasse dryers are classified as batch dryer and continuous dryers. A continuous type dryer is used in cases where drying at the rate of many tons per hour is required. On the other hand, a batch type dryer is suitable for drying at the rate of less than 100 kg per day. Dryers are also further divided by the type of heat supply; the heat needed for drying is supplied to the material by one of the following methods; Convective drying (using a drying medium, i.e., air), Contact drying (by conduction heat from a surface), Radiation drying, Dielectric drying and various combinations of drying. Ali K. Abdel-Rahman, 2015 [19] in general divide bagasse dryers as follows:

2.3.1 Tower Dryers

Tower dryer is the oldest type (see Fig. 1) which was built in 1910 by E. W. Kerr [2], [7]. It is a square tower with bagasse descending and stack gas rising in a countercurrent manner. The tower is equipped with deflectors to promote better gas-solid contact. This dryer was not used commercially.

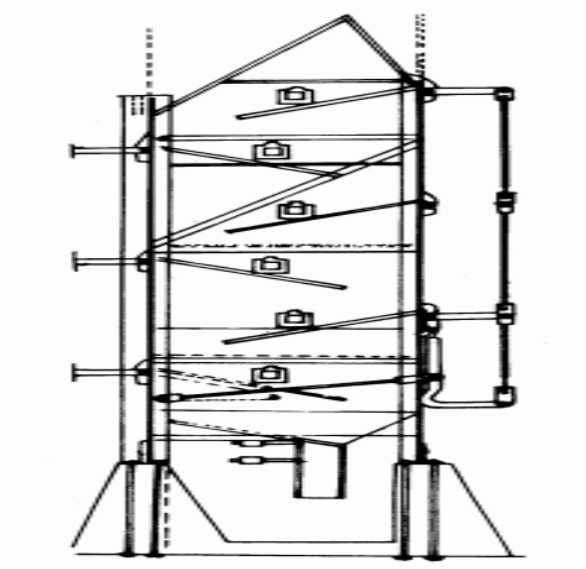

Figure 2-1: Schematic diagram of tower dryer[3]

2.3.2 Rotary Drum Dryers

The principle of single or multiple passage of hot gases contact in parallel with the bagasse to be dried inside a rotary drum type is similar to the sugar dryer [3], [5]. The dry bagasse is then separated from the wet gases in large diameter cyclone [3] as shown in figure below. Rotary drum dryers have the following advantages: (i) they can give uniform final moisture content with non-uniform particle size and inflow; (ii) they are more suitable for medium and large units; (iii) they tend to discharge less dust to atmosphere; (iv) its specific energy consumption is less than pneumatic dryers (it is 20 kWh/t-water evaporated) [29]. But they are big dryers, of low efficiency, occupying large areas [3], [5]. Their construction and installation are quite complex. They need an extra conveyor to transport bagasse to the drums and then back to the boilers.

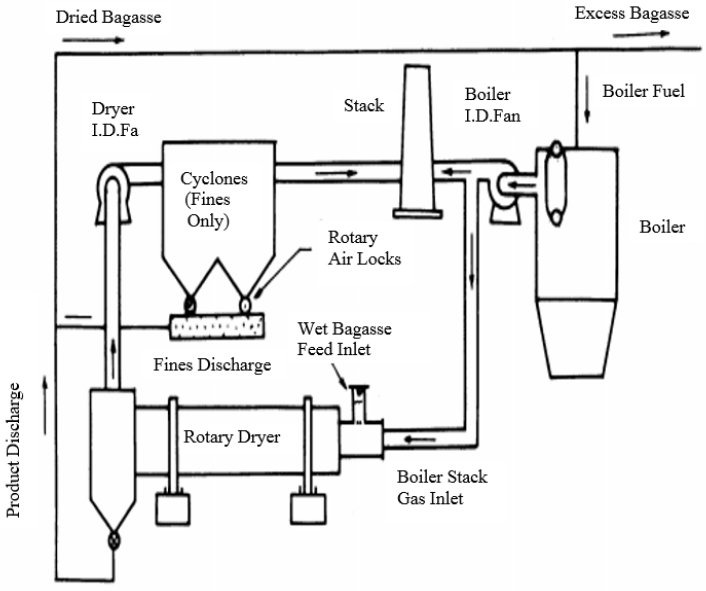

Figure 2-2: Rotary drum dryer[3]

2.3.3 Individual Dryers

This dryer can be mounted in front of the boiler individually to each furnace. It does not need any other installation of conveyors to bring and to take back the bagasse to the dryer. The hot gases are sucked before the air pre-heater and pulled by an auxiliary fan until the front side of the boiler by overhead or an underground duct. The wet bagasse falls down by gravity from the normal conveyor passing by a feeder that blocks the inlet of false air instead of going to the spreaders and diverted by a bypass porthole to the bagasse blending chamber with the hot gases. Thus the bagasse half spread is sucked by an auxiliary fan that raises the mixture through the dryer columns until the cyclone where the wet gases are separated from the dry bagasse. The wet gases go towards the chimney through big diameter ducts with an average temperature of 90^{o}C. The dry bagasse falls down by gravity into the cyclone and goes down by an air locker through the spreaders and feeds the furnace[3].

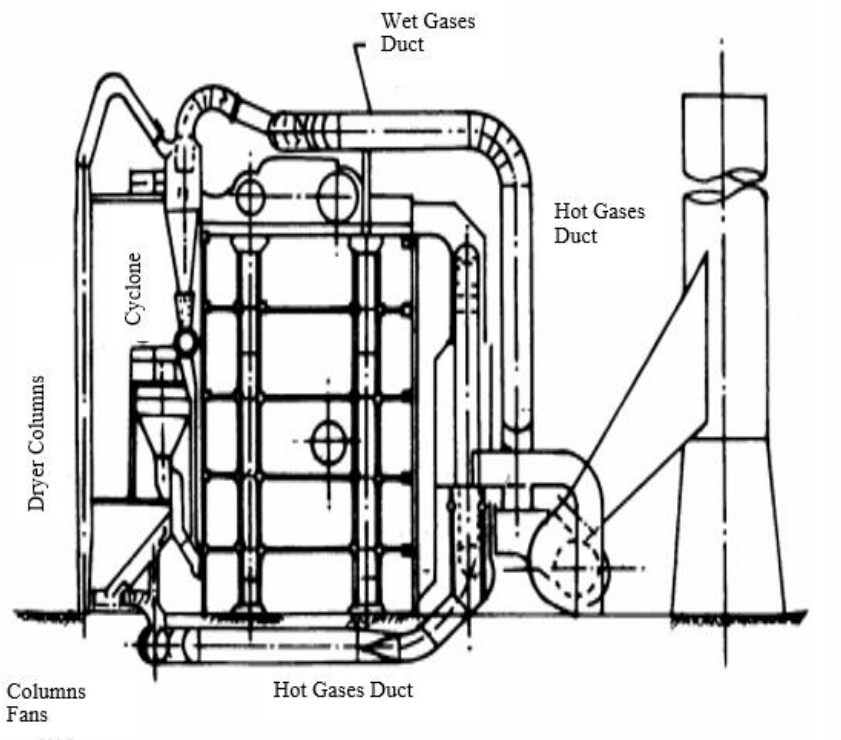

Figure 2-3: Individual dryer[3]

2.3.4 Fluidized-Pneumatic Dryers

Fluidized-Pneumatic dryers are much more efficient than rotary dryers due to the fact that they utilize drying columns where the bagasse is raised by a stream of hot gases and is separated from the wet gases after drying by one or two cyclones. Their cyclones are comparatively smaller and need less investment and operation costs. They are very safe as far as fire-hazards are concerned. Another important advantage is that during the drying, size classification of particles can be achieved. Fluidized-Pneumatic dryers can be classified into three types as below:

A. Fluidized Bed Dryers (FBD): It can be one of two main types: Static and Vibrating. How material moves through each dryer is fundamentally different.

I. Static FBD: In Static FBD (SFBD), the fluidized material bed is deep and the material acts like a liquid, flowing from a high level in the dryer to a low level.

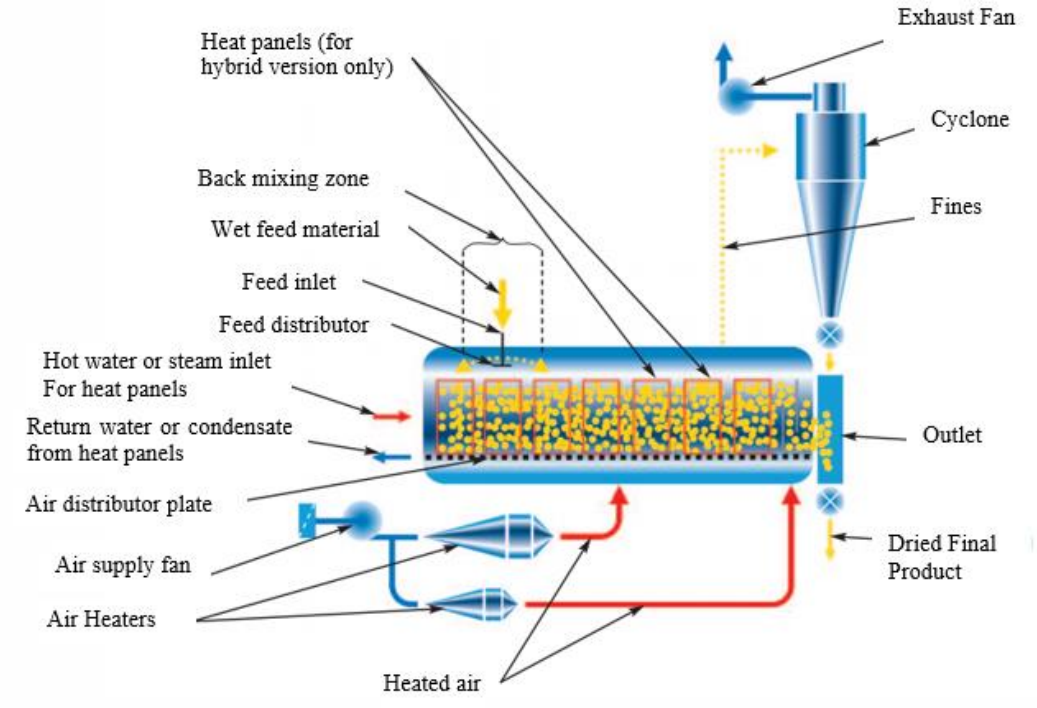

Figure 2-4: Static Fluidized Bed Dryer (SFBD)[20]

II. Vibrating FBD: In a Vibrating FBD (VFBD) the material bed is much shallower and the material is conveyed through the dryer not only by the same liquid-like flow from high to low but by a vibrating conveyor's vibratory action. In the vibrating dryer, the heated airflow's primary function is to dry the material by flowing upward through the conveyor's perforated pan.

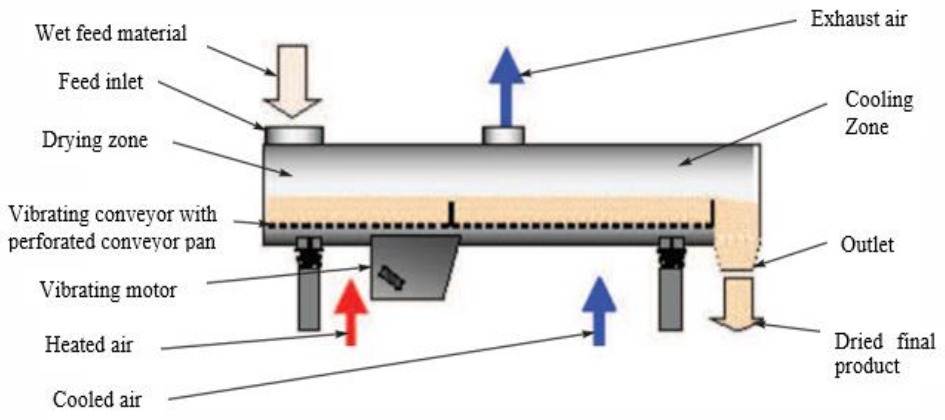

Figure 2-5: Vibrating Fluidized Bed Dryer (VFBD)[20]

B. Pneumatic transport dryers: such as the one shown in Fig. below:

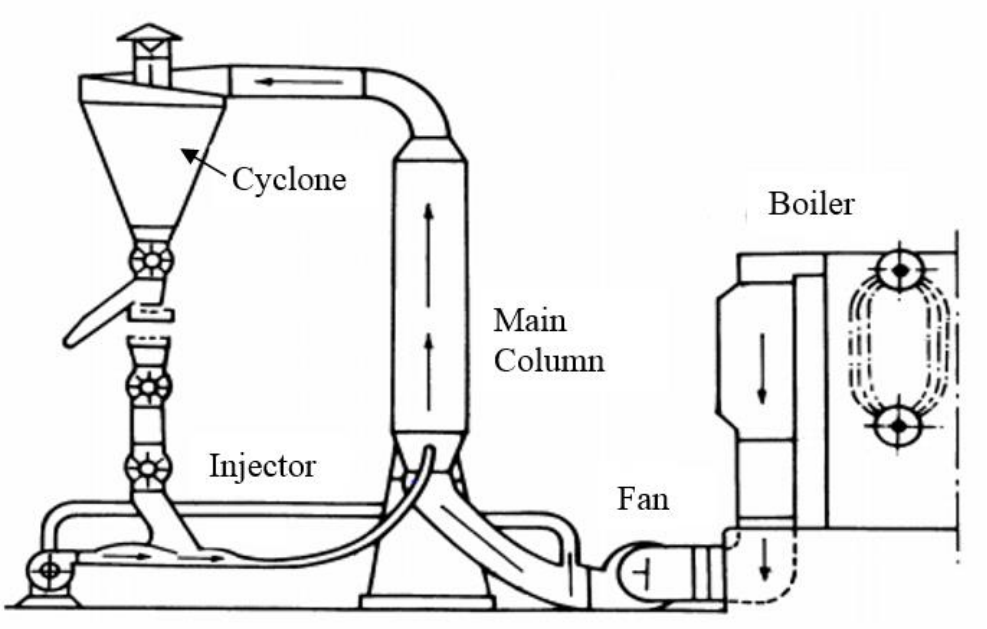

Figure 2-6: Pneumatic transport dryer[3]

C. Combined fluid bed-pneumatic transport dryers: such as the one shown in Fig. below:

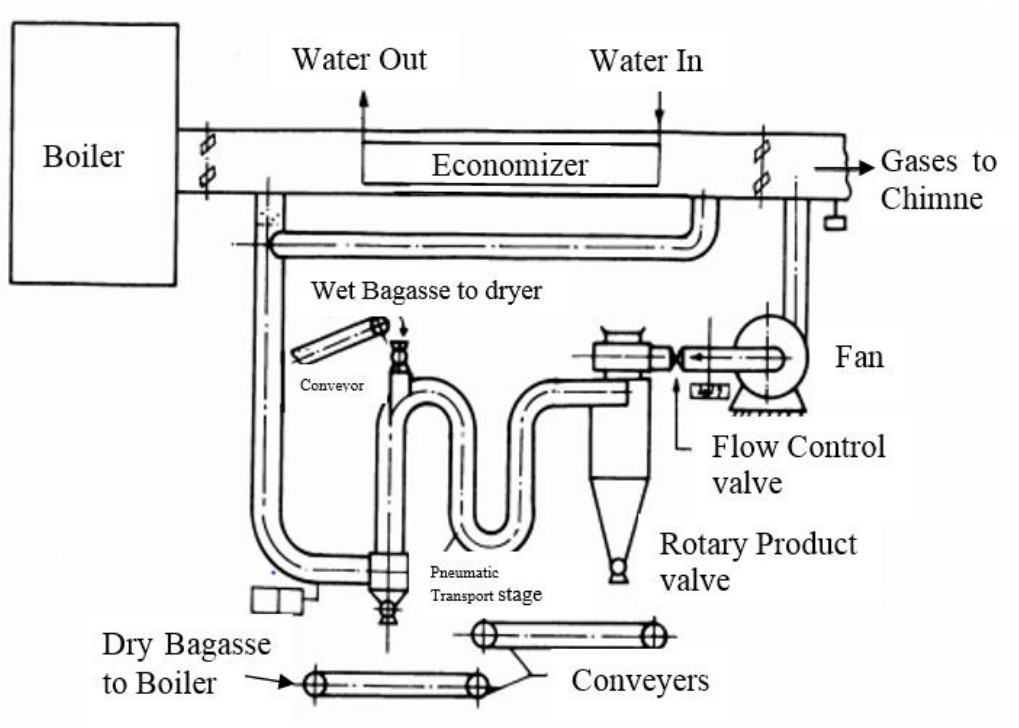

Figure 2-7: Combined fluid bed-pneumatic transport dryer[3]

The type of dryer should be selected based on the shape and size of the wet material, the amount of treatment and the drying conditions. The drying time required for a given product is also a key factor in the selection of the dryer. From the above types of bagasse dryers, the main types of dryers used for bagasse drying are the rotary drum and Fluidized Bed Dryers. Fluidized-bed dryer are

much more efficient than rotary dryers due to the fact that they utilize drying columns where the bagasse is raised by a stream of hot gases and is separated from the wet gases after drying by one or two cyclones. Their cyclones are comparatively smaller and need less investment and operation costs[19], [21]. Additionally, FBD have several advantages over other dryers such as; being more efficient, its large effective surface area of the material to be dried, and its low maintenance costs. Ali Kamel, 2015 reports that the cost of a pneumatic transport dryer is 47 % less than that of the rotary drum dryer. They are very safe as far as fire hazards are concerned. Another important advantage is that during the drying, size classification of particles can be achieved.

2.4 How Fluidized Bed Dryer Works?

A fluid bed dryer uses convection-heated air in direct contact with the wet feed to dry material suspended in a fluidized bed. In operation, air heated by a natural gas fueled air heater passes upward into the dryer through a perforated air distributor plate (or perforated conveyor pan). This fluidizes the wet feed material, as shown in figure below.

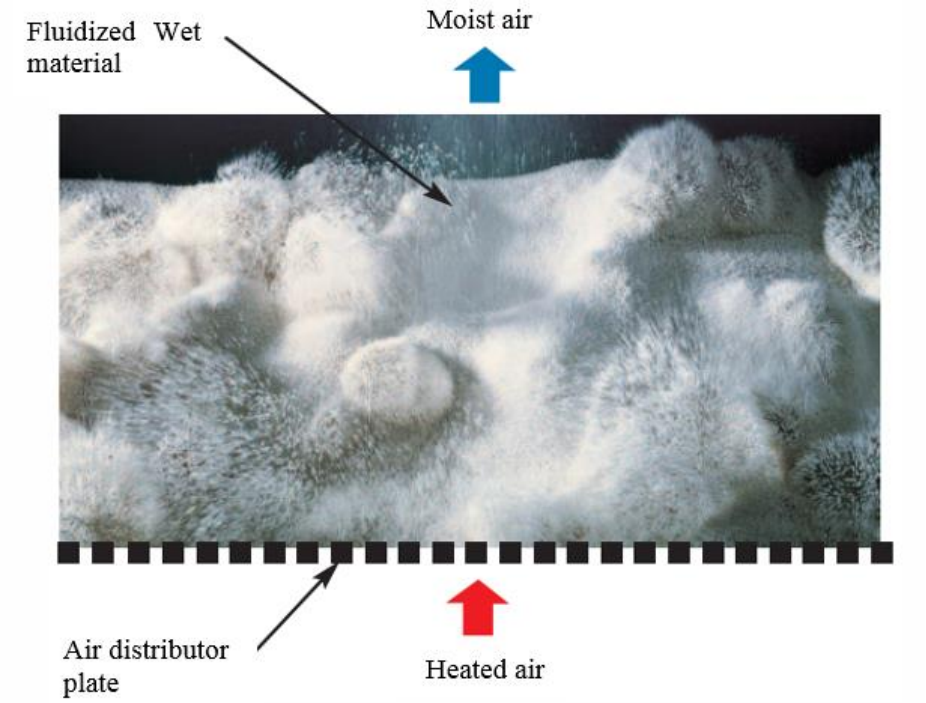

Figure 2-8: Material Suspended in Fluidized Bed Dryer(FBD)[20]

To obtain a final dried product with uniform moisture content, the air distribution plate's design must provide vertical airflow through the material without allowing air to bypass the material bed. As the heated air passes through the wet material, the air carries away the moisture, cools and is exhausted through a downstream cyclone, bag house, or other air-material separation equipment. The dried final product is conveyed by various means, depending on the dryer type, to the dryer's discharge.

The fluid-bed dryer's advantage over other dryers is that the fluid bed unit suspends the material in the heated air 100 percent of the time. In a conduction dryer (in which heat is indirectly transferred to the material through a hot surface, such as the dryer wall), only some of the material contacts the hot surface at one time, and in a convection dryer that doesn't suspend material, such as a rotary dryer, the material contacts the heated air only as the particles shower through the drying chamber with the dryer's rotation. Compared with these dryers, the fluid bed dryer has a very high heat-transfer rate and a smaller footprint, giving it higher heat efficiency. By intimately mixing the heated air and material close to equilibrium (that is, the same moisture content and temperature).

2.5 Fluidization Regimes

According to Wen-Ching Yang, 2003 and Maria Laura Passos et al., 2014, Fluidization is a process in which solids are caused to behave like a fluid by blowing gas or liquid upwards through the solid-filled reactor. When the solid particles are fluidized, the fluidized bed behaves differently as velocity, gas and solid properties are varied. It has become evident that there are number of regimes of fluidization, as shown in figure 2-9[22-24]. When the flow of a gas passed through a bed of particles is increased continually, a few vibrate, but still within the same height as the bed at rest. This is called a fixed bed (Figure 2.9A). With increasing gas velocity, a point is reached where the drag force imparted by the upward moving gas equals the weight of the particles, and the voidage of the bed increases slightly: this is the onset of fluidization and is called minimum fluidization (Figure 2.9B) with a corresponding minimum fluidization velocity, Umf. Increasing the gas flow further, the formation of fluidization bubbles sets in. At this point, a bubbling fluidized bed occurs as shown in figure 2.9C. As the velocity is increased further still, the bubbles in a bubbling fluidized bed will coalesce and grow as they rise. If the ratio of the height to the diameter of the bed is high enough, the size of bubbles may become almost the same as diameter of the bed. This is called slugging (Figure 2.9D). If the particles are fluidized at a high enough gas flow rate, the velocity exceeds the terminal velocity of the particles. The upper surface of the bed disappears and, instead of bubbles, one observes a turbulent motion of solid clusters and voids of gas of various sizes and shapes. Beds under these conditions are called turbulent beds as shown in Fig 2.9E. With further increases of gas velocity, eventually the fluidized bed becomes an entrained bed in which we have disperse, dilute or lean phase fluidized bed, which amounts to pneumatic transport of solids as shown in figure 2.9F.

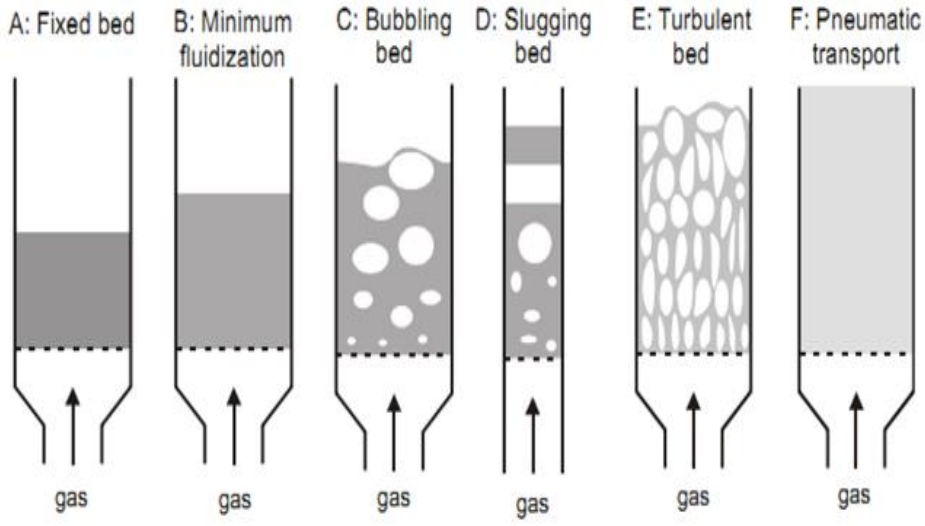

Figure 2-9: Schematic representation of fluidized beds in different regimes (based on Kunii and Levenspiel, 1991)[22]

2.6 Proximate and Ultimate Analysis of Bagasse

Proximate and ultimate analyses are used to determine the characteristics of carbonaceous materials that may be used as precursor for active carbons. Proximate analysis include fixed carbon, volatile materials, ashes, bricks and sucrose. Ultimate analysis describes the elemental composition, such as content of carbon, hydrogen, oxygen, nitrogen and metals. The tables below show Proximate and Ultimate analysis of sugarcane bagasse.

The proximate analysis defines that part of the fuel that gasifies below 750°C, called the volatiles, in relation to the fixed carbon[11], [25-27]. It provides an indication of its combustion properties especially the combustion stability[28]. A proximate analysis for Wonji/Shoa sugar factory bagasse is given in Table 2-1 below.

Table 2-1: Proximate Analysis of Wonji/Shoa Sugarcane Bagasse

Components	Percentage Composition
Fixed Carbon	12.73
Volatile Matter	81.76
Ash	2.5
Bricks	1
Sucrose	2

The ultimate analysis is the analysis of the fuel into its basic chemical elements. This analysis is used to obtain the theoretical air needed for combustion based on the stoichiometric equations of the various elements. It also provides a means to determine the quantity and composition of the flue gases[28]. Table 2 gives a typical ultimate analysis of Wonji/Shoa sugarcane bagasse.

Table 2-2: Ultimate Analysis of Wonji/Shoa Sugarcane Bagasse

Components	Percentage Composition
Carbon	46.4
Hydrogen	5
Nitrogen	0.45
Sulfur	0
Oxygen	47.3

2.7 Calorific Value of Sugarcane Bagasse

The calorific value of fuel is the heat released per unit mass of fuel at 25^0Cwith completed combustion. Generally, there are two calorific values: a gross calorific value (GCV) and a net calorific value (NCV). The GCV is the total energy released during the combustion process and can be accurately measured by using a bomb calorimeter. The NCV is the GCV without the latent heat of the water formed by the combustion process. Table 3 gives calorific values of sugarcane bagasse at 52% moisture content.

Table 2-3:Calorimetry/Calorific Values of Sugarcane Bagasse at 52% Moisture Content

Parameters	Value in kJ/kg
GCV or HHV	8956
NCV or LHV	7130

2.8 Composition of Flue Gas

The total weight of flue gases is given by Equation 3 as follows:

$$P = 5.76\ (1 - w)\ m + 1 \quad kg/kg$$

The weight of the individual gases is given by[10]:

a. Nitrogen

$$N_2 = 4.43(1-w)\ m \tag{5}$$

b. Oxygen

$$O_2 = 1.33(1-w)\ (m-1) \tag{6}$$

c. Water

$$H_2O = 0.585(1-w) + w \tag{7}$$

d. Carbon dioxide

$$CO_2 = 1.72(1-w) \tag{8}$$

Where w - is moisture content of bagasse

m - is excess air requirement

Substituting the values of m and w, and dividing by P, we may readily calculate the proportion by weight of each of these constituents in the flue gases.

Since the moisture content of bagasse is 52%, and the excess air required to burn the bagasse is ≤35%, the values of m and w is:

w = 0.52

m = 1.35

Therefore, P = 5.76 (1 - 0.52) 1.35 + 1 = 4.73 kg

And

N_2 = 4.43(1- 0.52)1.35 = 2.87 kg or $\frac{2.87\ kg}{4.73\ kg}$ = 60.7 %

O_2 = 1.33(1- 0.52)(1.35-1) = 0.22 kg or $\frac{0.22\ kg}{4.73\ kg}$ = 4.72 %

H_2O = 0.585(1- 0.52) + 0.52 = 0.8 kg or $\frac{0.8\ kg}{4.73\ kg}$ = 16.93 %

CO_2 = 1.72(1- 0.52) = 0.82 kg or $\frac{0.82\ kg}{4.73\ kg}$ = 17.45 %

Table 2-4: Composition of Flue Gases

Components	**Percentage Composition by Volume (Vol. %)**	**Volume Fraction**
Nitrogen	60.7 %	$\frac{0.607}{0.998}$ = 0.6082
Oxygen	4.72 %	$\frac{0.0472}{0.998}$ =0.0473
Water	16.93 %	$\frac{0.1693}{0.998}$ = 0.1696
Carbon dioxide	17.45 %	$\frac{0.1745}{0.998}$ =0.1748
Total	99.8 % or 0.998	0.9999

By using this percentage composition, we can determine other properties of flue gas using Flue Gas Properties Calculator as shown in Appendix C:

CHAPTER THREE: METHODOLOGY

In this present research study, Fluidized Bed Dryer is going to be designed and thermal energy analysis of this dryer will also done. The design and thermal energy analysis is done analytically and using ANSYS Fluent software. The data used to design and analyze thermal energy of FBD is directly collected from the Wonji/Shoa sugar factory. The model of FBD is developed using CAD software's and the simulation is done using analysis software ANSYS Fluent. Moreover, the relationship between bagasse moisture content and boiler efficiency will also determine. Additionally, the installation of FBD is shown in this paper. The following figure shows the overall design sequence of a FBD that going to be designed.

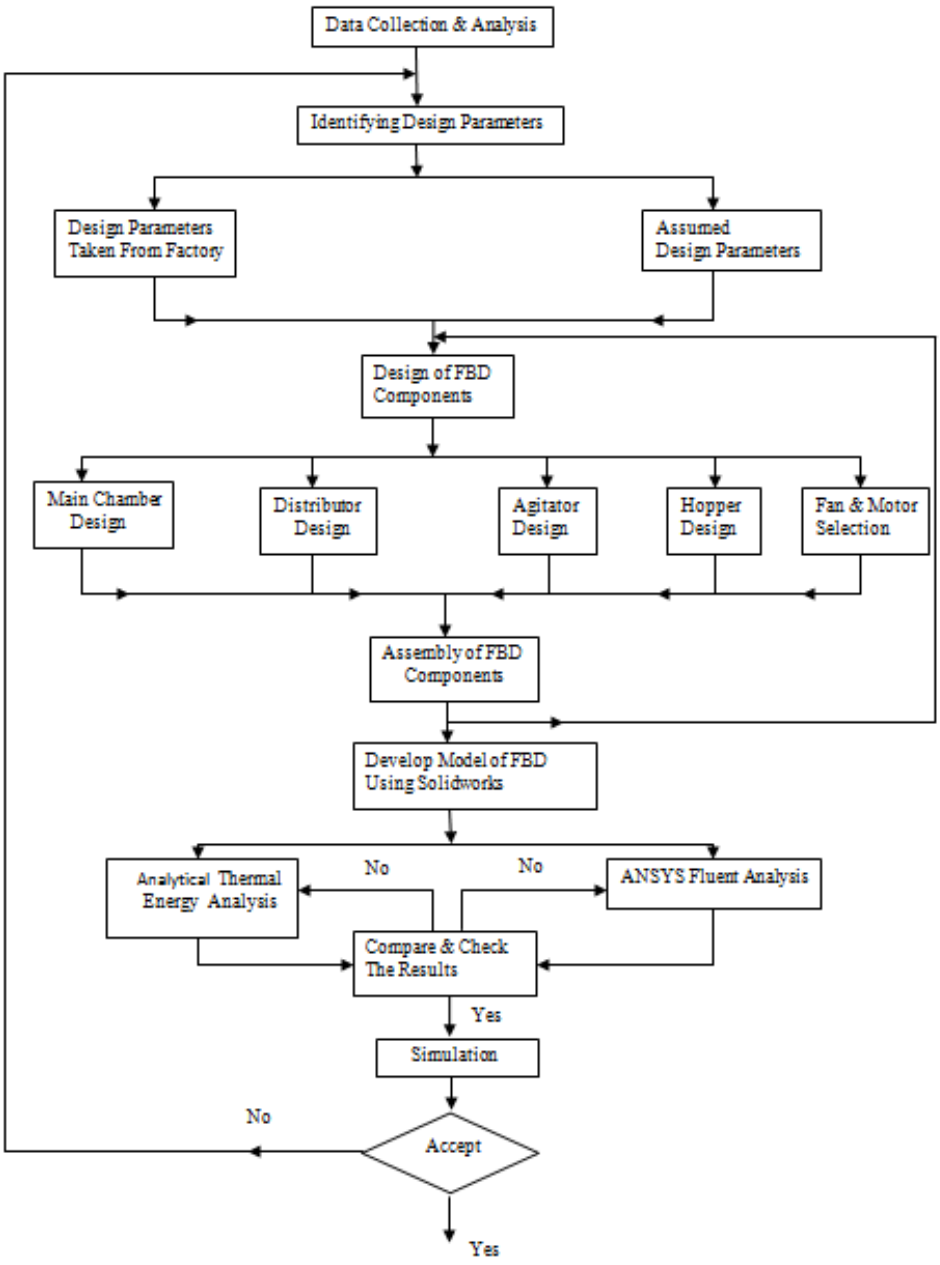

Figure 3-1: Overall Design Sequence for a FBD

The FBD going to be designed is a type of direct contact or open parallel flow heat exchanger in which the exchange of heat takes place by direct mixing of hot flue gases and moist bagasse, hence transfer of heat and mass takes place simultaneously. Direct contact with hot flue gases gives high heat transfer rates, short residence times and uniform drying. The hot flue gases mixes with the moist bagasse and gives its latent heat to moist bagasse and gets cooled. According to the relative direction of flow of moist bagasse and hot flue gases, this FBD is classified as parallel-flow heat exchanger type, because the two fluids flow in the same directions. To remove bagasse easily out of the drying chamber, it is better if the orientation of the dryer is vertical rather than being horizontal. The flow arrangement and temperature distribution for such a heat exchanger are shown schematically in the figure below. Parallel-flow FBD gives maximum rate of heat transfer for a given surface area. That is why direct contact parallel flow type of FBD is going to be designed.

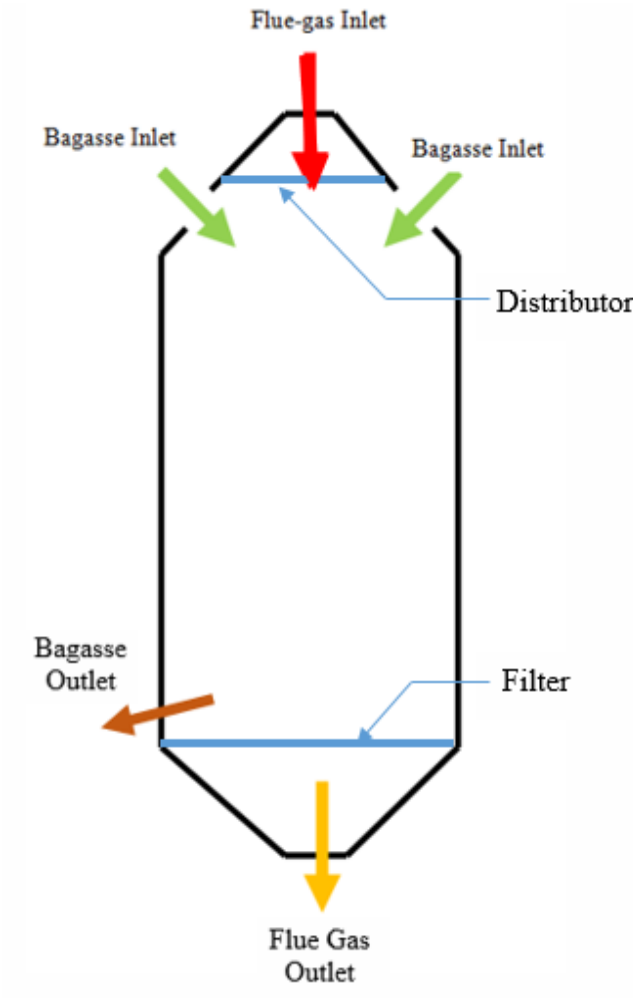

a) Flow Arrangement

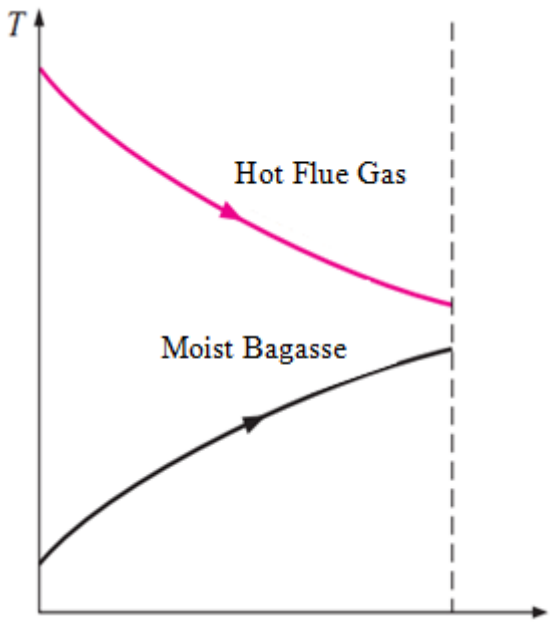

b) Temperature Distribution

Figure 3-2: Direct Contact Parallel Flow FBD

3.1 Design Data of Fluidized Bed Dryer

The following data is obtained from Wonji/Shoa sugar factory and used as a design data:

Table 3-1: Design Data (Actual)

Parameters	Value
Bagasse Moisture Content	52%
Mill Cane Crushing Capacity	6250 ton/hr
Bagasse Production	30-33% of total sugarcane crushed by mill
Bagasse Consumed by One Boiler	55.55 ton/hr
Flue Gas Temperature	270^{o}C at Economizer Outlet
Bagasse Temperature After Mill	35^{o}C or 308K
Atmospheric Temperature	25^{o}C or 298K
Atmospheric Pressure	1atm
Flue Gas Density at 270^{o}C	0.678 kg/m^3
Bagasse Density	250 kg/m^3
C_p of bagasse	0.46 kJ/kg K
C_p of flue gas	0.23 kJ/kg K
Mass flow rate of bagasse	15.43kg/s
Mass flow rate of flue gas	73 kg/s

Table 3-2: Design Data (Assumption & From Literature)

Parameters	Value
Environment air velocity	4m/s
Height of main chamber	20m [Assumption]
Discharge coefficient(C_d)	0.8 [Ref 22]
Distributor/grid thickness(t)	25mm [Ref 22]

The reason why the height of main chamber is assumed to be 20m is to match with Economizer location and to get good performance of the dryer. Presently the Economizer of Wonji/Shoa sugar factory were installed at a height of about 22m near to boiler. The flue gas which enter the main chamber is taken from Economizer. So to avoid losses of flue gases during entrance of dryer, the height of main chamber is assumed to be 20m. The left 2m is occupied by the upper hopper of dryer.

3.2 Part Design of Fluidized Bed Dryer

3.2.1 Design of Main Chamber

Main chamber is a place where mixture of wet bagasse and hot flue gases takes place.

Wonji sugar factory mills crushes 6250 tons of sugarcane per hour.

- By crushing 6250 tons of sugarcane per hour, 1968.75tons of bagasse obtained per hour since bagasse represents 30 - 33% of the total sugarcane mass[10-11] by taking the average value 31.5%, 0.315 x 6250tons/hr which is equal to 1968.75tons/hr. There are two boilers, one boiler consumes 55.55tons per hour and totally the two boilers consumes 111.1tons of bagasse per hour.
- Drying 111.1tons of bagasse in one dryer is difficult and it cannot be efficient. So a number of dryers required with a capacity of 55.55 tons per hour. Therefore:
- Number of dryers = $\frac{111.1\ ton}{55.55\ ton} = 2$ dryers are required
- Volume required for 55.5 tons:

$$V = \frac{\text{Mass}}{\text{Density}} = \frac{55550\ \text{kg}}{250\frac{\text{kg}}{\text{m}^3}} = 222.2\text{m}^3 \quad (9)$$

This volume is the volume bagasse required. For fluidization to take place additional space is needed. Therefore, the total volume of main chamber is obtained from the relation:

$$V_T = 1.25V = 1.25(222.2\text{m}^3) = 277.75\text{m}^3 \quad (10)$$

- From conventional formula, the volume of chamber is:

$$V_T = \pi r^2 h \quad (11)$$

From this conventional formula, the radius of the chamber is obtained:

$$r = \sqrt{\frac{V}{\pi h}} = \sqrt{\frac{277.75m^3}{3{,}14\ X\ 20m}} = 2.1\text{m} \quad (12)$$

- Cross Sectional Area of the chamber(A_c):

$$A_c = \pi r^2 \text{ or } \frac{\pi D^2}{4} \quad (13)$$

$= 3.14 \text{ x } (2.1\text{m})^2$

$= 13.9\text{m}^2$

To decrease the corrosive action of flue gases, it is better if the material of main chamber is gray cast iron. In a cylindrical pipe or a spherical shell, the additional insulation increases the conduction resistance of insulation, but decreases the convection resistance of the surface because of the

increase in the outer surface area. Due to these opposite effects, a critical radius/critical thickness of insulation is defined as the outer radius that provides maximum rate of heat transfer. For a cylindrical layer, it is defined as[34 – 36]:

$$r_{cr} = k / h \quad (14)$$

Where k is the thermal conductivity of insulation and h is the external convection heat transfer coefficient.

For insulation material Asbestos is preferred because it has tremendous thermal stability, it is good insulator, it is non-flammable even at very high temperatures and is extremely flexible and durable. The thermal conductivity of asbestos, loosely packed is 0.015W/m.K[36]. Hence the critical radius of insulation is:

$$r_{cr} = \frac{0.015 \text{W/m.K}}{6.29 \text{ W}/m^2 \text{.K}} = 0.0024\text{m}$$

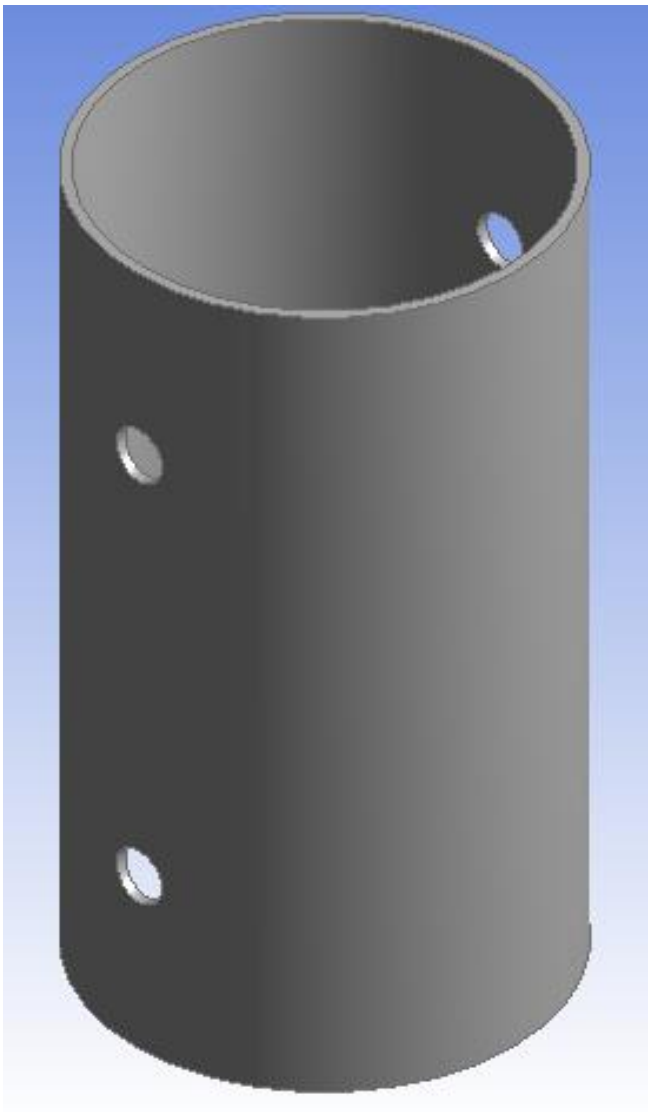

Figure 3-3: Main chamber

3.2.2 Design of Distributor or Grid

Distributor is used to distribute the hot flue gases uniformly to the main chamber. It is assembled at the top of main chamber and its diameter is depend on the diameter of the main chamber and the preferable diameter of the distributor/grid is three forth(3/4) of that of main chamber which is 3/4 x 4.2 = 3.15m[22]. The hole diameter of distributor is constrained by some main factor: If the hole size is small, it can become blocked by dust. If the number of holes is less, the larger distance between the holes can lead to a non-uniform distribution of gas. Hence a hole diameter of about 20 up to 30 mm would be optimum[22].

The following equations can be used to design distributor/grid:

- Pressure drop across the chamber

$$\Delta P_{chamber} = g\,\rho_F\,L_C \quad (15)$$

$$= 9.81 m/s^2 \times 0.678 kg/m^3 \times 20m$$

$$= 0.133 kPa$$

Where g is gravitational acceleration, ρ_F is density of flue gas, L_C is length of chamber.

According to *Wen-Ching Yang, 2003*, thus as a rule of thumb, the criteria for good gas distribution based on the direction of gas entry are:

1. For upwardly and laterally directed flow:
   $\Delta P_{grid} > 0.3\Delta P_{chamber}$
2. For downwardly directed flow:
   $\Delta P_{grid} > 0.1\Delta P_{chamber}$
3. Under no circumstances should the pressure drop across a large-scale commercial grid be less than 2500 Pa, i.e.,
   $\Delta P_{grid} > 2{,}500 Pa$

Since the direction of flue gas entry is downward for this case:

$$\Delta P_{grid} > 0.1\Delta P_{chamber}$$

$$\geq 0.1 \times 0.133 kPa$$

$$\geq 0.0133 kPa$$

The minimum pressure drop across the grid should not be greater than 0.0133kPa, unless good gas distribution is not obtained.

- The gas velocity through the grid hole (orifice equation):

$$U_h = C_d\sqrt{\frac{2\Delta P_{grid}}{\rho_{g,c}}} \quad (16)$$

$$= 0.8\sqrt{\frac{2 \text{ x } 13.3}{0.678}} = 5.01\text{m/s}$$

Where C_d is orifice discharge coefficient and a typical value of C_d for a grid hole is about 0.8. Actually, the value of C_d depends on the grid plate thickness and the hole pitch, $\rho_{g,c}$ is density of the gas entering the chamber.

- Volumetric flow rate of gas:

$$Q = U_h \frac{\pi D^2}{4} \quad (17)$$

$$= 5.01 \text{ x } \frac{\pi \text{ x } 3.15^2}{4}$$

$$= 39.04\text{m}^3/\text{s}$$

Or

$$Q = N\frac{\pi d_h^2}{4} U_h \quad (18)$$

where N is number of holes on distributor/grid, d_h is diameter of hole/hole pitch which is between 20 up to 30mm[22](Take average hole diameter 25mm). Also the grid plate thickness is recommended to be between 35mm and 40mm[22](Take average grid plate thickness 37.5mm).

From equation 18, the number of holes on distributor (N) is given by:

$$N = \frac{4Q}{\pi d_h^2 U_h}$$

$$= \frac{4 \text{ x } 39.04}{\pi \text{ x } 0.025^2 \text{ x } 5.01}$$

$$= 15876$$

- The hole density (holes per unit area of the grid):

$$N_d = \frac{N}{\frac{\pi D^2}{4}} \quad (19)$$

$$= \frac{15876}{\frac{\pi \text{ x } 3.15^2}{4}}$$

$$= 2037/\text{m}^2$$

3.2.2.1 Hole Size

To increase the gas residence time in the chamber, it is desirable to introduce the greatest number of small gas bubbles as possible into the bed. This can be achieved by maximizing N at the expense of d_h in equation (17) (within the limits of mechanical, cost, and scale up constraints). To minimize stagnant zones, the number of grid holes per m^2 should be greater than 20. The hole diameter(d_h) is preferable between 20mm and 30mm [22], hence the average 25mm is used for design purpose.

3.2.2.2 Hole Layout

To increase the uniformity of fluidization, it is common to lay out the holes in triangular or square pitch, as shown in Figure below. All the holes in a grid with triangular pitch are equidistant. This is not the case for a grid with square pitch. Triangular pitch will also result in more holes per unit area. The relationship between the grid hole pitch, L_h, and the number of hole density (holes per unit area of the bed), N_d, depends on whether the holes are laid out in triangular or square pitch.

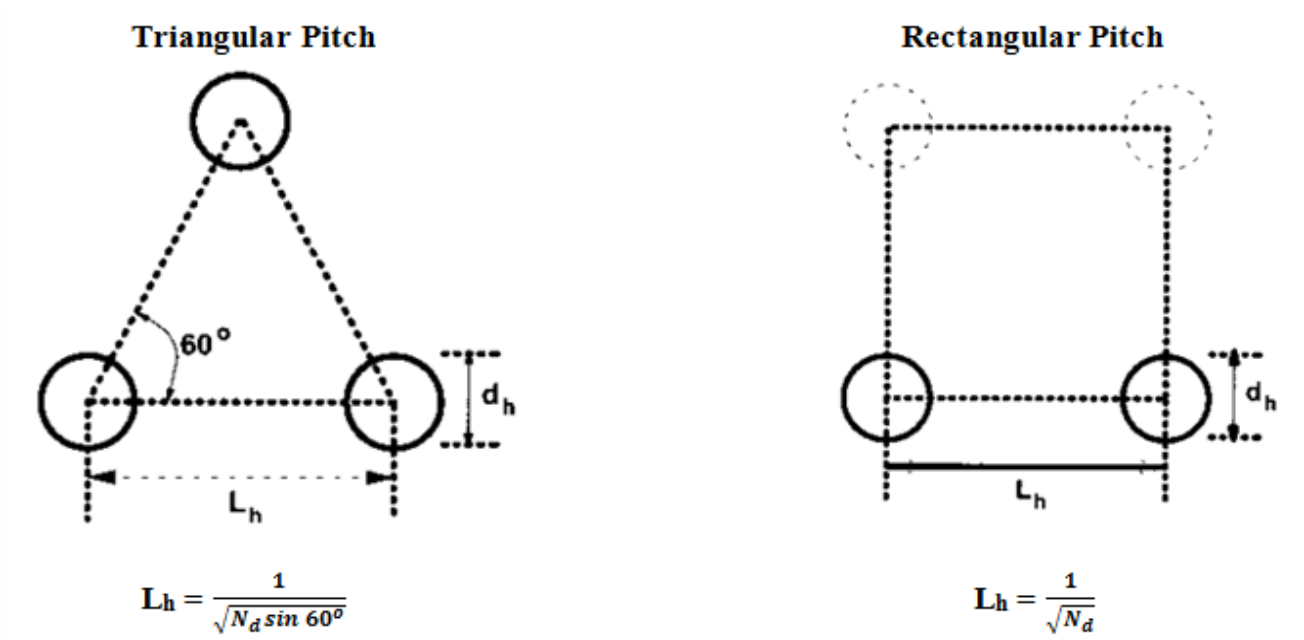

Figure 3-4: The relationship between hole density and grid hole pitch for both triangular and square pitch[22]

Since all the holes in a grid with triangular pitch are equidistant, so triangular pitch orientation is more preferable than square pitch for this studies. Therefore, the grid hole pitch (L_h) or distance between each hole is given by:

$$L_h = \frac{1}{\sqrt{N_d \sin 60}} = \frac{1}{\sqrt{2037 \sin 60}} = 0.024\text{m}$$

Figure 3-5: Distributor/Grid

3.2.3 Design of Agitator

Agitator is used to provide the continuous mixing of the wet bagasse with the hot flue gases for effective drying. If the agitator is not used, the bagasse particles would settle down and resulting in non-uniform drying. Agitator is installed in main chamber. Its length is equal with the diameter of main chamber 4.2m plus the both side thickness of chamber (thickness of main chamber 5cm) and insulator thickness. So its length is 4.2m + 2(0.05m) + 2(0.0024m) = 4.3m ≈ 4.5m. Since it rotate inside the main chamber, its width should be less than the diameter of main chamber. Take it 4.15m. There are different types of agitators to facilitate mixture of fluids and their blade orientation also depends on the purposes required. Since this agitator is only used to facilitate the mixture of bagasse and flue gas, its blade complexity is not necessary, the following blade model is better enough. The holes on agitator blade is used to provide the passage of flue gas during the rotation of agitator. The diameter of this holes is the same with the diameter of distributor holes 25mm.

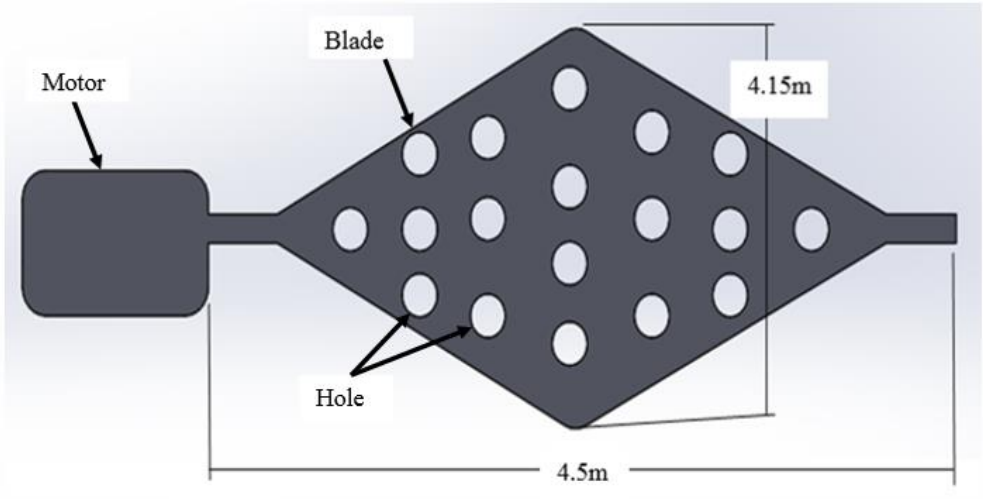

Figure 3-6: Agitator with motor

3.2.4 Design of Hopper

Hopper shapes can be cylindrical, trapezoidal or conical. For this study conical shape of hopper is more preferable because its shape easily matches the required purposes. There are two hoppers, upper and lower hopper. Upper hopper is used to feed wet bagasse to the main chamber while the lower hopper is used to collect cooled flue gases and vapors formed in the main chamber.

Volume of Truncated cone hopper is given by[29]:

$$V = \frac{\pi h}{12}[D - d]^2 \quad (20)$$

Where, V = volume of cone, m^3

h = height, m

D = larger diameter of truncated cone, m

d = smaller diameter of truncated cone, m

From this equation the smaller diameter of truncated cone (d) is:

$$d^2 - 2Dd + D^2 - \frac{12V}{\pi h} = 0$$

From conventional formula, the volume of cone is given by;

$$V = \pi\left(\frac{d^2}{4}\right)\left(\frac{h}{3}\right) \quad (21)$$

Hence,

$$d^2 - 2Dd + D^2 - \frac{12\left(\pi\left(\frac{d^2}{4}\right)\left(\frac{h}{3}\right)\right)}{\pi h} = 0,$$

$$d^2 - 2Dd + D^2 - d^2 = 0$$

$$d = \frac{D^2}{2D}$$

$$d = \frac{4.2^2}{2(4.2)}$$

$$= 2.1m$$

The larger diameter of both upper and lower hopper must be equal to the diameter of main chamber 4.2m. The smaller diameter of lower hopper is 2.1m, while the diameter of upper hopper should be one fourth of the smaller diameter of lower hopper [29], which is $(\frac{1}{4}$ x 2.1) = 0.525m. The two inlets of bagasse is assumed to be 0.5m x 0.5m. For both hopper 45° cone angle is used and the corresponding height is:

Upper Hopper

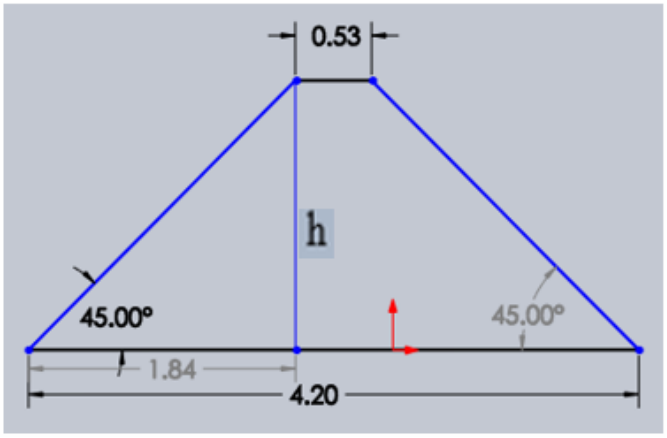

Using tan law:

$\tan 45 = \frac{h}{1.84}$

h = 1.84 (tan 45)

h = 1.84m

Lower Hopper

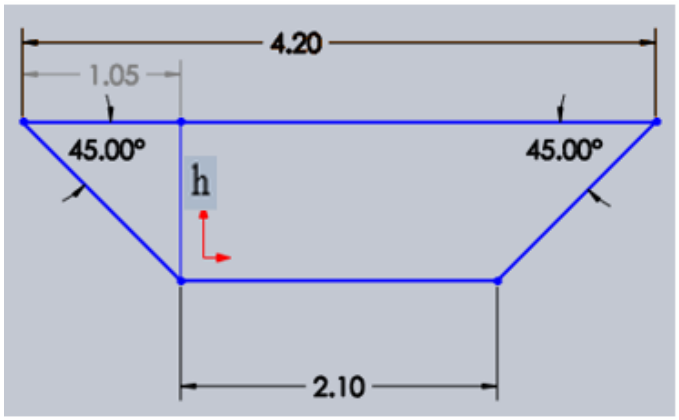

Using tan law:

$\tan 45 = \frac{h}{1.05}$

h = 1.05(tan 45)

h = 1.05

The figure given below shows the designed upper hopper, lower hopper.

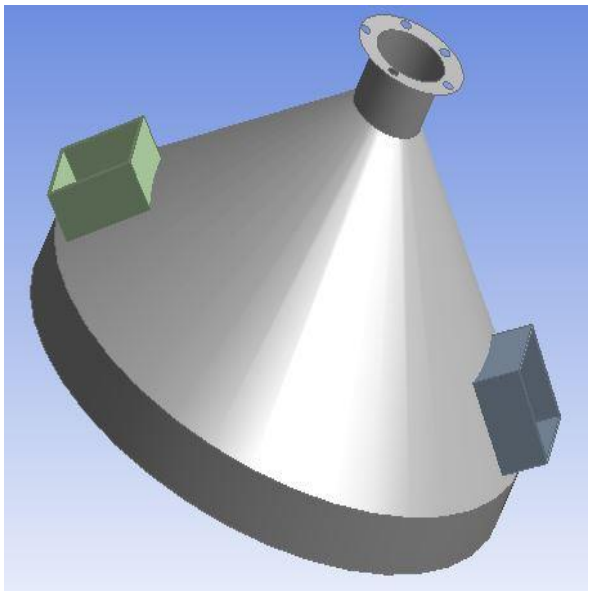

Figure 3-7: Upper Hopper

Figure 3-8: Lower Hopper

3.2.5 Filter

Filter is used to prevent the escaping of bagasse particles from the induced draught fan or it is used to separate the particles of bagasse that moved with cooled flue gas and vapor formed. It is installed between the lower hopper and the lower end of main chamber. Its diameter is equal to the diameter of main chamber 4.2m and its thickness is assumed to be 37.5mm similar to thickness of distributor. The size of its hole is assumed based on the size of fiber bagasse 2mm to 4mm. The filter plate is inclined at an angle for the purpose of increasing solids discharge from the chamber.

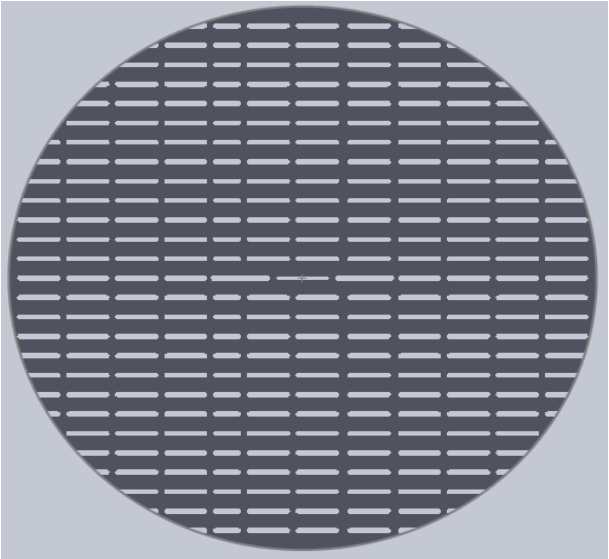

Figure 3-9: Filter

3.2.6 Fan Selection

Fan can be either axial, centrifugal or mixed based on flow type and are generally driven by electric motor. Axial type fan is used for low pressure and higher flow rate applications while centrifugal type fan is used for high pressure and lower flow rate applications. For this purpose axial type fan is preferable. Also fan can be classified as forced draft(F.D) and induced draft(I.D). Also, F.D and I.D fans can be either of the axial or centrifugal type. F.D is used to blow the hot flue gas into the main chamber while I.D is used to suck out the vapor from the main chamber.

From the mass-flow rate through the fan, velocity of flue gas is given by[30]:

$$V = \frac{\dot{m}}{\rho A} \tag{22}$$

$$= \frac{73\ \text{kg/s}}{0.678\frac{kg}{m^3}\ X\ 13.9m^2}$$

= 7.75m/s

The power required to drive the fan is given by[30]:

$$P = \dot{m}(\Delta h_o)_{st} = \dot{m}C_p(\Delta T_o)_{st} \quad (23)$$

If the flow velocities at the entry and exit of the fan stage are equal or small, the values of static and stagnation enthalpy changes are identical. The same is true for changes in pressure and temperature across the stage[30]. Hence, assume flow velocities at the entry and exit of the fan stage are equal, so take static and stagnation enthalpy and temperature changes are equal.

$$P = 73\text{kg/s} \times (0.23\text{kJ/kg.K})\,(270\text{ K})$$
$$= 4.53\text{kW}$$

So, for this purpose a fan with mass-flow rate of 73kg/s and power 4.53kW is needed to meet the requirements.

These all above parts assembled together and give the new modified fluidized bed dryer which requires small space for installation. A review of literature reveals that the vertical orientation is useful in two ways. First, it takes advantage of the gravitational effect of particles falling and second, it allows for operation at much lower gas velocities than could be used if the tube was horizontal[18], [21].

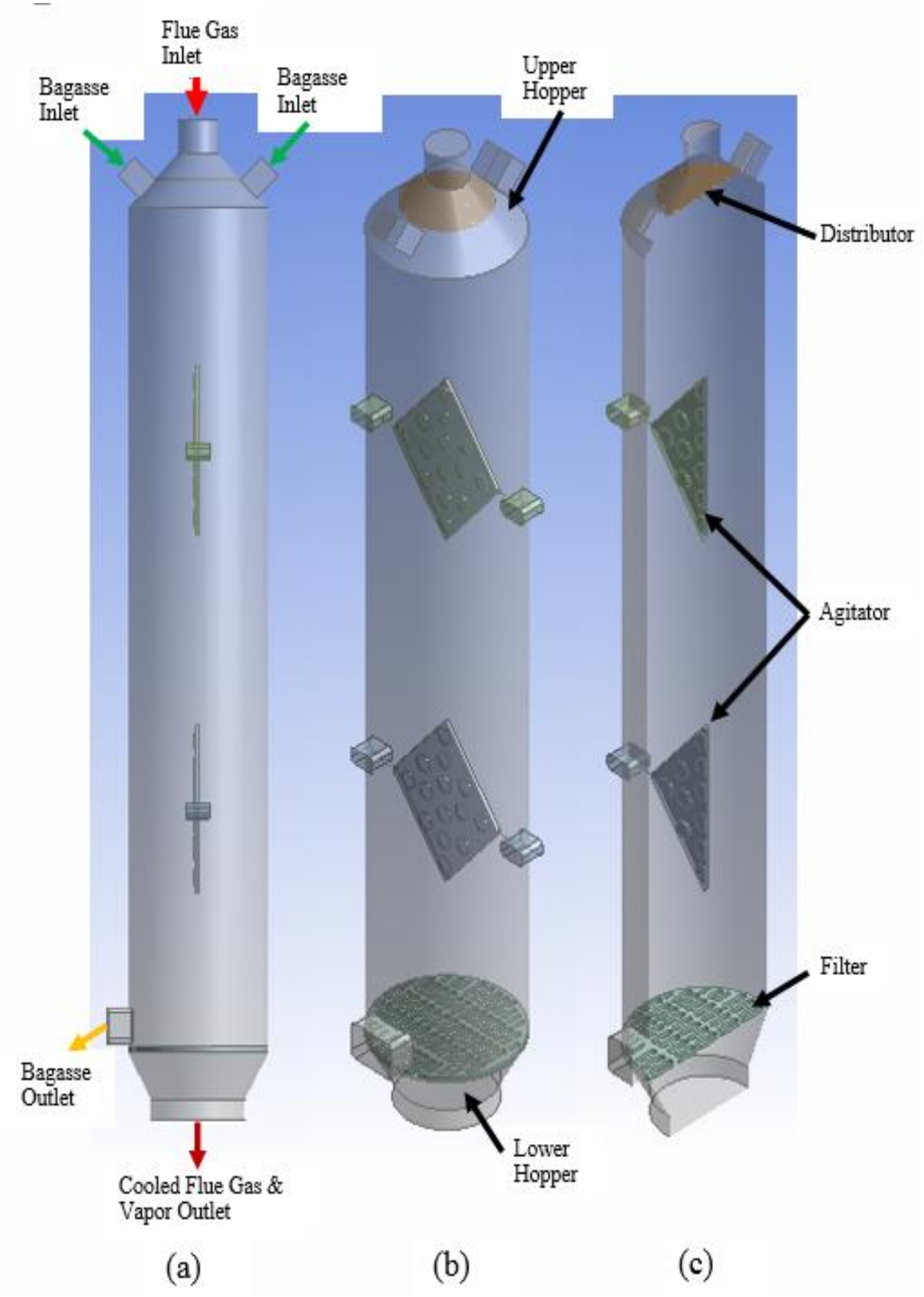

Figure 3-10: Assembled FBD (a) Front View (b) Isometric View (c) Sectional View

3.3 Working Principle of Fluidized Bed Dryer (FBD)

The wet bagasse is fed through the hopper to the main chamber. In main chamber agitator makes rotation by motors and this rotation of agitator and the hot flue gases from the Forced draught fan controls the settling of bagasse and causes vigorous mixing of hot air and bagasse. This vigorous mixing leads to the fluidization (Mixture of hot flue gases and wet bagasse's). The high velocity flow of hot flue gases across the agitated wet bagasse enables the removal of moisture in bagasse in form of vapors. This vapors and cooled flue gases in main chamber gets sucked by the Induced draught fan and released to the environment. After some hour, the dried bagasse is taken out from the main chamber by moving the distributor. The below flow diagram shows the process of bagasse drying.

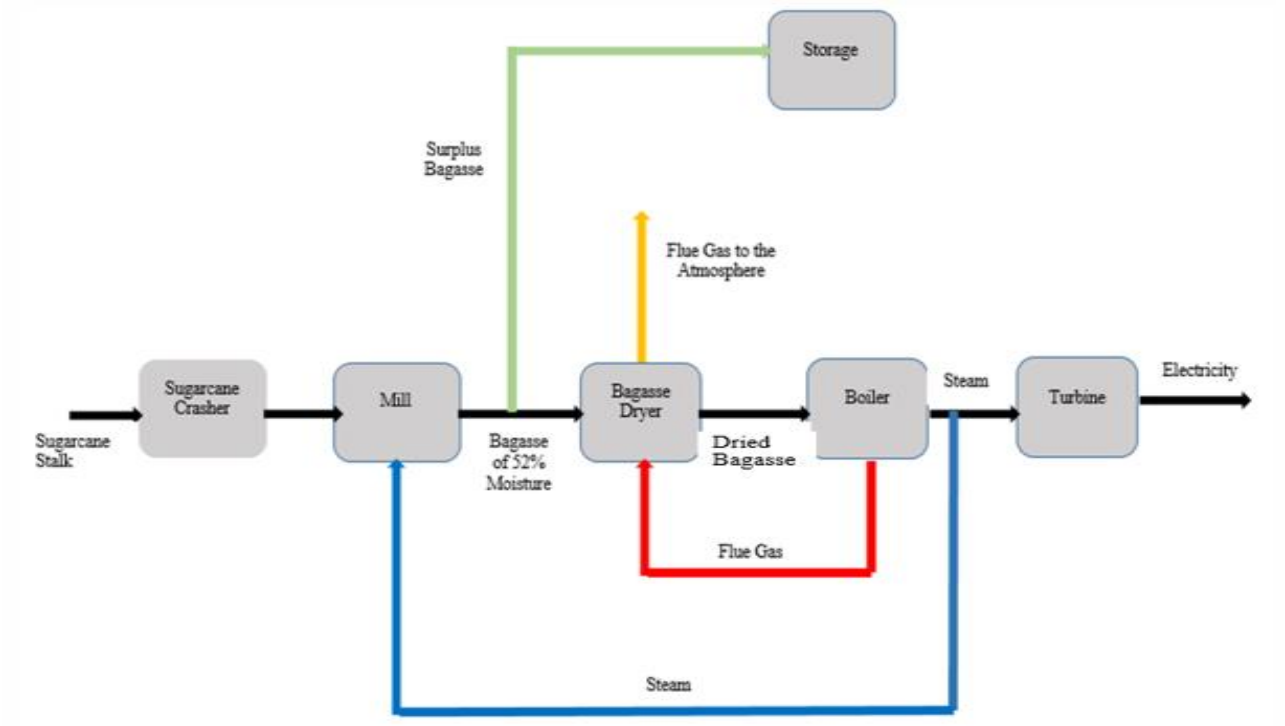

Figure 3-11: Flow Diagram of Bagasse Drying

3.4 Thermal Analysis of Fluidized Bed Dryer

3.4.1 Inside of dryer

The flue gas flow regime (whether the flow is laminar, transitional or turbulent) is indicated by the value of Reynolds number:

$$\mathrm{Re} = \frac{\boldsymbol{Vd}}{\nu} \tag{24}$$

Where V - is velocity of flue gas,

d - is diameter of main chamber and

ϑ - is kinematic viscosity

The kinematic viscosity(ϑ) of flue gas at temperature T in ^oC is approximated by the following relation[31] or calculated using Lauterbach Verfahrenstechnik(LV) software as attached in appendix D:

$$\vartheta = (0.1335 + 0.925x10^{-3}t) \times 10^{-4} \quad m^2/s \tag{25}$$

Where t - is internal temperature in main chamber

The temperature of gas in main chamber is 543K or 270^{o}C. So the kinematic viscosity becomes:

$$\vartheta = (0.1335 + 0.925x10^{-3} \times 543) \times 10^{-4} = 0.0000636\ m^2/s$$

The velocity of flue gas is given by the relation[32]:

$$V = \frac{\dot{m}}{\rho A_c} \tag{26}$$

Where $\dot{m}$ - is mass flow rate of flue gas

ρ - is density of flue gas

A_c - is cross-sectional area of main chamber

$$V = \frac{73kg/s}{\frac{0.678kg}{m^3} X\ 13.9m^2} = 7.75\text{m/s}$$

The Reynolds number for a flue gas velocity (V) of 7.75m/s in a dryer of 4.2m diameter (d) is:

$$Re = \frac{7.75 \times 4.2}{0.0000636} = 511792.45$$

This value of Re number indicate us the flow is in turbulent regime. Since the emissivity of the flue gas is low, hence the predominant mode of heat transfer is forced convection. A relationship for forced convection from a turbulent gas flow inside a cylindrical tube is given by [33]:

$$Nu = 0.023\ Re^{0.8}\ Pr^{0.4} \tag{27}$$

where Nu - is Nusselt number and also given by[31]:

$$Nu = \frac{h_i\ d_i}{k} \tag{28}$$

Pr - is Prandl number and given by:

$$Pr = c_p\mu/k \tag{29}$$

Most gases have a value of Pr of about 0.74, and this value is substantially independent of temperature[31], hence the above equation simplifies to:

$$Nu = 0.02\ Re^{0.8}$$

$$= 0.02 \times (511792.45)^{0.8} = 738.42$$

From equation 28, the internal heat transfer coefficient (h_i) of the dryer becomes:

$$h_i = \frac{Nu \times k}{d_i} \quad W/m^2.K \tag{30}$$

Where k - is thermal conductivity of flue gas and its value can be approximated using the following relation[31] or calculated using Lauterbach Verfahrenstechnik (LV) software as attached in appendix D:

$$k = 0.02442 + 0.6992\times10^{-4}\, t \ W/m.K \tag{31}$$

$$= 0.02442 + (0.6992x10^{-4}) \times 543$$

$$= 0.0624 \ W/m.K$$

Hence, $hi = \frac{738.42 \times 0.0624}{4.2} = 10.97 W/m^2.K$

3.4.2 Outside of the Dryer

The heat transfer processes taking place on the outside surface of the dryer are rather more complex than the inside surface coefficient. Radiation heat transfer does have a part to play-the surface of the dryer will exchange heat by radiation to the surrounding environment, and the convective heat loss will be affected by the prevailing wind speed. In calm conditions, the convective heat transfer from the outside surface of the dryer will be by natural convection. As the wind velocity increases, forced convection will become the dominant mechanism.

For external flow normal to a dryer Nusselt number is given as follows [31, 33]:

$$Nu=0.26\ Re^{0.6}Pr^{0.3} \tag{32}$$

Assuming a constant value for Prandtl number of 0.74, this expression simplifies to:

$$Nu = 0.24Re^{0.6} \tag{33}$$

In this case the Reynolds and Nusselt numbers refer to the outside diameter (d_o) of the dryer. Then the outside convective heat transfer coefficient ($h_{c,o}$) of the dryer is given by:

$$h_{c,o} = \frac{Nu \times k}{d_o} \tag{34}$$

The outside temperature of dryer is 25°C or 298K. At 298K the kinematic viscosity and thermal conductivity of air is calculated by equation 25 and 31 respectively:

$$\nu = (0.1335 + 0.925x10^{-3} \times 298) \times 10^{-4} = 0.000041\ m^2/s$$

$$k = 0.02442 + (0.6992\times10^{-4}) \times 298 = 0.045\ W/m.K$$

The Reynolds number at environment air velocity of 4m/s is:

$$Re = \frac{Vd}{\nu}$$

$$= \frac{4 \text{ x } 4.2}{0.000041} = 409756.1$$

From Eq. 33, the Nusselt number is:

$$Nu = 0.24(409756.1)^{0.6} = 559.4$$

The outside diameter (d_o) of dryer is equals to internal diameter (d_i) of dryer plus the thickness of dryer which is 2cm. From equation 34, the outside convective heat transfer is:

$$h_{c,o} = \frac{559.4 \text{ x } 0.045}{4.24} = 5.94 \text{ W/m}^2\text{.K}$$

The heat transfer from the outside surface of the chamber to the environment also contains a contribution from a radiative exchange to the surroundings. This is not an easy mechanism to quantify accurately, as radiative heat transfer is a non-linear process with respect to temperature and is affected by the nature and configuration of the participating surfaces. However, in circumstances such as these a linear approximation can be made to the radiative heat transfer component and an outside film coefficient defined in terms of the convective and radiative components[31] thus:

$$h_o = h_{c,o} + \varepsilon h_{r,o} \quad (35)$$

Where ε - is the emissivity of the surface and

$h_{r,o}$ - is a linearized radiation surface heat transfer coefficient, which is dependent on the surface temperature of the dryer and the temperature of the surroundings.

For typical situations a reasonable value for $h_{r,o}$ is 5 W/m^2/K. The emissivity will depend on the outside finish of the dryer steel metal finish (ε=0.07)[12].

$$h_o = 5.94 + (0.07 \text{ x } 5) = 6.29 \text{ W/m}^2\text{.K}$$

The overall heat transfer coefficient for the dryer is given by[34]–[36]:

$$U = \frac{1}{\frac{1}{h_i} + \frac{L_c}{K_c} + \frac{L_{ins}}{K_{ins}} + \frac{1}{h_o}} \quad (36)$$

Where L_{ins} – is thickness of insulation material(0.0024m), K_{ins} – is thermal conductivity of insulation material(2W/m.K)[34], L_c – is thickness of main chamber(0.02m) and K_c – is thermal conductivity of chamber(Gray Cast Iron). The thermal conductivity of gray cast iron is 47-80W/m.K[34], take the average value 63.5W/m.K.

$$= \frac{1}{\frac{1}{10.97} + \frac{1}{6.29} + \frac{0.0024}{2} + \frac{0.02}{63.5}} = 4 \text{W/m}^2\text{.K}$$

3.4.3 Heat Transfer Rate Analysis of Bagasse Dryer

The first law of thermodynamics/Energy balance, requires that the rate of heat transfer from the hot flue gas should be equal to the rate of heat transferred to the moist bagasse plus the latent heat of evaporation of moisture contained in bagasse plus heat loss to the surrounding(since the dryer is insulated, the heat loss to the surrounding is zero). That is[34–37]:

The rate of heat transfer from the hot flue gas or sensible heat given off by flue gas:

$$\dot{Q} = \dot{m}_f C_{pf} (T_{f,\,in} - T_{f,\,out}) \quad (37)$$

The rate of heat transferred to the moist bagasse or sensible heat gained by bagasse:

$$\dot{Q} = \dot{m}_b C_{pb} (T_{b,\,out} - T_{b,\,in}) \quad (38)$$

In general,

Sensible heat given off by flue gas = Sensible heat gained by bagasse + Latent heat of evaporation of moisture + Heat loss to the surrounding

$$\dot{m}_f C_{pf} (T_{f,\,in} - T_{f,\,out}) = \dot{m}_b C_{pb} (T_{b,\,out} - T_{b,\,in}) + \dot{m}_w L + q_{loss}$$

Where, $\dot{m}_{f,}$ $\dot{m}_b$ and $\dot{m}_w$ - mass flow rate of flue gas, bagasse and moisture in bagasse respectively

$C_{pb,}$ C_{pf} - specific heat of bagasse and flue gas at constant pressure respectively

$T_{b,\,out,}$ $T_{f,\,out}$ - outlet temperature of bagasse and flue gas respectively

$T_{b,\,in}$, $T_{f,\,in}$ - inlet temperature of bagasse and flue gas respectively

L – Latent heat of evaporation of water (2256J/kg)[32]

$q_{loss} = 0$ (because the dryer is insulated)

In dryer analysis, it is often convenient to combine the product of the *mass flow rate* and the *specific heat* of a fluid into a single quantity which is called the *heat capacity rate* and it is defined for the hot and cold fluid streams as follows[34]:

$$C_h = \dot{m}_h C_{ph} \quad (39)$$

And $$C_c = \dot{m}_c C_{pc} \quad (40)$$

Where the subscripts *c* and *h* stand for cold and hot fluids, respectively. In this case the hot fluid represents flue gas and the cold fluid represents moist bagasse. The heat capacity rate of a fluid stream represents the rate of heat transfer needed to change the temperature of the fluid stream by 1°C as it flows through a dryer.

With the definition of the heat capacity rate the above equations, Equation 37 and 38 can be simplified as:

$$\dot{Q} = C_c\,(T_{b,\,out} - T_{b,\,in}) \tag{41}$$

$$\dot{Q} = C_h\,(T_{f,\,in} - T_{f,\,out}) \tag{42}$$

The heat transfer rate in a dryer is equal to the heat capacity rate of either fluid multiplied by the temperature change of that fluid. Note that the only time the temperature rise of a cold fluid (bagasse) is equal to the temperature drop of the hot fluid (flue gas) is when the heat capacity rates of the two fluids are equal to each other. Refer figure 3-17.

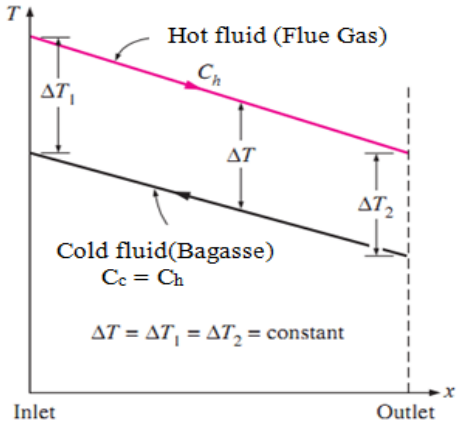

Figure 3-12: When the heat capacity rates of the two fluids are equal to each other

When the heat capacity rates of the two fluids are equal to each other, it experience the same temperature change in a well-insulated dryer. A bagasse dryer can be designed by two methods:
i) The LMTD (Logarithmic Mean Temperature Difference) when inlet and outlet conditions are specified. However, when the problem is to determine the inlet or exit temperatures for a bagasse dryer, ii) the analysis is performed more easily by using a method based on effectiveness of the dryer and number of transfer units. The dryer effectiveness (ε) is defined as the ratio of actual heat transfer to the maximum possible heat transfer [34], [35], [37]. Thus

$$\varepsilon = \frac{\dot{Q}}{\dot{Q}_{max}} = \frac{\text{Actual heat transfer rate}}{\text{Maximum possible heat transfer rate}} \tag{43}$$

The actual heat transfer rate in a dryer can be determined from an energy balance on the hot or cold fluids and can be expressed as:

$$\dot{Q} = C_h\,(T_{f,\,in} - T_{f,\,out}) = C_c\,(T_{b,\,out} - T_{b,\,in}) + \dot{m}_w L \tag{44}$$

The maximum possible heat transfer rate in a dryer is:

$$\dot{Q}_{max} = C_{min}(T_{f,in} - T_{b,in}) \tag{45}$$

Where C_{min} is the smaller value of $C_h = \dot{m}_h\,C_{ph}$ and $C_c = \dot{m}_c\,C_{pc}$.

Also the dryer effectiveness ε, is calculated according to the formula given in appendix A, table 7.1 [34]–[37]. Thus,

$$\varepsilon = \frac{1-\exp[-\mathrm{NTU}(1+c)]}{1+c} \quad (46)$$

Then, once the effectiveness of the dryer is known, the actual heat transfer rate $\dot{Q}$ can be determined from Equation 43 as follows:

$$\dot{Q} = \varepsilon \dot{Q}_{max} = \varepsilon\, C_{min}(T_{f,in} - T_{b,in}) \quad (47)$$

The number of transfer units NTU of the dryer is expressed as[34]–[37]:

$$\mathrm{NTU} = \frac{\mathrm{UA_s}}{\mathrm{C_{min}}} = \frac{\mathrm{UA_s}}{(\dot{m}\mathrm{C_p})_{\mathrm{min}}} \quad (48)$$

Where A_s - is the heat transfer area

Another option to find NTU is given in appendix B, table 7.2.

Since the problem is to determine the exit temperatures of a bagasse dryer, out of the two methods, to design bagasse dryer the effectiveness method is more preferable than the LMTD (Logarithmic Mean Temperature Difference) method.

Hence from equation 41, the rate of heat transferred to the moist bagasse is:

$\dot{Q} = C_c\,(T_{b,\,out} - T_{b,\,in})$

$= \dot{m}_c\, C_{pc}\,(T_{b,\,out} - T_{b,\,in})$

From table 3-1 (Design Data), the values of $\dot{m}_c$, C_{pc}, & $T_{b,in}$ are 15.43kg/s, 0.46kJ/kg.K & 308K respectively

$= 15.43\text{kg/s} \times 0.46\text{kJ/kg.K}\,(T_{b,\,out} - 308\text{K})$

$= 7.1\text{kJ/m.K}\,(T_{b,\,out} - 308\text{K})$

So, temperature of bagasse at outlet is:

$$T_{b,\,out} = \frac{\dot{Q}}{7.1\text{kJ/s.K}} + 308\text{K} \quad (49)$$

But the actual heat transfer rate $\dot{Q}$ is:

$$\dot{Q} = \varepsilon C_{min}(T_{f,in} - T_{b,in})$$

Now let compare C_h & C_c to select the values of C_{min} & C_{max}:

$C_h = \dot{m}_h\, C_{ph} = 73\text{kg/s} \times 0.23\text{kJ/kg.K} = 16.79\text{kJ/s.K}$

$C_c = \dot{m}_c\, C_{pc} = 15.43\text{kg/s} \times 0.46\text{kJ/kg.K} = 7.1\ \text{kJ/s.K}$

Hence, $C_c = C_{min}$ = 7.1 kJ/s.K & $C_h = C_{max}$ = 16.79kJ/s.K

From equation 48, NTU is:

$$NTU = \frac{UA_s}{C_{min}}, \qquad \text{where } A_s = \pi Dh = \pi(4.2m)(20m) = 269.9m^2$$

$$= \frac{4\,\frac{W}{m^2.K} \times 269.9m^2}{7100J/s.K}$$

$$= 0.152$$

From equation 46, the dryer effectiveness ε is:

$$\varepsilon = \frac{1-\exp[-NTU(1+c)]}{1+c} \qquad \text{Where } c = \frac{C_{min}}{C_{max}} = \frac{7.1\ kJ/s.K}{16.79kJ/s.K} = 0.42$$

$$= \frac{1-\exp[-0.152(1+0.42)]}{1+0.42}$$

$$= 0.137$$

Thus the actual heat transfer rate $\dot{Q}$ is:

$$\dot{Q} = (0.136)\ (7.1\ kJ/s.K)\ (543K-308K)$$

$$= 228.81kJ/s$$

Hence, the temperature of bagasse at outlet is:

$$T_{b,\,out} = \frac{228.81kJ/s}{7.1kJ/s.K} + 308K$$

$$= 340.23K \text{ or } 67.23^oC$$

Now we find the temperature of flue gas after heat rejection, from the first law of thermodynamics that states the rate of heat transfer from the hot flue gas should be equal to the rate of heat transferred to the moist bagasse or heat given by the flue gas should be equal to the heat taken by the bagasse since there is no heat dissipation.

$$\dot{m}_f\, C_{pf}(T_{f,in} - T_{f,out}) = \dot{m}_b C_{pb}(T_{b,out} - T_{b,in}) + \dot{m}_w L$$

So temperature of flue gas after heat rejection is:

$$T_{f,\,out} = T_{f,\,in} - \frac{\dot{m}_b C_{pb}(T_{b,out} - T_{b,in}) + \dot{m}_w L}{\dot{m}_f\, C_{pf}}$$

$$= 543K - \frac{15.43\frac{kg}{s} \times 0.46\frac{kJ}{kg.K}(340.23K - 308K) + (0.52 \times 15.43\frac{kg}{s})(2256\frac{J}{kg})}{73kg/s \times 0.23kJ/kg.K}$$

$$= 528.3K \text{ or } 255.3^oC$$

3.4.4 Moisture Reduction Analysis of Bagasse

Enthalpy change in moisture is given by the following relation[31], [38]:

$$\Delta H = M_f h_{b,out} + [M_i - M_f] \times h_{f,out} - M_i h_{b,in} \quad (50)$$

Where, M_f - is final moisture content in the bagasse

M_i - is initial moisture content in the bagasse

$h_{b,in}$ - is specific enthalpies of H_2O at temperature $T_{b,in}$ or 35°C

$h_{b,out}$ - is specific enthalpies of H_2O at temperature $T_{b,out}$ or 67.23°C

$h_{f,out}$ - is specific enthalpies of H_2O at temperature $T_{f,out}$ or 255.3°C

From steam table the values of $h_{b,in}$, $h_{b,out}$ & $h_{f,out}$ are 146.59kJ/kg, 281.41kJ/kg & 1681.65kJ/kg respectively.

The energy balance equation for the bagasse dryer is given by:

$$\dot{Q} = \Delta H \quad (51)$$

$$\dot{m}_f C_{pf}(T_{f,in} - T_{f,out}) = M_f h_{b,out} + [M_i - M_f] \times h_{f,out} - M_i h_{b,in} \quad (52)$$

Or

$$\dot{m}_b C_{pb}(T_{b,out} - T_{b,in}) = M_f h_{b,out} + [M_i - M_f] \times h_{f,out} - M_i h_{b,in} \quad (53)$$

Solve for final moisture content M_f from equation 52:

$$M_f = \frac{\dot{m}_f C_{pf}(T_{f,in} - T_{f,out}) + M_i h_{b,in} - M_i h_{f,out}}{h_{b,out} - h_{f,out}}$$

$$= \frac{\frac{73kg}{s} x \frac{0.23kJ}{kg}.K(543K - 529.38K) + 0.52 \times 146.59\frac{kJ}{kg} - 0.52 \times 1681.65\frac{kJ}{kg}}{281.41\frac{kJ}{kg} - 1681.65\frac{kJ}{kg}}$$

= 0.41 or 41%

Again solve for final moisture content M_f from equation 53:

$$M_f = \frac{\dot{m}_b C_{pb}(T_{b,out} - T_{b,in}) + M_i h_{b,in} - M_i h_{f,out}}{h_{b,out} - h_{f,out}}$$

$$= \frac{\frac{15.43kg}{s} x \frac{0.46kJ}{kg}.K\,(340.23K\,K - 308K) + 0.52 \times 146.59\frac{kJ}{kg} - 0.52 \times 1681.65\frac{kJ}{kg}}{281.41\frac{kJ}{kg} - 1681.65\frac{kJ}{kg}}$$

= 0.41 or 41%

Both equations gives almost the same result, so the final moisture content of bagasse is reduced to 41% from 52% or 11% moisture reduction. According to Hugot equation 1% moisture reduction increases GCV by 196 kJ/Kg[10], [19]. Thus total increased GCV is 11 x 196 = 2156kJ/kg. In

general 1% reduction in moisture in bagasse increases boiler efficiency by 0.5%[11], [31]. Thus boiler efficiency increased from 70% to 75% theoretically.

3.5 ANSYS Fluent Analysis of FBD

For this paper ANSYS FLUENT is used to analyze and simulate FBD. Because ANSYS FLUENT/ CFD provides high-fidelity database for diagnosing flow field. CFD gives an insight into flow patterns that are difficult, expensive, or impossible to study using the traditional (experimental) techniques. The five major advantages of CFD over experimental fluid dynamics are given below:

a) Lead time in design and development is significantly reduced.
b) CFD can simulate flow conditions that are not reproducible in experimental tests.
c) CFD provides more detailed information.
d) CFD is increasingly more cost effective than wind tunnel testing.
e) CFD produces lower energy consumption.

The Eulerian-Eulerian two-fluid model is widely employed for computational fluid dynamics (CFD) simulations of the gas-solid flows, since it requires economical computational resources and enables large-scale reactor modeling. The two-fluid model treats gas and solid phases as fully interpenetrating continua, which typically involves two sets of averaged Navier-Stokes equations. These governing equations are closed with the interfacial transfer models and the kinetic-frictional models for the description of granular phase [44]. The commercial CFD packages FLUENT and CFX gain many practices in Eulerian-based modeling of gas-solid flows. FLUENT uses a phase-coupled SIMPLE (Semi-Implicit Method for Pressure-Linked Equations) algorithm.

All CFD codes contain three main elements:

(1) ***A pre-processor***: In the pre-processing stage, formulation of the problem, i.e., governing equations and boundary conditions, and construction of a computational mesh, i.e., set of nodes and control volumes, are carried out.

(2) ***A flow solver***: In the flow solver stage, governing equations are discretized, and the resulting algebraic equations are solved. There are four different methods used as a flow solver:

(i) Finite difference method;
(ii) Finite element method,
(iii) Finite volume method, and
(iv) Spectral method.

(3) ***A post-processor***: In the post-processing stage, visualization, i.e., graphs and plots of the solution, and the analysis of results, i.e., calculation of forces, flow rates, pressure drop, heat transfer, etc., are carried out.

Mathematical models/Governing equations

The following fundamental laws can be used to derive governing differential equations that are solved in a Computational Fluid Dynamics (CFD):

- ✓ Conservation of mass
- ✓ Conservation of linear momentum (newton's second law)
- ✓ Conservation of energy (First law of thermodynamics)

The continuity equations of the flue gas and solid bagasse phases are written as:

$$\frac{\partial(\alpha_g \rho_g)}{\partial t} + \nabla.(\alpha_g \rho_g U_g) = 0$$

$$\frac{\partial(\alpha_b \rho_b)}{\partial t} + \nabla.(\alpha_b \rho_b U_b) = 0$$

Where ρ_g- is the gas phase density, ρ_b- is the solid bagasse phase density, Ug - is the gas phase velocity, U_b - is the bagasse solid phase velocity, Ug - is the gas phase velocity, α_g and α_b are the volumetric fractions of gas and solid phases, α_g = 1 - α_b.

The continuity equation is re-formulated as:

$$\frac{\partial \alpha_b}{\partial t} + \nabla.(U\alpha_b) + \nabla.(\alpha_g U_r \alpha_b) = 0$$

Where U is the mixture velocity, U = $\alpha_b U_b + \alpha_g U_g$, and U_r is the relative velocity,

$$U_r = U_b - U_g$$

The momentum equations of the flue gas and solid bagasse phases are given as:

$$\frac{\partial(\alpha_g \rho_g U_g}{\partial t} + \nabla.(\alpha_g \rho_g U_g U_g) = -\alpha_g \nabla p + \nabla.(\alpha_g \tau_g) + \beta(U_s - U_g) + \alpha_g \rho_g g$$

$$\frac{\partial(\alpha_b \rho_b U_b}{\partial t} + \nabla.(\alpha_b \rho_b U_b U_b) = -\alpha_b \nabla p - \nabla p_b + \nabla.(\alpha_b \tau_b) + \beta(U_g - U_s) + \alpha_b \rho_b g$$

Where p is the pressure, p_b is the solid bagasse phase pressure, τ_g and τ_b are the stress tensors of flue gas and solid bagasse phases, β is the interphase momentum transfer coefficient, and g is the gravitational acceleration.

The gas phase is assumed as a Newtonian fluid, and its stress tensor is defined using the Newtonian stress-strain relation as:

$$\tau_g = \mu_g[\nabla U_g + (\nabla U_g)^T] - \frac{2}{3}\mu_g(\nabla . U_g)I$$

Where μ_g is the shear viscosity of gas phase and I is the unit tensor. Similarly, the shear stress tensor of solid phase is expressed as:

$$\tau_b = \mu_b[\nabla U_b + (\nabla U_b)^T] + (\lambda_b - \frac{2}{3}\mu_b(\nabla . U_b)I$$

Where μ_b is the solid shear viscosity and λ_b is the solid bulk viscosity.

In general the following governing equations are used to govern the fluid flow.

Continuity $\frac{\partial \rho}{\partial t} + \nabla . (\rho V) = 0$

Momentum $\rho \frac{DV}{Dt} = \nabla . \tau_{ij} - \nabla p + \rho F$

Energy $\rho \frac{De}{Dt} + p(\nabla . V) = \frac{\partial Q}{\partial t} - \nabla . q + \Phi$

Where ρ - is the fluid density, V - is the fluid velocity vector, τ_{ij} - is the viscous stress tensor, p - is pressure, F - is the body forces, e - is the internal energy, Q - is the heat source term, t – is time, Φ - is the dissipation term, and ∇.q - is the heat loss by conduction.

These governing equations can also written in form of:

Continuity Equation: $\frac{\partial \rho}{\partial t} + \frac{\partial(\rho u)}{\partial x} + \frac{\partial(\rho v)}{\partial y} + \frac{\partial(\rho w)}{\partial z} = 0$

Navier Stokes Equation:

$$\rho \frac{\partial u}{\partial t} + \rho u \frac{\partial u}{\partial x} + \rho v \frac{\partial u}{\partial y} + \rho w \frac{\partial u}{\partial z} = -\frac{\partial \hat{p}}{\partial x} + \mu \left[\frac{\partial^2 u}{\partial x^2} + \frac{\partial^2 u}{\partial y^2} + \frac{\partial^2 u}{\partial z^2} \right]$$

$$\rho \frac{\partial v}{\partial t} + \rho u \frac{\partial v}{\partial x} + \rho v \frac{\partial v}{\partial y} + \rho w \frac{\partial v}{\partial z} = -\frac{\partial \hat{p}}{\partial y} + \mu \left[\frac{\partial^2 v}{\partial x^2} + \frac{\partial^2 v}{\partial y^2} + \frac{\partial^2 v}{\partial z^2} \right]$$

$$\rho \frac{\partial w}{\partial t} + \rho u \frac{\partial w}{\partial x} + \rho v \frac{\partial w}{\partial y} + \rho w \frac{\partial w}{\partial z} = -\frac{\partial \hat{p}}{\partial z} + \mu \left[\frac{\partial^2 w}{\partial x^2} + \frac{\partial^2 w}{\partial y^2} + \frac{\partial^2 w}{\partial z^2} \right]$$

The three primary unknowns that can be obtained by solving these equations are (actually there are five scalar unknowns if we count the three velocity components separately)

- ✓ velocity vector

- ✓ pressure
- ✓ temperature

But in the governing equations the following four additional variables solved numerically.

- ✓ Density, ρ
- ✓ Enthalpy, h (or internal energy, e)
- ✓ Viscosity, μ
- ✓ thermal conductivity, k

Pressure and temperature can be treated as two independent thermodynamic variables that define the equilibrium state of the fluid. Four additional variables listed above are determined in terms of pressure and temperature using tables, charts or additional equations. However, for many problems it is possible to consider ρ, μ and k to be constants and h to be proportional to T with the proportionally constant being the specific heat c_p.

In ANSYS FLUENT (CFD) analysis, there are a lot of steps to complete the analysis as shown below:

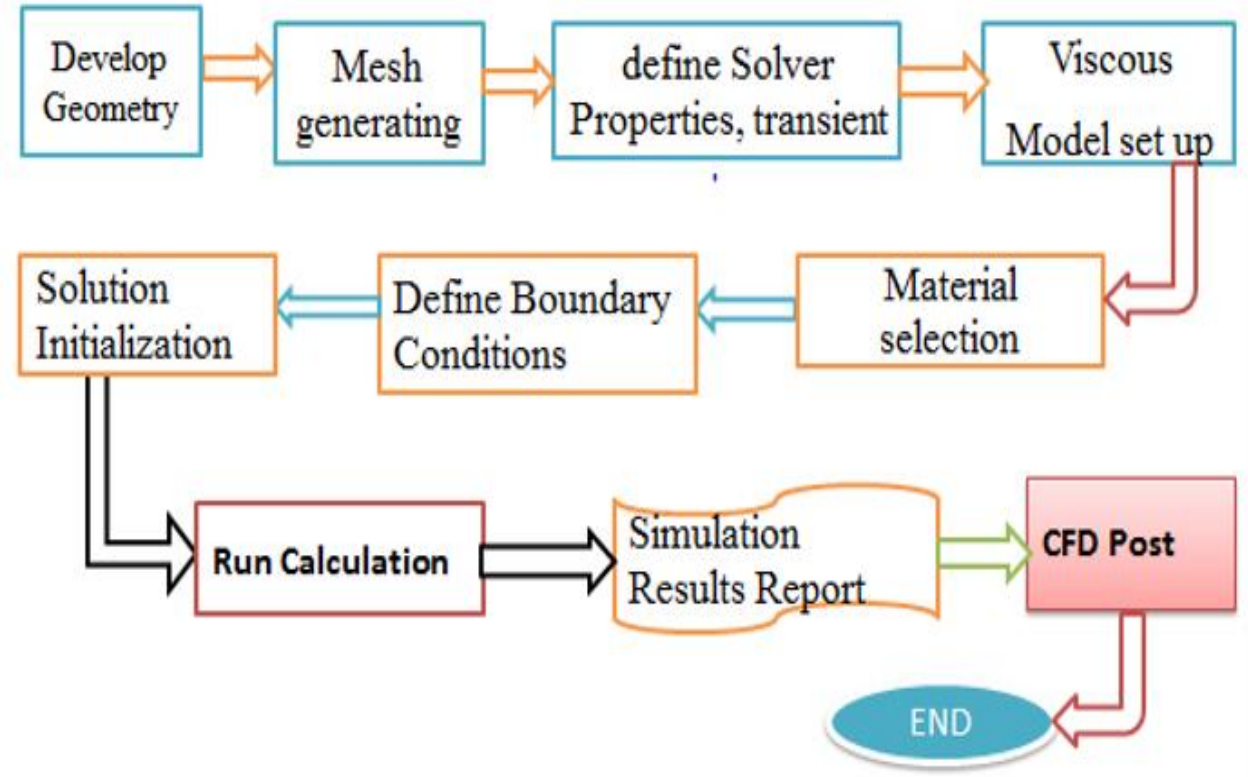

In this main steps, there are also some specific steps which shows detail how ANSYS FLUENT used to analyze and simulate the designed FBD.

a) **Develop Geometry**

In this step the geometry of the FBD is developed based on the dimensions obtained in part design section. So the geometry looks like below:

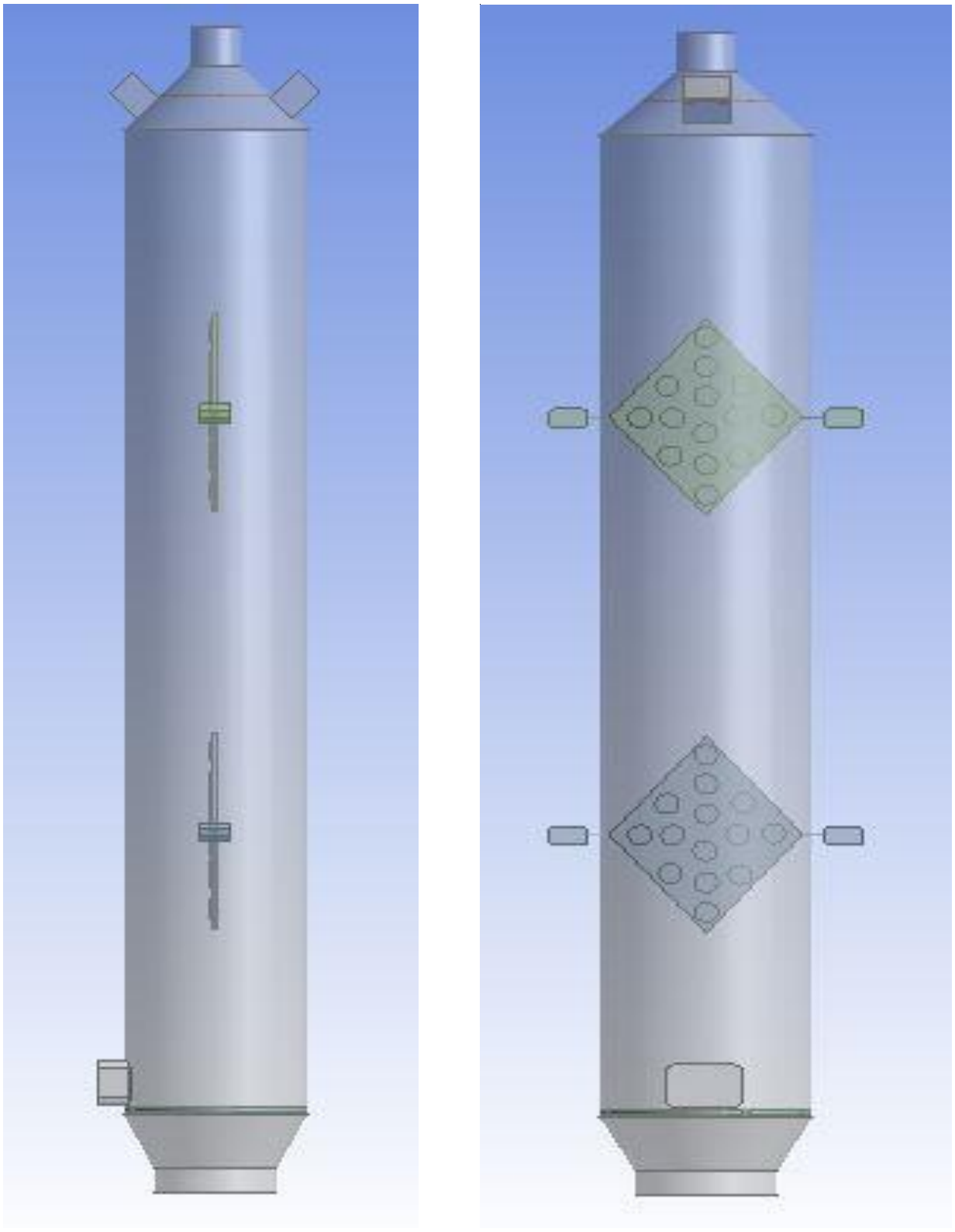

a) Front View b) Side View

Figure 3-13: FBD Geometry

b) Meshing

Mesh is developed like below.

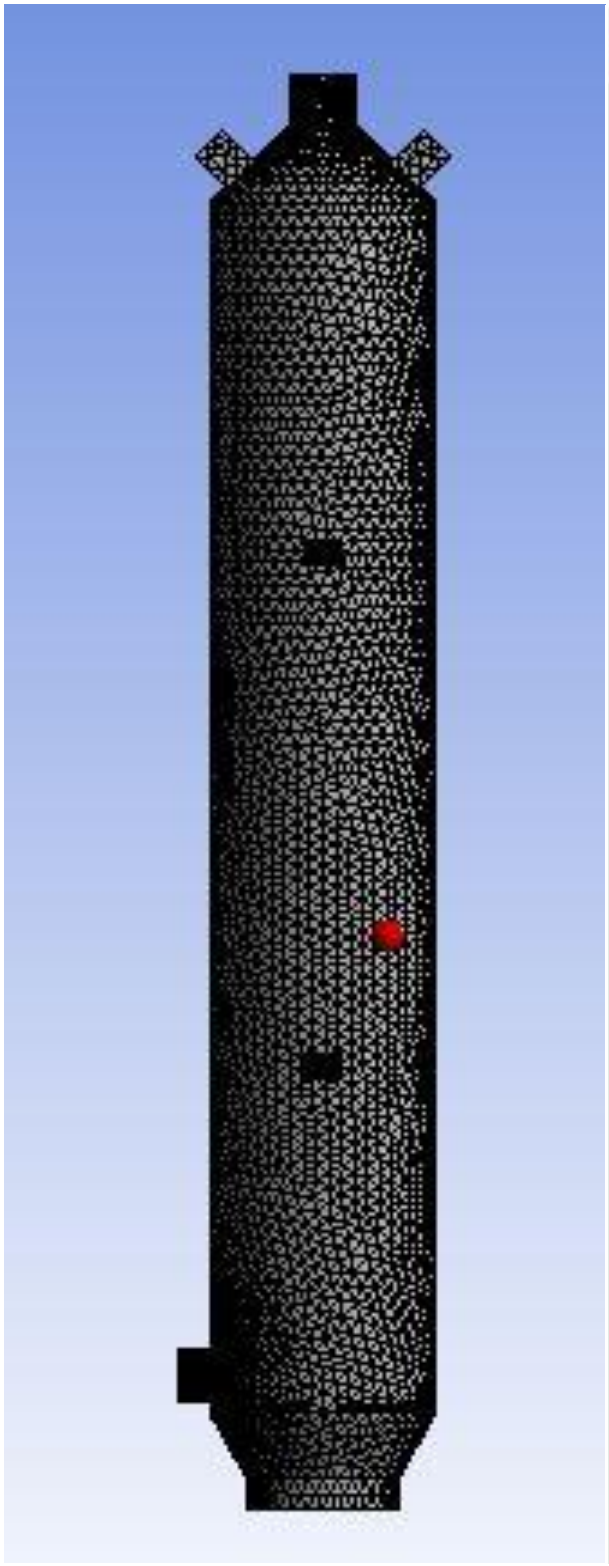

Details of "Mesh"

Defaults	
Physics Preference	CFD
Solver Preference	Fluent
Relevance	100
Sizing	
Use Advanced Size Function	On: Curvature
Relevance Center	Fine
Initial Size Seed	Active Assembly
Smoothing	High
Transition	Slow
Span Angle Center	Fine
Curvature Normal Angle	Default (12.0 °)
Min Size	Default (2.4637e-003 m)
Max Face Size	1.e-002 m
Max Size	1.e-002 m
Growth Rate	Default (1.10)
Minimum Edge Length	8.857e-002 m
Inflation	
Assembly Meshing	
Method	None
Patch Conforming Options	
Triangle Surface Mesher	Program Controlled
Patch Independent Options	
Topology Checking	Yes
Advanced	
Defeaturing	
Statistics	

Figure 3-14: Meshing and Mesh Details

For more detail report of geometry and mesh refer appendix E.

c) Setup

In this step there are different sections:

i) Solution Setup

- The first solution setup is *"**General**"*. For general, *pressure based type* and *transient time solver* is selected with gravity as shown below. The pressure-based solver is applicable for a wide range of flow regimes from low speed incompressible flow to high-speed compressible flow. It requires less memory (storage) and allows flexibility in the solution procedure[44].

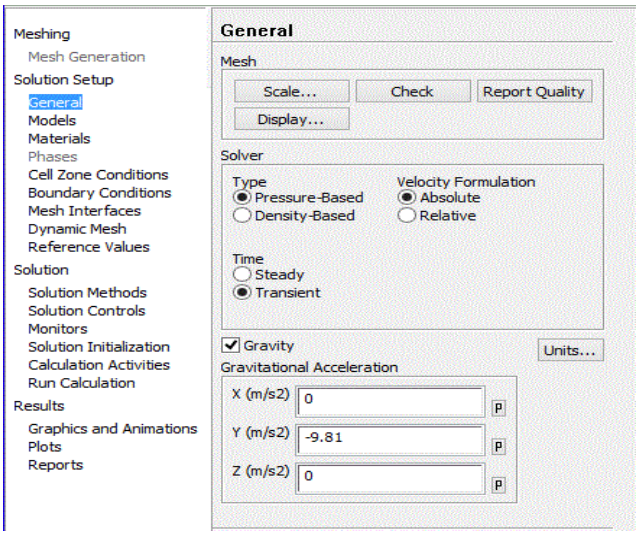

- The second solution setup is *"**Models**"*. Here *energy model* is on and for *viscous model* since the flow is turbulent, *standard k-epsilon equation* is selected. The k-epsilon (k-ϵ) model for turbulence is the most common to simulate the mean flow characteristics for turbulent flow conditions. This is a two equation model which gives a general description of turbulence by means of two transport equations (PDEs). The 2 transported variables are turbulent kinetic energy k, which determine the energy in turbulence, and turbulent dissipation ϵ, which determines the rate of dissipation of the turbulent kinetic energy. The turbulence kinetic energy k, and its rate of dissipation ϵ, are obtained from the following transport equations[44]:

$$\frac{\partial}{\partial t}(\rho k) + \frac{\partial}{\partial x_i}(\rho k u_i) = \frac{\partial}{\partial x_j}\left[\left(\mu + \frac{\mu_t}{\sigma_k}\right)\frac{\partial k}{\partial x_j}\right] + G_k + G_b - \rho\epsilon - Y_M + S_k$$

And

$$\frac{\partial}{\partial t}(\rho\epsilon) + \frac{\partial}{\partial x_i}(\rho\epsilon u_i) = \frac{\partial}{\partial x_j}\left[\left(\mu + \frac{\mu_t}{\sigma_\epsilon}\right)\frac{\partial \epsilon}{\partial x_j}\right] + C_{1\epsilon}\frac{\epsilon}{k}(G_k + C_{3\epsilon}G_b) - C_{2\epsilon}\rho\frac{\epsilon^2}{k} + S_\epsilon$$

In the k–ε turbulence model, the correlation term in the flow velocity variations is represented in a Reynolds' stress term by averaging the values of the Navier–Stokes equation over time under the assumption that a turbulent flow velocity varying in time can be divided into a time average flow velocity and a variant flow velocity. Each equation follows the laws of conservation of mass and momentum, suitable for analyzing the effect of turbulence on each boundary surface in an arbitrary inspection volume set to analyze the flow.

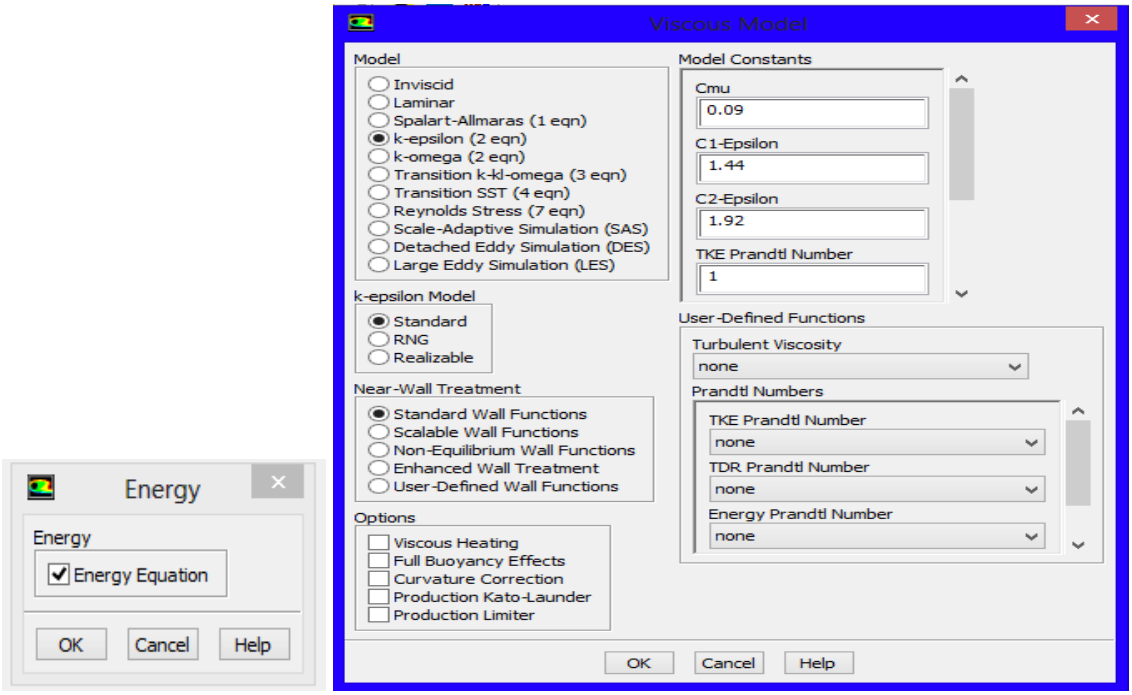

- The third solution setup is *"**Materials**"*. Here for materials bagasse and flue gas are used as working medium while steel is selected for FBD wall.

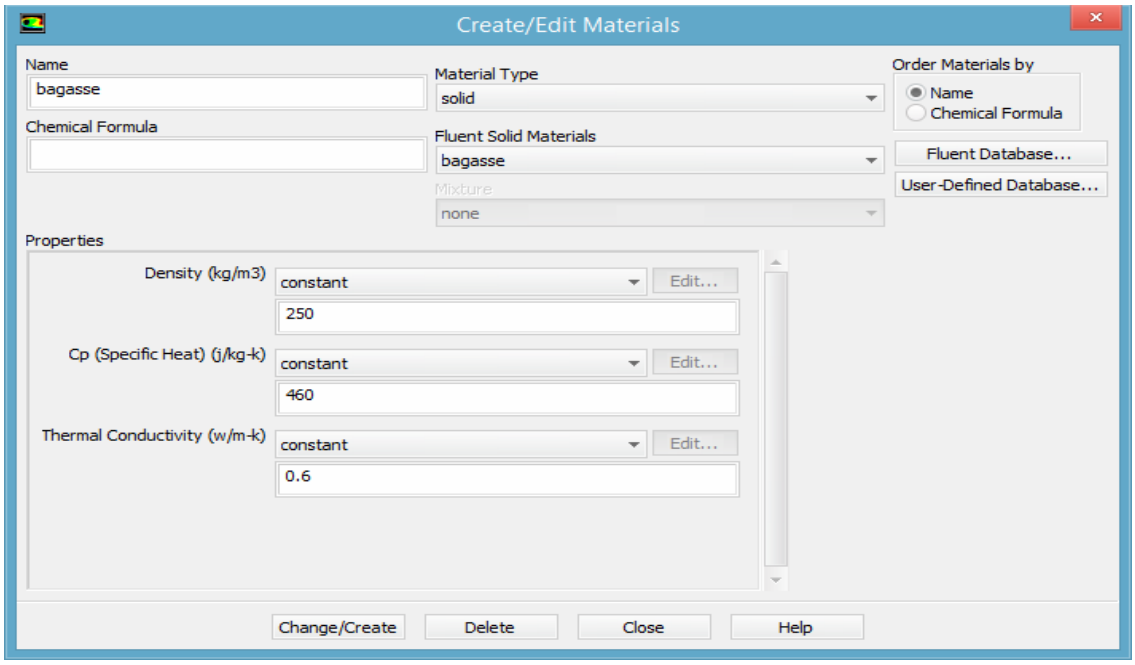

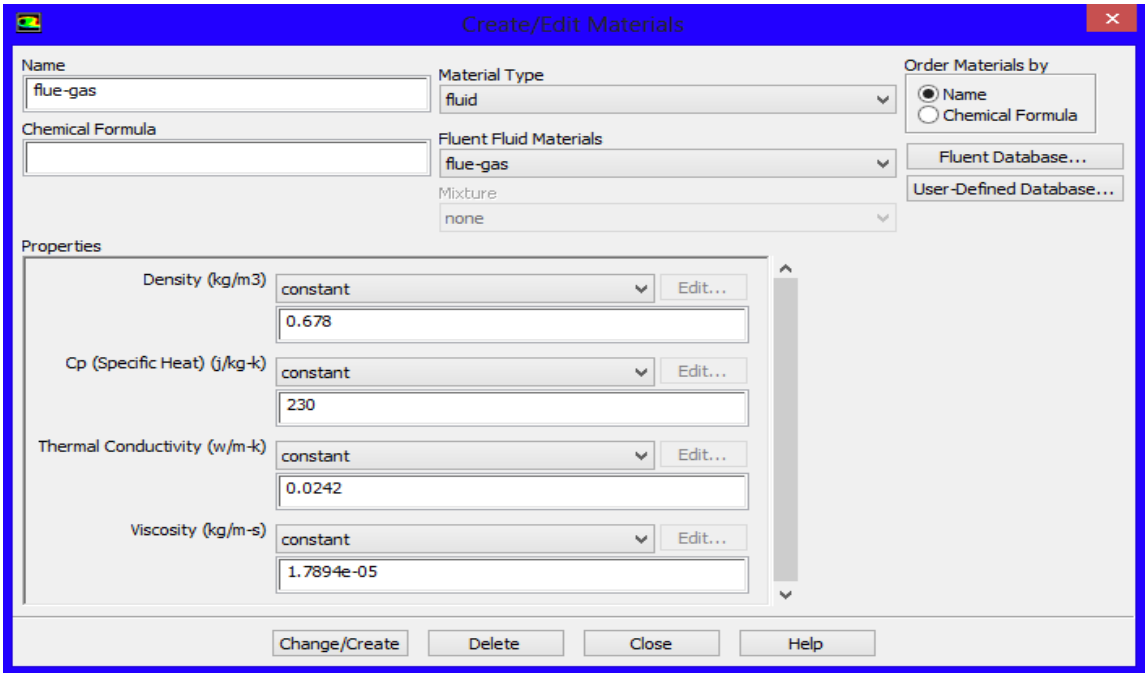

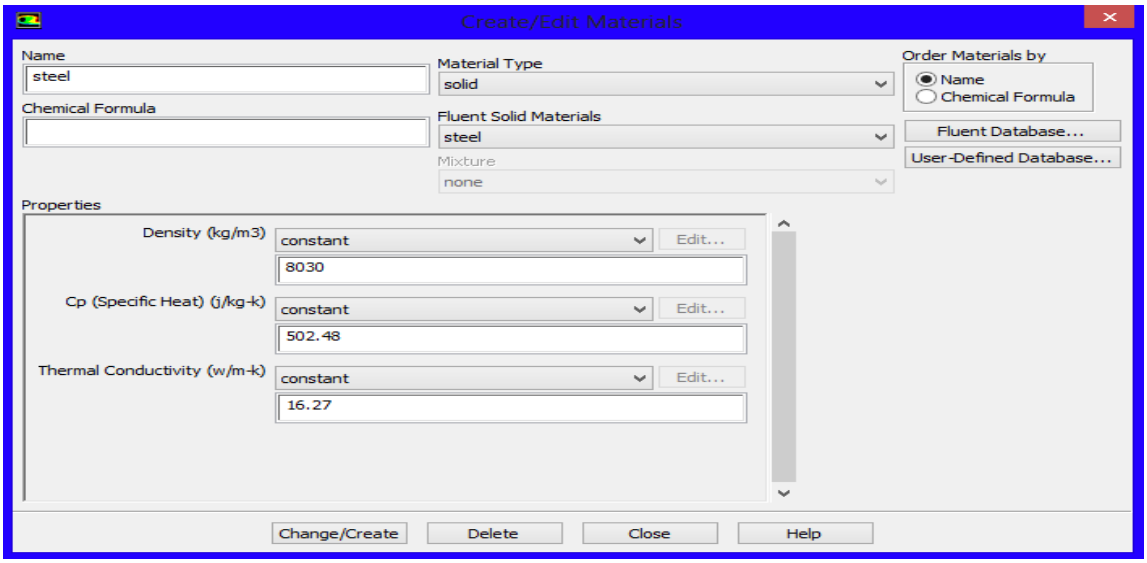

- The fourth solution setup is *"**Cell Zone Conditions**"*. Here zone name is given and material is selected for the zone.

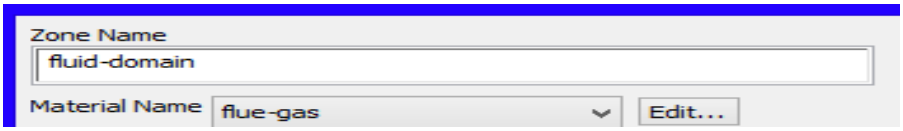

- The fifth solution setup is *"**Boundary Conditions**"*. For boundary condition here there are five zones: *bagasse inlet, flue gas inlet, bagasse outlet, flue gas and vapor outlet* and *wall-solid.*

➢ For **bagasse inlet**, *Mass-Flow Inlet* type boundary condition is selected and mass flow rate 15.43 kg/s and temperature 308K is filled.

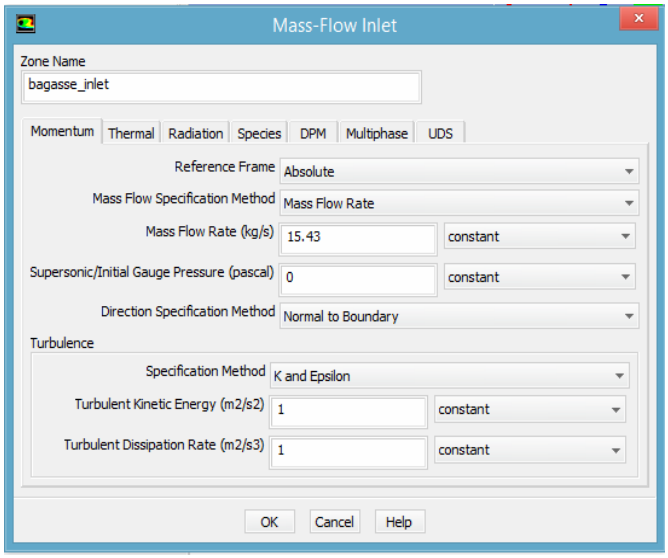

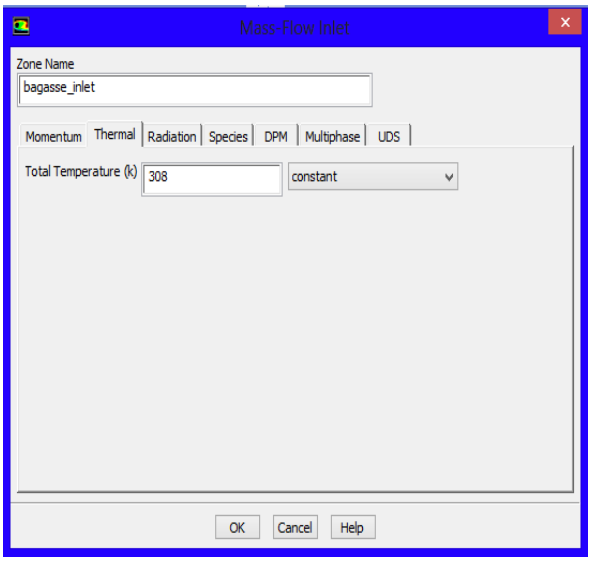

- For **flue gas inlet**, *Velocity inlet* type boundary condition is selected and velocity of flue gas 7.75m/s and temperature 543K is filled.

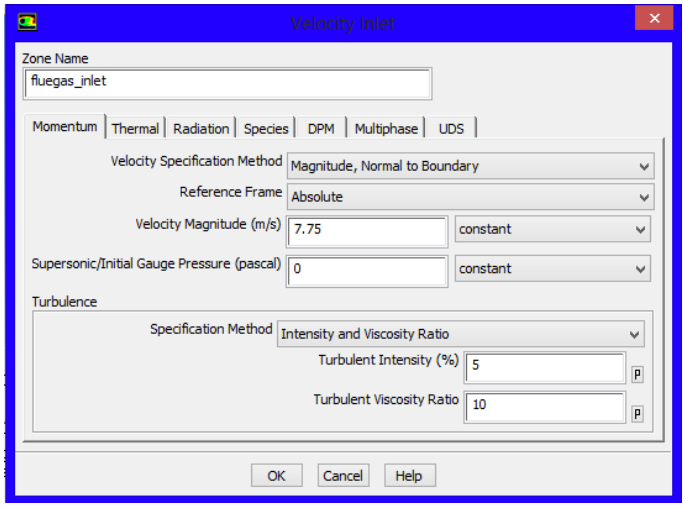

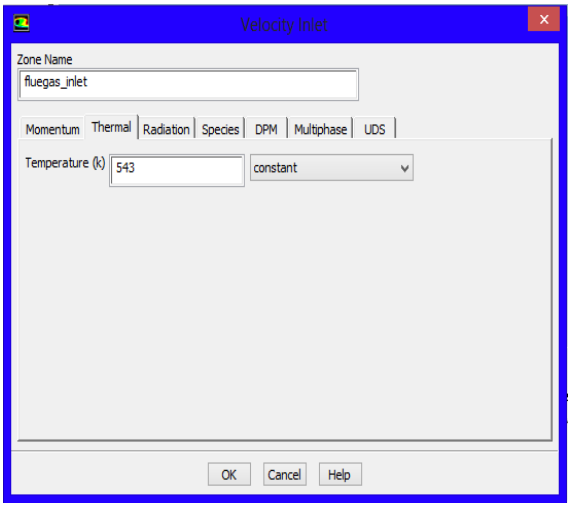

- For **bagasse outlet**, *Pressure Outlet* type boundary condition is selected.

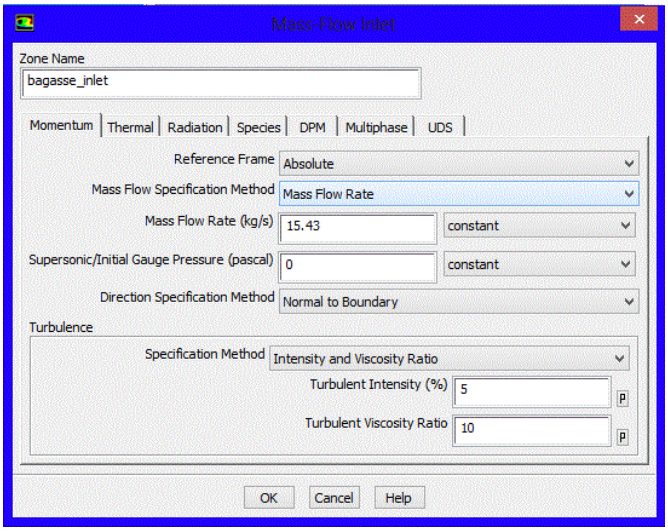

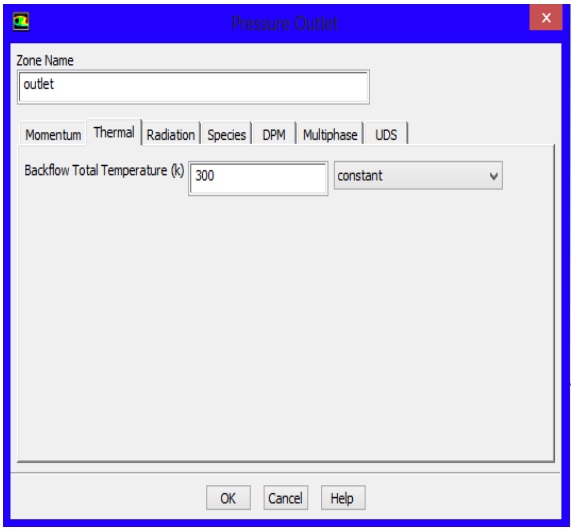

- Also for **flue gas and vapor outlet**, *Pressure Outlet* type boundary condition is selected.

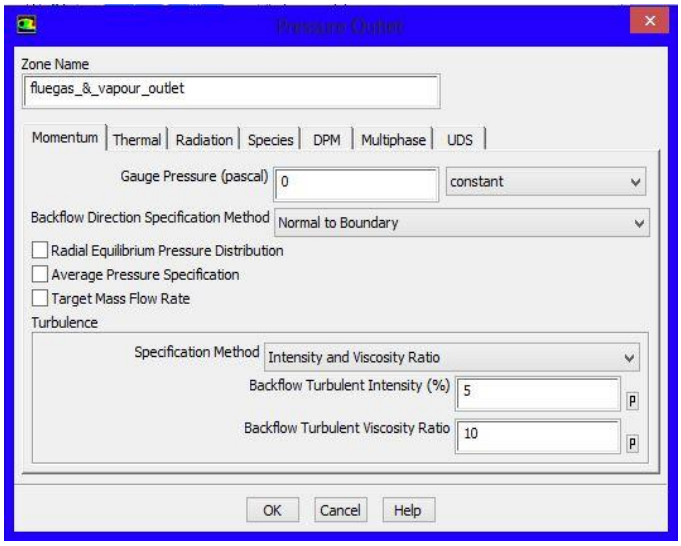

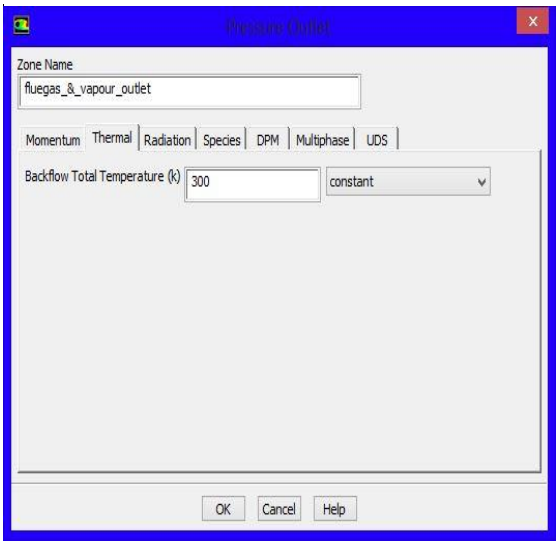

- For **wall-solid**, *Wall* type boundary condition is selected.

  Wall boundary conditions are used to bound fluid. Wall boundaries can be either stationary or moving. The stationary boundary condition specifies a fixed wall, whereas the moving boundary condition can be used to specify the translational or rotational velocity of the wall, or the velocity components. For this case, since the wall of dryer is fixed, stationary wall is selected as shown below. There are six types of thermal conditions are available at walls. These are heat flux(for a fixed heat flux condition), temperature(to specify the temperature at the wall surface), convection(when heat transfer coefficient and free stream temperature is known), radiation(when external emissivity and external radiation temperature is known), mixed(when the convection and radiation boundary conditions combines) and via system coupling. For this case, temperature boundary condition is selected as shown below.

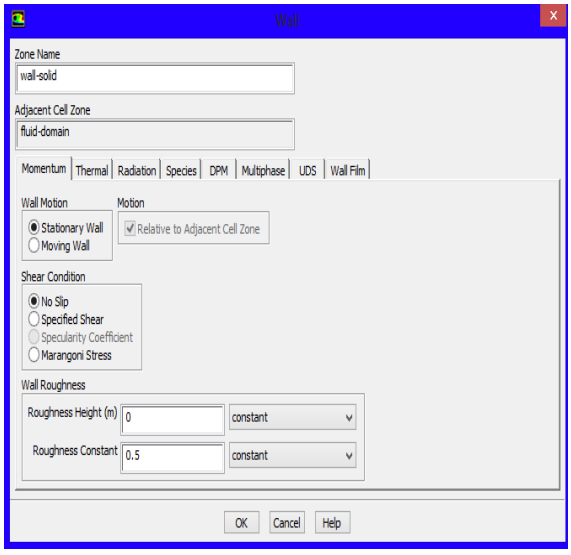

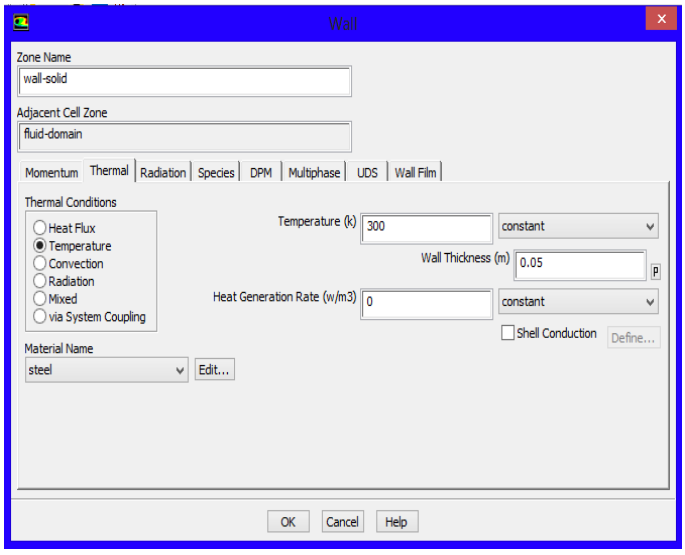

ii) Solution

- Here the solution methods are selected as follow:

  Pressure-velocity coupling refers to the numerical algorithm which uses a combination of continuity and momentum equations to derive an equation for pressure (or pressure correction) when using the pressure-based solver. There are four algorithms are available in FLUENT[44].

  i) Semi-Implicit Method for Pressure-Linked Equations (SIMPLE)
  - The default scheme, robust

  ii) SIMPLE-Consistent (SIMPLEC)
  - Allows faster convergence for simple problems

  iii) Pressure-Implicit with Splitting of Operators (PISO)
  - Useful for unsteady flow problems or for meshes containing cells with higher than average skewness

  iv) Fractional Step Method (FSM) for unsteady flows.
  - Used with the NITA scheme; similar characteristics as PISO.

  The gradients of solution variables at cell centers can be determined using three approaches[44]:

  i) Green-Gauss Cell-Based – The default method; solution may have false diffusion (smearing of the solution fields).

  ii) Green-Gauss Node-Based – More accurate; minimizes false diffusion; recommended for tri/tet meshes.

  iii) Least-Squares Cell-Based – Recommended for polyhedral meshes; has the same accuracy and properties as Node-based Gradients.

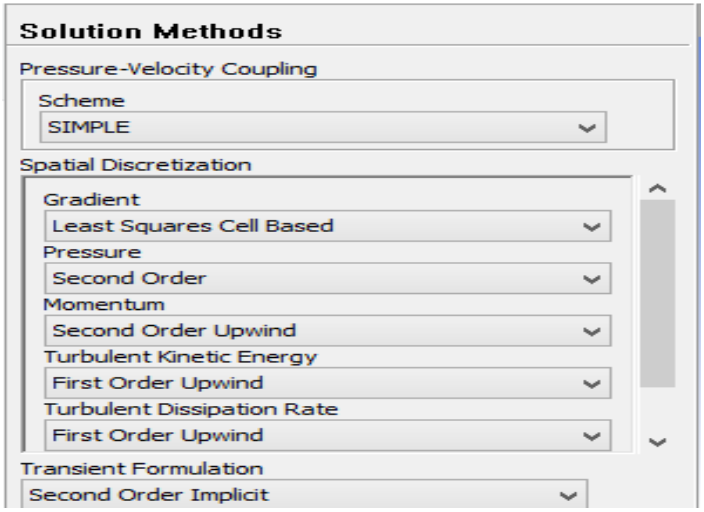

- Solution controls and monitors are taken as default value.

- For solution initialization, *Hybrid Initialization* is selected. Standard initialization allows to specify all the variables directly as initial guesses. Fluent is setup to allow you to easily specify the initial x-velocity, y-velocity, z-velocity, temperature, pressure, etc. all as constant fields over the whole domain. Hybrid initialization is a bit more complex. It uses the boundary conditions and then solves an Euler problem. It uses the solution to this Euler problem as the initial guess. In standard initialization you must provide the initial guess. In hybrid, Fluent guesses them for you.

- Run Calculation is selected as follows:

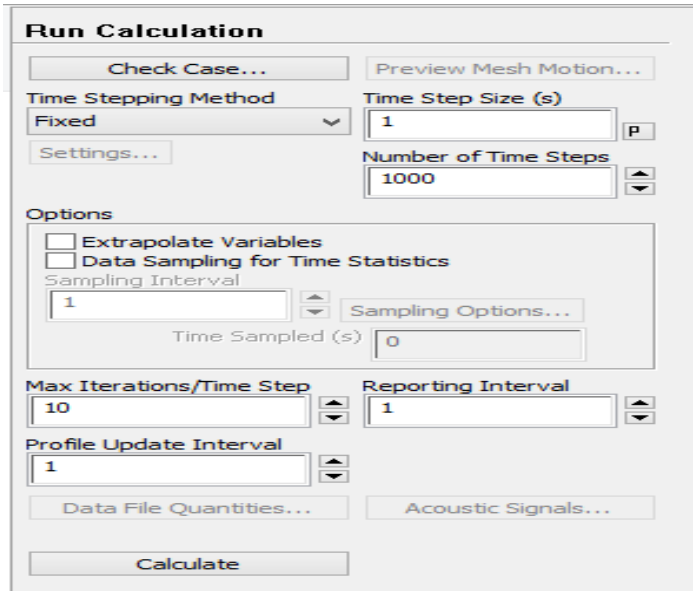

After 10,000 iterations the result which presented in result and discussion chapter is obtained. For more detail information of input summary, refer appendix F.

3.6 Energy Balance of Fluidized Bed Dryer

The fluidized bed drying system is divided into the following subsystems: the feeder(hopper, fan, etc), the heater(flue gas) and the drying column(main chamber). For fluidized bed drying, the most significant subsystems/component is the drying column or chamber. Therefore, the thermal balance is derived by applying mass, energy and entropy balances to the drying column. The drying process in a fluidized bed is modeled by assuming a perfect mixing of particles. The process occurs during an isobaric process due to simultaneous heat and mass transfer between gas and solid. The thermodynamic state of the particle is described by enthalpy (h_m), entropy (s_m), and moisture content (w).

3.6.1 Mass & Energy Balances

The following diagram shows the mass & energy balances of FBD:

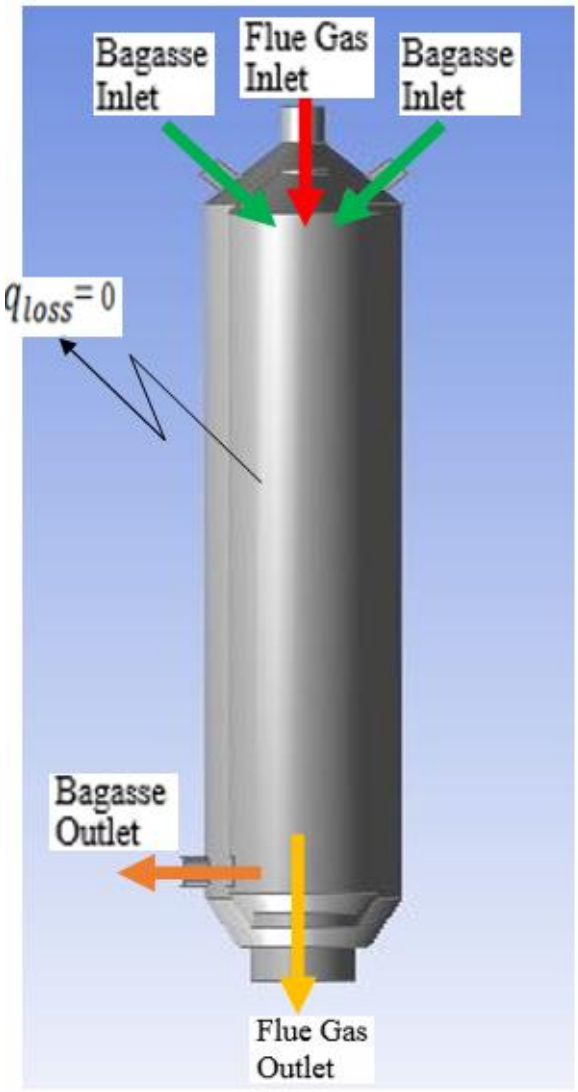

Where:

$\dot{m}_b$ - is mass flow rate of bagasse

T_{bi} - is temperature of bagasse at inlet

w_{bi} - is moisture content of bagasse at inlet

T_{bo} - is temperature of bagasse at outlet

w_{bo} - is moisture content of bagasse at outlet

$\dot{m}_f$ - is mass flow rate of flue gas

T_{fi} - is temperature of flue gas at inlet

W_i - is specific humidity at inlet

T_{fo} - is temperature of flue gas at outlet

W_o - is specific humidity at outlet

q_{loss} - is energy loss from the dryer

Figure 3-15: Energy Balance Diagram

3.6.1.1 Mass Balance

Mass balance depend on the *"Law of Conservation of Mass"* which states that mass is constant through the process. For general case, the mass balance equation is given by[32], [39], [40]:

$$m_{in} - m_{out} = \Delta m_{cv} \quad (54)$$

It can also be expressed in rate form as

$$\frac{dm_{cv}}{dt} = \dot{m}_i - \dot{m}_o \quad (55)$$

Where $\dot{m}_i$ and $\dot{m}_o$ denote, respectively, the rate of mass at inlet and exit of the dryer.

The mass balance equation for above diagram (Fig. 3-15) can be written as follows:

$$\dot{m}_{fo} W_o + \dot{m}_{bi}\ w_{bi} = \dot{m}_{fi}\ W_i + \dot{m}_{bo}\ w_{bo} \quad (56)$$

3.6.1.2 Energy Balance

Energy balance depend on the *"Law of Conservation of Energy"* which states that energy is neither created nor destroyed unless it changed from one form to another form. The energy balance for any system undergoing any process can be expressed as[34], [39]:

$$E_{in} - E_{out} = \Delta E_{system} \quad (57)$$

Or, in the rate form, as

$$\dot{E}_{in} - \dot{E}_{out} = \frac{dE_{system}}{dt} \quad (58)$$

The energy balance equation for above diagram (Fig. 3-24) can be written as follows:

$$\dot{m}_f H_{fo} + \dot{m}_b H_{bi} = \dot{m}_f H_{fi} + \dot{m}_b H_{bo} + q_{loss} \quad (59)$$

Or

$$\dot{m}_b C_{pb} (T_{b,out} - T_{b,in}) = \dot{m}_f C_{pf} (T_{f,in} - T_{f,out}) + q_{loss} \quad (60)$$

Thus;

- H_{fo} & H_{fi} - are thermal energy of flue gas at outlet & inlet respectively. It is calculated by:

$$H_f = C_{pf} (T_f - T_O) + WH_L \quad (61)$$

Where, C_{pf} - is specific heat of flue gas

H_L - is latent heat of vaporization of water (kJ/kg) at the average temperature of the moist bagasse.

- H_{bi} & H_{bo} -are thermal energy of bagasse at inlet & outlet respectively. It is calculated by:

$$H_b = C_{Pb} (T_b - T_o) + wC_{Pw} (T_b - T_o) \quad (62$$

Where, C_{Pb} - is specific heat of bagasse,

C_{Pw} - is specific heat of water &

T_o - is a reference temperature & its value is assumed to be 0^oC.

From equation 62:

$H_{bi} = C_{Pb} (T_{bi} - T_o) + wC_{Pw} (T_{bi} - T_o)$

$= 0.46kJ/kg.K(308K – 273K) + 0.52(4.186kJ/kg.K)(308K – 273K)$

$= 92.28kJ/kg$

$$H_{bO} = C_{Pb}(T_{bo} - T_o) + wC_{Pw}(T_{bo} - T_o)$$

$$= 0.46kJ/kg.K(340.23K-273K) + 0.52(4.186kJ/kg.K)(340.23K-273K)$$

$$= 177.27kJ/kg$$

Hence, the thermal energy of bagasse is increased by 85 kJ/kg from 92.28kJ/kg to 177.27kJ/kg.

The change in the total energy of a system during a process is the sum of the changes in its internal, kinetic, and potential energies and can be expressed as[32]:

$$\Delta E = \Delta U + \Delta KE + \Delta PE \quad (63)$$

Where $\Delta U = m(u_2 - u_1)$

$\Delta KE = \frac{1}{2}m(v_2^2 - v_1^2)$

$\Delta PE = mg(z_2 - z_1)$

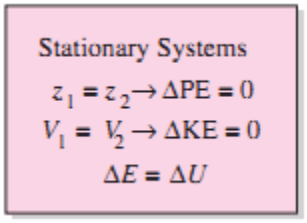

Figure 3-16: Stationary Systems

Most systems encountered in practice are stationary, that is, they do not involve any changes in their velocity or elevation during a process (Fig.21). Thus, for stationary systems, the changes in kinetic and potential energies are zero (that is, $\Delta KE = \Delta PE = 0$), and the total energy change relation in Eq. 28 reduces to $\Delta E = \Delta U$ for such systems. Therefore, since the bagasse dryer is stationary all kinetic and potential energy effects can be ignored during energy analysis. Mass and energy are conserved quantities, but entropy is never conserved. To account for these entropy transfers, the entropy balance has to be performed.

3.6.2 Entropy and Exergy Balances

3.6.2.1 Entropy Balance

Entropy can be viewed as a measure of molecular disorder or disorganization, or molecular randomness in a system. As a system becomes more disordered, the positions of the molecules become less predictable and the entropy increases. Thus, it is not surprising that the entropy of a substance is lowest in the solid phase and highest in the gas phase[32].

The entropy balance for the drying column becomes[32], [39], [40]:

Entropy change = entropy transfer + entropy generation

$$\Delta S = \int_1^2 \frac{\delta Q}{T} + S_{gen} \quad (64)$$

Where Q - is heat transfer, T - is temperature & S_{gen} - is the entropy generation in the dryer column,

$$S_{gen} = (S_2 - S_1) - \int_1^2 \frac{\delta Q}{T} \geq 0 \quad (65)$$

Where,

$$S_2 - S_1 = \int_1^2 c(T)\frac{dT}{T} \cong c_{avg} \ln \frac{T_2}{T_1} \ \text{(kJ/kg.K)} \quad (66)$$

Where c_{avg} - is the average specific heat of the bagasse over the given temperature interval.

Hence, entropy change is:

$$\Delta S = c_{avg} \ln \frac{T_2}{T_1} \ \text{(kJ/kg.K)}$$

$$= 0.46\text{kJ/kgK}(\ln \frac{340.23}{308})$$

$$= 0.046 \text{ kJ/kgK}$$

Entropy generation is a measure of the magnitudes of the irreversibilities present during that process. The greater the extent of irreversibilities, the greater the entropy generation. Therefore, entropy generation can be used as a quantitative measure of irreversibilities associated with a process & also serves as a criterion in determining whether a process is reversible, irreversible, or impossible[32]. Thus;

$$S_{gen} \begin{cases} > 0 \ \text{Irreversible process} \\ = 0 \ \text{Reversible process} \\ < 0 \ \textit{Impossible proces} \end{cases}$$

3.6.2.2 Exergy Balance

The property exergy is the work potential of a system in a specified environment and represents the maximum amount of useful work that can be obtained as the system is brought to equilibrium with the environment.

The exergy balance for the drying column is given by:

$$\dot{E}_{b2} - \dot{E}_{b1} = \dot{E}_{dfg1} - \dot{E}_{dfg2} + \dot{E}_{evap} \quad (67)$$

$\dot{E}_b$ and $\dot{E}_{dfg}$ are the exergy transfer rate of the bagasse and drying flue gas, respectively; $\dot{E}_{evap}$ is the exergy evaporation rate. The specific exergies at inlets (e_{b1}) and outlets (e_{b2}) of the bagasse are given by:

$$e_{b1} = (h_{b1} - h_0) - T_0(S_{b1} - S_0) \quad (68)$$

$$e_{b2} = (h_{b2} - h_0) - T_0(S_{b2} - S_0) \quad (69)$$

The specific exergies associated with a stream of drying flue gas entering and leaving the column are:

$$e_{dfg1} = (h_1 - h_0) - T_0(s_1 - S_0) \quad (70)$$

$$e_{dfg2} = (h_2 - h_0) - T_0(S_2 - S_0) \quad (71)$$

where e_{dfg1} and e_{dfg2} are the specific exergy transfers of flue gas at inlets and outlets, respectively; h_o, S_o denote the specific enthalpy and specific entropy at the temperature of dead state T_o (temperature at thermodynamic equilibrium with the environment which values is 25°C. At the dead state, a system is at the temperature and pressure of its environment (in thermal and mechanical equilibrium); it has no kinetic or potential energy relative to the environment (zero velocity and zero elevation above a reference level); and it does not react with the environment (chemically inert). The dead-state temperature and pressure are taken to be T_0= 25°C (77°F) and P_0= 1 atm (101.325kPa or 14.7psia))[32] respectively; h_1 and S_1 denote the specific enthalpy and the specific entropy at the temperature of drying air entering the column (T_{da1}); h_2 and S_2 denote the specific enthalpy and the specific entropy of drying air at the temperature of the drying air exiting the column, respectively.

From equation (68 – 71), the specific exergies of bagasse and drying flue gas are:

$$e_{b1} = (146.68 - 104.89) - 298(0.5053 - 0.3674)$$

= 0.696 kJ/kg

$$e_{b2} = (280.45 - 104.89) - 298(0.91819 - 0.3674)$$

= 11.42 kJ/kg

$$e_{dfg1} = (549.54 - 297.68) - 298(2.308575 - 1.69359)$$

= 68.59 kJ/kg

$$e_{dfg2} = (533.98 - 297.68) - 298(2.27967 - 1.69359)$$

= 61.65 kJ/kg

The value of h and s can be taken from steam table.

From exergy balance for the drying column(equation 67), $\dot{E}_{evap}$ is:

$$\dot{E}_{evap} = \dot{E}_{b2} - \dot{E}_{b1} - \dot{E}_{dfg1} + \dot{E}_{dfg2}$$

= 11.42 kJ/kg - 0.696 kJ/kg - 68.59 kJ/kg + 61.65 kJ/kg

= 3.78 kJ/kg

3.7 Efficiency of Fluidized Bed Dryer

The potential for using fluidized bed dryers is strongly dependent on an efficient use of energy. In this section, two methods to determine the efficiency of fluidized bed drying are described. These are energy efficiency based on the First Law of Thermodynamics and exergy efficiency based on the First Law and the Second Law of Thermodynamics.

3.7.1 Energy efficiency

Energy efficiency of the dryer chamber based on the First Law of Thermodynamics can be derived by using the energy balance equation. The thermal efficiency of the drying process can be defined as:

$$\eta_{th} = \frac{\text{Energy transmitted to the bagasse}}{\text{Energy incorporated in the drying flue gas}} \tag{72}$$

The thermal efficiency can be expressed in terms of energy efficiency using the energy rate balance equation as[39], [41]:

$$\eta_e = \frac{W_d\,[\,h_{fg}(M_{P1} - M_{P2}) + c_m(T_{m2} - T_{m1})]}{\dot{m}_{da}(h_1 - h_0)\Delta t} \tag{73}$$

where, W_d = Weight of dry material (kg), h_{fg}= Latent heat of vaporization of water (kJ/kg water), M_{P1}= Initial particle moisture content, dry basis (kg water/kg solid), M_{P2}= Final particle moisture content, dry basis (kg water/kg solid), $\dot{m}_{da}$= Mass flow rate of the drying air (kg/s), h_1= Initial specific enthalpy (kJ/kg), h_0= Final specific enthalpy (kJ/kg), Δt = Change in time (sec).

3.7.2 Exergy efficiency

Exergy efficiency of the dryer column based on the First Law and the Second Law of Thermodynamics can be derived using the exergy rate balance equation. The exergy efficiency provides a true measure of the performance of the drying system from the thermodynamic viewpoint. In defining the exergy efficiency it is necessary to identify both the product and the fuel. In this study, the product is the rate of exergy evaporation and the fuel is the rate of exergy drying air entering the dryer column. The exergy efficiency of the dryer is the ratio between product and fuel. Where the product is only the rate of exergy evaporation process and the fuel is the rate of exergy drying air enters the dryer column, the exergy efficiency on the basis of the exergy rate balance is given as[39], [41]:

$$\eta_{ex} = \frac{\dot{E}_{evap}}{\dot{E}_{dfg1}} \tag{74}$$

Where, $\dot{E}_{evap}$= Rate of exergy evaporation (kJ/s), $\dot{E}_{dfg1}$= Exergy of drying flue gas entering the dryer (kJ/s).

From equation 74,

$$\eta_{ex} = \frac{3.78\ \text{kJ/kg}}{68.59\ \text{kJ/kg}}$$

$$= 0.55$$

3.8 Installation of Bagasse Dryer

The Bagasse dryer is installed between the boiler ID fan and the chimney. Most boilers have economizer and air heaters which substantially reduce the flue gas temperatures. Further reduction in the flue gas temperature will require additional heat exchanger in the economizer or air heaters. But passing the flue gas through a bagasse dryer rather than adding heating surface in economizer or air heaters is an effective way of reducing both the bagasse moisture content and the final flue gas exit temperature. There are two bagasse dryer arrangements as shown in figure below:

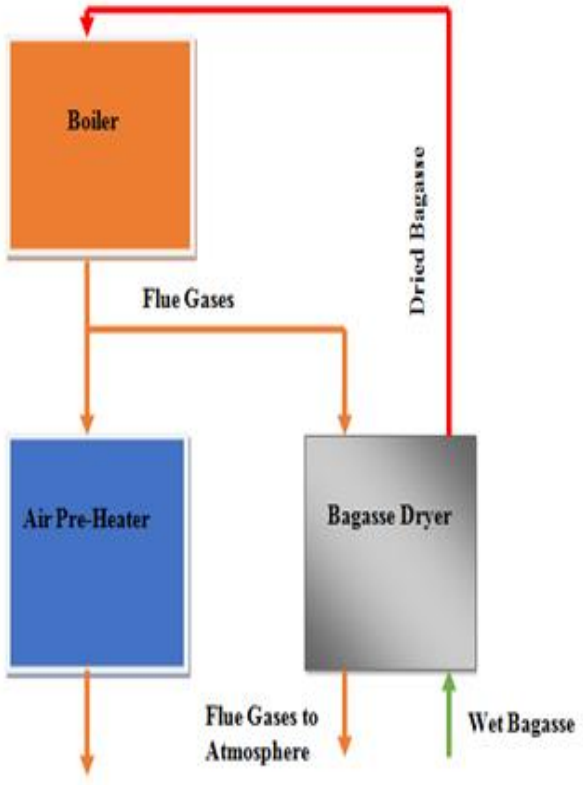

Figure 3-17: Parallel Arrangement

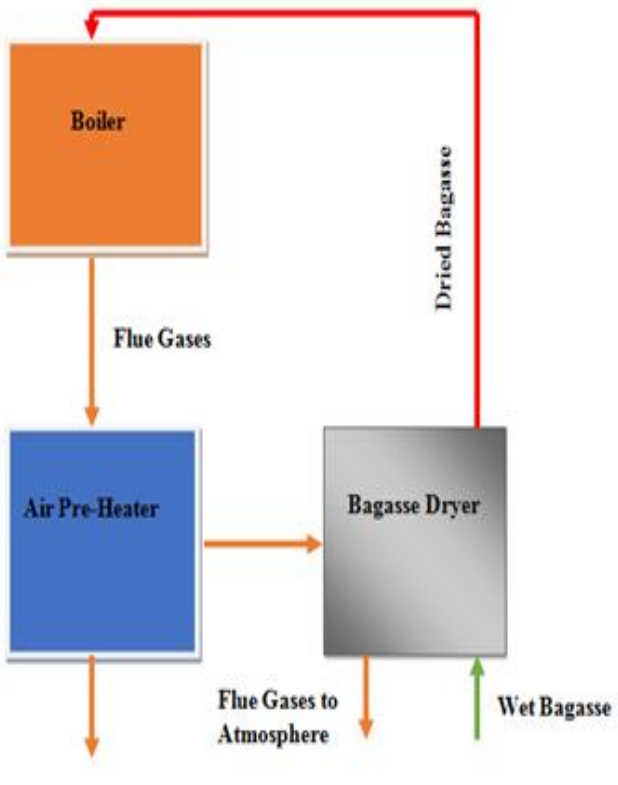

Figure 3-18: Sequence Arrangement

According to ***Ali K. Abdel-Rahman, 2015*** study, if the hot gases are taken after air pre-heater at 220^{o}C, the moisture can be decreased by 10 points. But, if the gases are taken before the air pre-heater which has a temperature of 300^{o}C, the moisture will be decreased by 15 points[3]. Therefore, the parallel arrangement is more preferable than sequence arrangement.

3.9 Determination of Calorific Values and Thermal Efficiency of Boiler

Typically the mill wet bagasse contains around 48% to 52% moisture with a gross calorific value (GCV) of around 2270 Kcal/kg (~9500 kJ/kg)[42] and a sugar content (s) which of the order of 1.5 to 2 % by weight[3]. Higher moisture content in bagasse reduces its GCV and also results in higher energy loss because the fuel moisture carries that latent heat of vaporization up the stack. The GCV and NCV of bagasse can be determined by using equation 1 & 2 Hugot equation[10];

GCV = 4.1839[4,600 - 12s - 46w], in kJ/kg

NCV =4.1839[4,250 - 12s -48.5w], in kJ/kg

Now by using the above formula the relation between moisture content and GCV/NCV when the sugar content of the bagasse is 2%(the sugar content of Wonji/Shoa bagasse) is calculated as shown in Table 3.3 below:

Table 3-3: Relation between Moisture Content and GCV/NCV

Moisture Content (w), %	GCV, kJ/kg	NCV, kJ/kg	% increase of GCV	% increase of NCV
52	9137.6	7129.4	0	0
51	9330.1	7332.3	2.1	2.8
50	9522.5	7535.2	4.2	5.7
49	9715.0	7738.1	6.3	8.5
48	9907.5	7941.0	8.4	11.8
47	10,099.9	8144.0	10.5	14.2
46	10,292.4	8346.9	12.6	17.1
45	10484.8	8549.8	14.7	19.9
44	10677.3	8752.7	16.8	22.8
43	10869.8	8955.6	18.9	25.6
42	11062.2	9158.6	21.1	28.5
41	11254.7	9361.5	23.2	31.3
40	11447.2	9564.4	25.3	34.2

As the above calculation indicates, the bagasse drying process increases the gross calorific value (GCV) and net calorific values (NCV) of bagasse with the respective decrease in moisture content. NCV is increased by 2.8 % for a one percent drop in moisture content.

Study shows that 1% reduction of moisture in bagasse increases its calorific value by 196kJ/kg (47 Kcal/kg) and also 1% reduction of moisture in bagasse increases boiler efficiency by 0.5% if it is used as a fuel in boiler[31]. But the above calculation show that 1% reduction of moisture in bagasse increases its calorific value by 192.5kJ/kg. This little deviation is due to round off or some minor calculation error. Graphically, the relation looks like below:

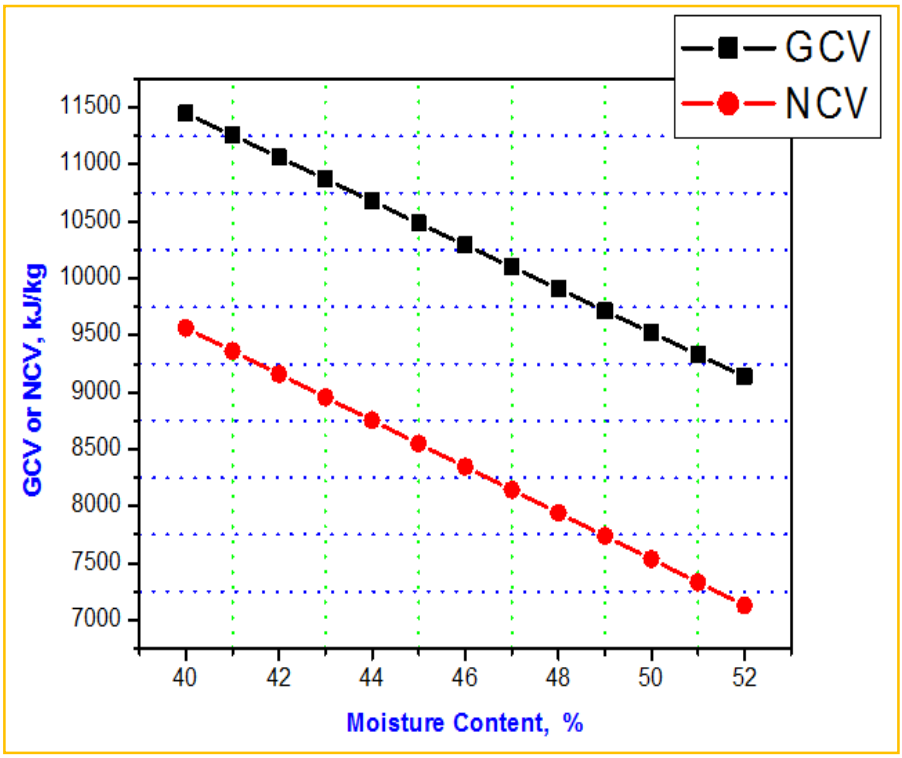

Figure 3-19: Relation between moisture content and calorific values (GCV and NCV)

It can be clearly seen from the graph that, both GCV and NCV are increased with the moisture content decreased.

The table given below shows the relation between moisture content and boiler efficiency.

Table 3-4: Relation between Moisture Content and Thermal Efficiency of Boiler[10]

Moisture Content (w), %	Thermal Efficiency of Boiler (η), %
52	70
51	70.5
50	71
49	71.5
48	72
47	72.5

46	73
45	73.5
44	74
43	74.5
42	75
41	75.5
40	76

As bagasse moisture decreases, boiler efficiency will increase. They are inversely proportional. Therefore, when the bagasse moisture is reduced from 52% to 40.68% the thermal efficiency of boiler is increased by 5.66%.

3.10 Bill of Materials

The quantities and price of material needed for this work are summarized in Table 9 below: The source of this material cost is based on Alibaba and Amazon.com.

Table 3-5: Bill of Materials

S/n	Materials	Specifications	Quantity	Rate	Cost(Birr)
1	Gray Cast Iron	G18 4.2m x 20m x 0.02m	1	1,036,200	1,036,200
2	Sheet Metal	Galvanized Sheet Metal	2	4846.59	9,693.18
3	Forced Draft Fan		1	2237	2237
4	Induced Draft Fan		1	2237	2237
5	AC Electric Motor	Single Phase, 220V	2	5592	11,184
6	Fan Motor	AC Single Phase, 220V	2	419.4	838.8
7	Conveyor Belt	PVC Coated	2	41,940	83,880
8	Steel Tube	Galvanized Round Tube 0.525m x 4m	1	989.1	989.1
9	Bearing	Ball Bearing	4	100	400
10	Bolts and Nuts	Carbon Steel Hex Head	20	30	600
11	Metal Distributor	Circular Galvanized Sheet Metal 2mm Thick	1	1161.52	1,161.52
12	Metal Filter Plate	Circular Galvanized Sheet Metal 2mm Thick	1	912.26	912.26
13	Paints	Metal Paints	1 Gallon	350	700
14	Manufacturing and Installation Cost				30,000
15	Miscellaneous				10,000
Total					1,191,032.86

Adding 10% contingency to the total cost give the total design cost to be 1,310,136.146 ETB.

Adding 25% margin to the total design cost, the machine can be sold at a price of 1,637,670.18 ETB.

3.11 Benefit Expected After Bagasse Dryer Installation

Net Calorific Value (NCV) of bagasse at 52% moisture = 7129.4kJ/kg (1704kcal/kg)(refer table 3-3), NCV of bagasse at 41% moisture = 9361.5kJ/kg (2237.4kcal/kg). Energy available at 52% moisture of bagasse of 55.55Ton Per Hour (TPH) = 94,657,200kcal/hr, Energy available at 41% moisture of bagasse of 55.55TPH = 124,287,570kcal/hr.

Excess energy available after drying = 124,287,570 - 94,657,200= 29,630,370kcal/hr, Unit of power that can be produced by that excess energy, 1 kcal/hr = 0.001163KW.hr, Thus 29,630,370kcal/hr = 34,460 kWh. Power consumption by dryer is 7.5 kWh, Net extra power available = 34,460 - 7.5 = 34452.5 kWh.

The present electricity tariff in Ethiopia is 0.018$ or 0.504ETB per kWh. So the factory get extra revenue of 34452.5kWh x 0.504ETB = 17,364ETB per day. So the factory can pay back the cost within $\frac{1,637,670.18}{17,364}$ = 94.31days or 3.14 months.

CHAPTER FOUR: RESULT AND DISCUSION

4.1 Analytical Design Result

In this study, a FBD was designed to reduce the moisture content of bagasse to achieve the research objectives mentioned in chapter one and the following dimensional values tabulated in table 4-1 are obtained from analytical designs for FBD based on raw data collected from Wonji/Shoa sugar factory.

Table 4-1: Dimensions obtained for FBD

Parameters	Dimensions Obtained
Main/Drying Chamber Height	20m
Main/Drying Chamber Diameter	4.2m
Distributor/Grid Diameter	3.15m
Number of Holes on Distributor	15872
Distributor/Grid Hole Diameter	25mm
Thickness of Distributor/Grid	37.5mm
Length of Agitator	4.5m
Width of Agitator	4.15m
Upper Hopper Height	1.84m
Larger Diameter of Upper Hopper	4.2m
Smaller Diameter of Upper Hopper	0.525m
Lower Hopper Height	1.05m
Larger Diameter of Lower Hopper	4.2m
Smaller Diameter of Lower Hopper	2.1m
Filter Diameter	4.2m
Filter Thickness	37.5mm

Additionally, from the thermal analysis done on the FBD, the temperature of bagasse and flue gas at the inlet of this dryer were 308K and 543K respectively. After drying process, the analytical analysis or design results indicates that the temperature of bagasse at FBD outlet is increased to 340.23K by losing the moisture content of the bagasse.

4.2 ANSYS Fluent Analysis Result

The following snapshots indicate the post-process of ANSYS Fluent analysis result

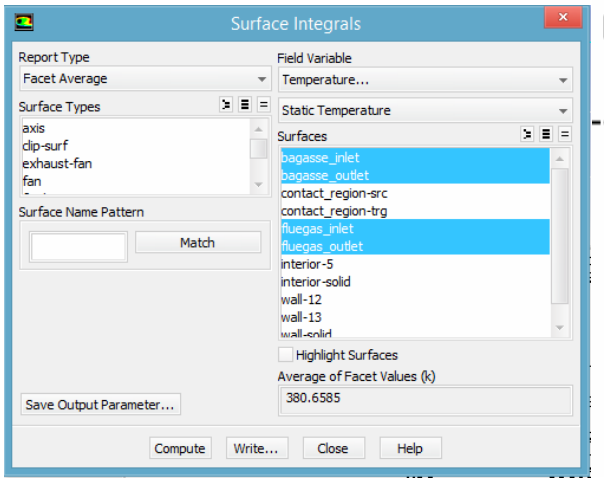

Average of Facet Values

Static Temperature	(k)
bagasse_inlet	308
bagasse_outlet	338.30878
fluegas_inlet	543
fluegas_outlet	354.09372
Net	380.65848

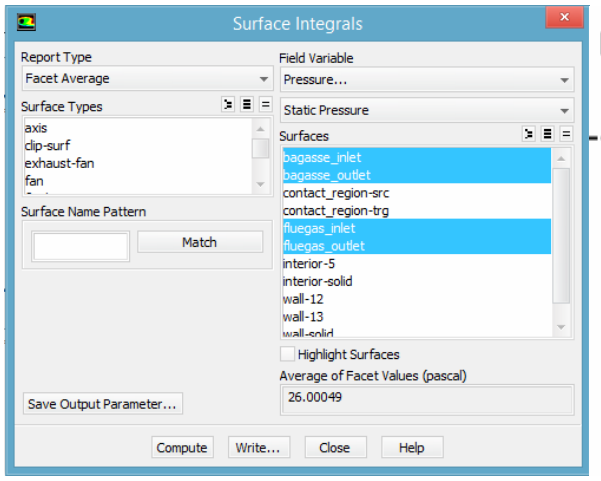

Average of Facet Values

Static Pressure	(pascal)
bagasse_inlet	111.71786
bagasse_outlet	-0.05242011
fluegas_inlet	104.79855
fluegas_outlet	0
Net	26.000492

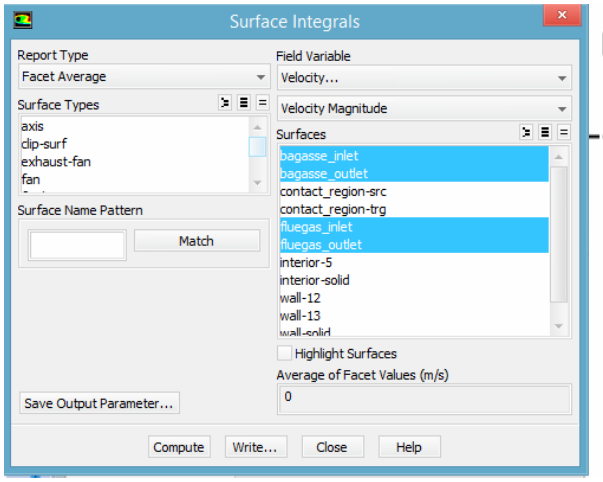

Average of Facet Values

Velocity Magnitude	(m/s)
bagasse_inlet	23.706367
bagasse_outlet	5.6739435
fluegas_inlet	7.75
fluegas_outlet	5.2005215
Net	6.8753319

Figure 4-1: CFD Post Results

The snapshot of simulation result is shown as follows:

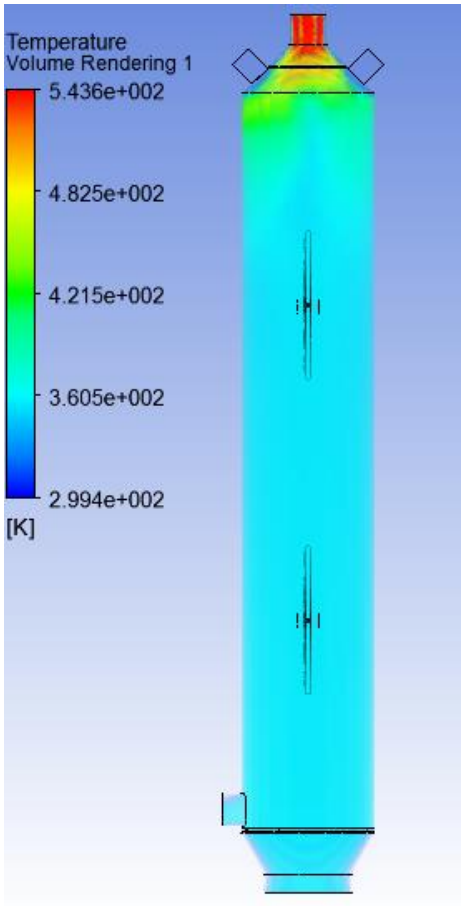
Temperature
Volume Rendering 1
5.436e+002
4.825e+002
4.215e+002
3.605e+002
2.994e+002
[K]

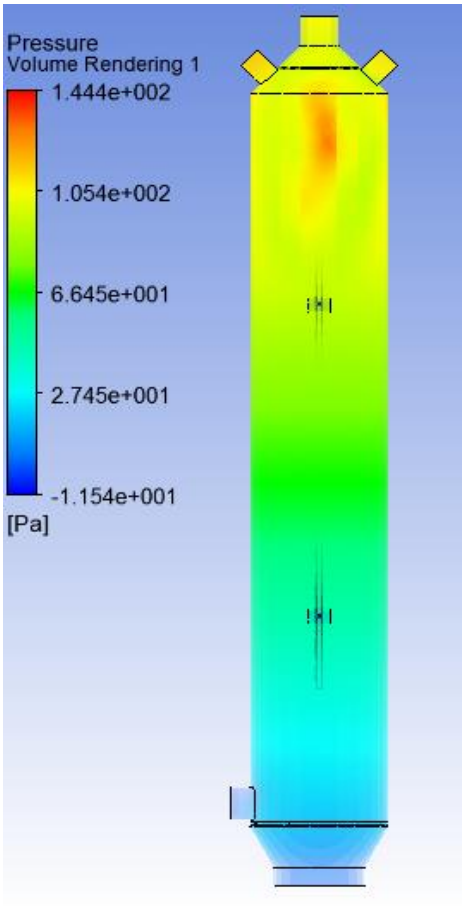
Pressure
Volume Rendering 1
1.444e+002
1.054e+002
6.645e+001
2.745e+001
-1.154e+001
[Pa]

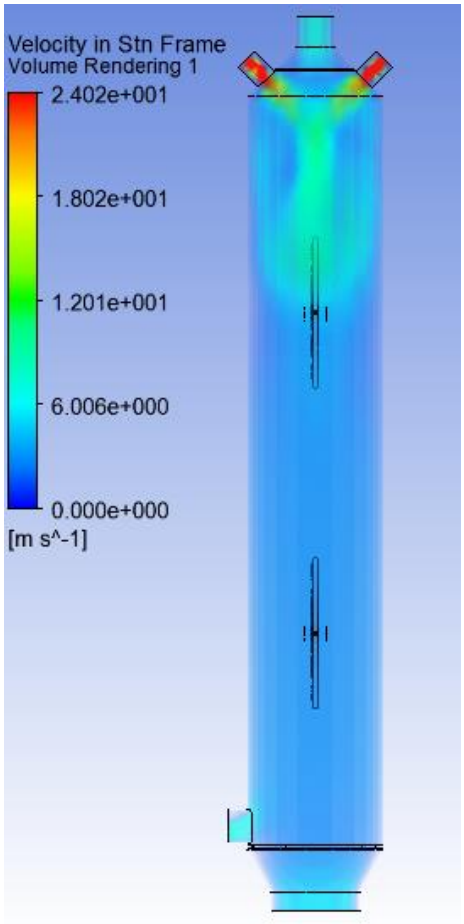
Velocity in Stn Frame
Volume Rendering 1
2.402e+001
1.802e+001
1.201e+001
6.006e+000
0.000e+000
[m s^-1]

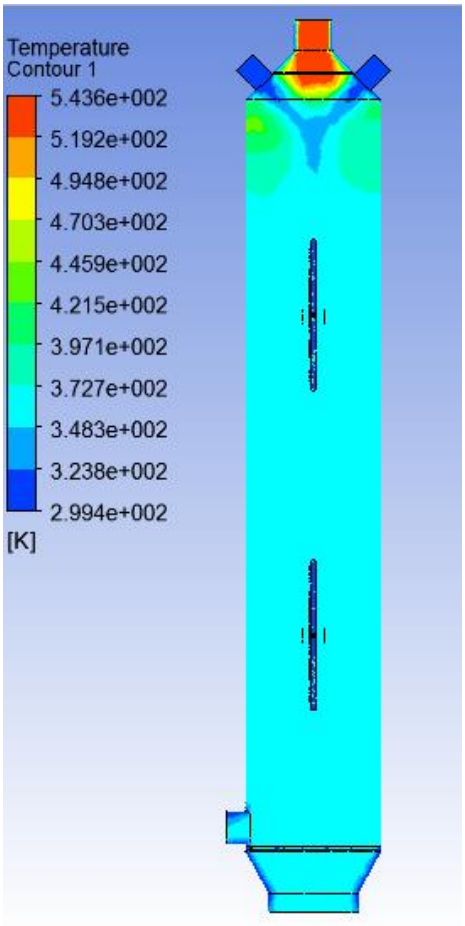
Temperature
Contour 1
5.436e+002
5.192e+002
4.948e+002
4.703e+002
4.459e+002
4.215e+002
3.971e+002
3.727e+002
3.483e+002
3.238e+002
2.994e+002
[K]

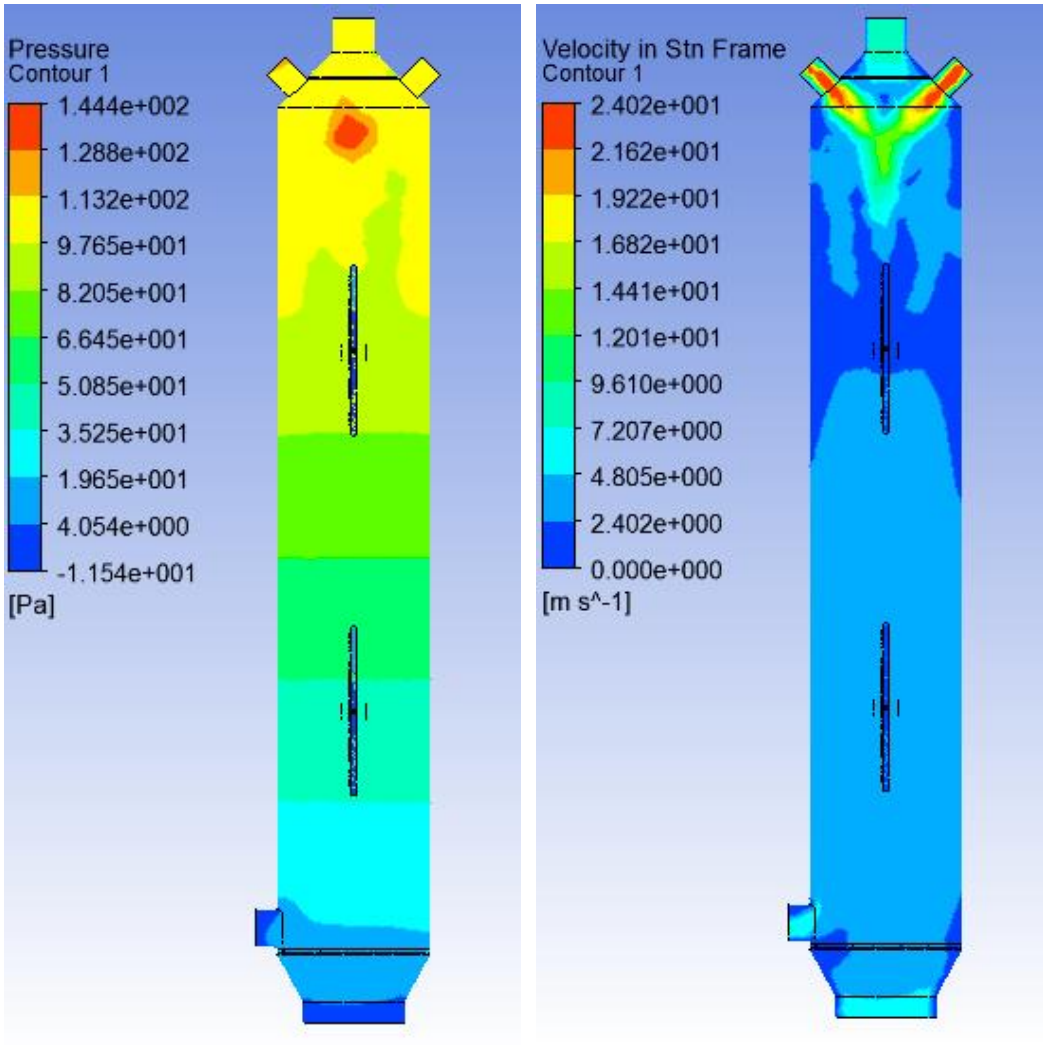

Figure 4-2: CFD Post Simulation

As the Fluent analysis report indicates, the bagasse temperature obtained at outlet of FBD is 338.3K. The analytical analysis also gives the temperature of bagasse at dryer outlet 340.23K. This indicate that, the results obtained from analytical and simulation analysis are almost equal. Hence the FBD increases the temperature of bagasse by 32.23K.

To summarize, both analysis gives almost the same result, so the moisture content of bagasse is reduced by 11% from 52% to 41%. According to Hugot, 1% moisture reduction increases GCV by 196 kJ/Kg[10], [19]. Thus total increased GCV is 11 x 196 = 2156kJ/kg. Also 1% reduction in moisture in bagasse increases boiler efficiency by 0.5%[11], [31]. Thus boiler efficiency increased by 5.5%, from 70% to 75.66% theoretically. Figure 4-2 shows the temperature, pressure and velocity simulation happened in the dryer.

4.3 Parameters Affecting Drying Capacity of a FBD

There are several parameters which influence the drying capacity of a fluidized-bed dryer, these include:

- Gas inlet temperature,
- Gas flow rate,
- Humidity of the drying gas at the inlet,
- Feeding rate of bagasse, and
- Inlet moisture content.

Figure 4-3 shows the effect of bagasse temperature and the time bagasse stay inside the drying chamber. Clearly the graph shows the temperature of bagasse or reduction of moisture content increased as the duration of bagasse inside the drying chamber increases.

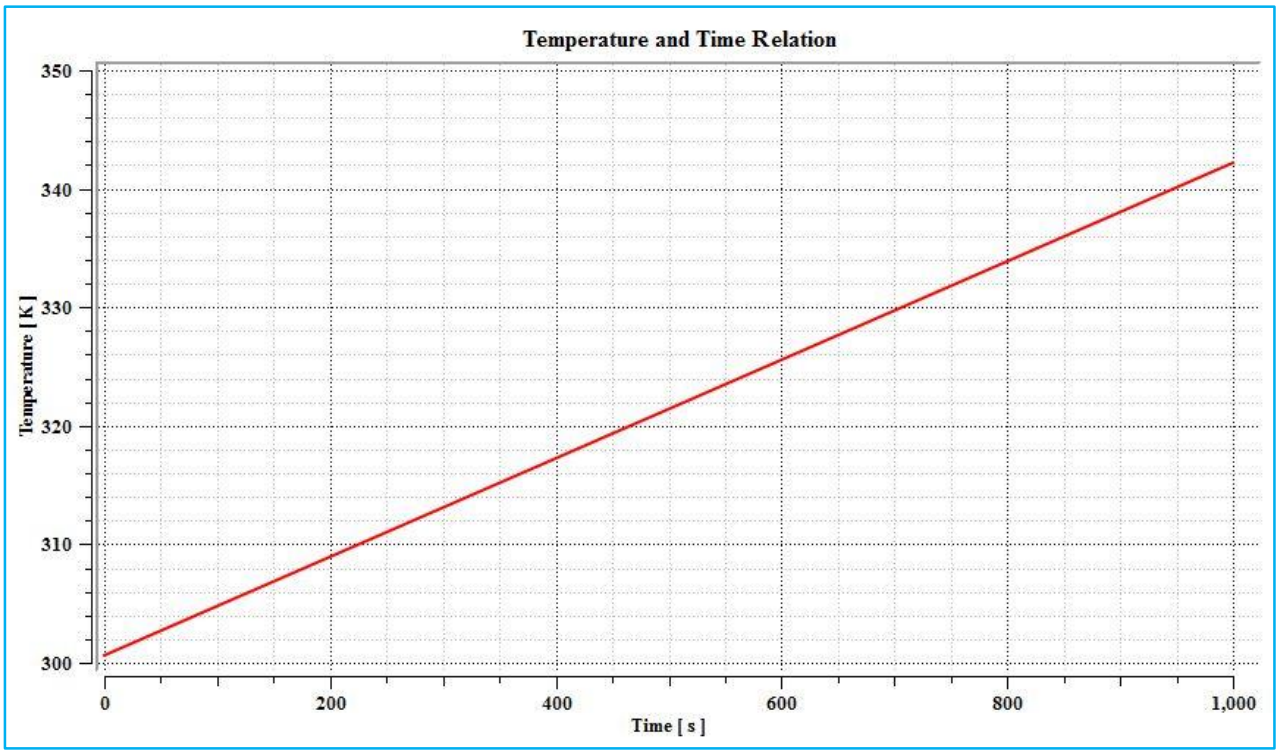

Figure 4-3: Effect of Bagasse Temperature and Time (Duration of Bagasse in Drying Chamber)

Generally from the experiences developed, if the flue gas inlet temperature is increased, the rate of bagasse drying will increase. But if the inlet temperature of flue gas becomes above 281^{o}C to 316^{o}C, it causes fire hazards. Because, the burnout temperature of bagasse is between 281^{o}C to 316^{o}C according to the experiments conducted on sugarcane bagasse by thermogravimetric analysis to investigate burnout temperatures of bagasse by *Jau-Jang Lu & Wei-Hsin Chen*[43]. Also when flue gas flow rate increase, the rate of bagasse drying will increase. When feeding rate of bagasse & inlet moisture content increase, the rate of bagasse drying will decrease.

CHAPTER FIVE: CONCLUSION AND RECOMMENDATION

5.1 Conclusion

An extensive study for the subject of bagasse drying has been made in this research paper. The aim of the study was to reduce the moisture content of sugarcane bagasse in order to improve boiler efficiency. To do that FBD were designed to dry bagasse and the results obtained show clearly that these aims were achieved. The moisture content reduced from 52% to 41% and the boiler efficiency was improved from 70 to 75.5%. The design and thermal energy analysis of the FBD were performed analytically and using analysis software ANSYS Fluent.

5.2 Recommendation

Based on the results obtained and the experiences gained from the present study, some recommendations for future research are given below:

- In this study for drying sugarcane bagasse flue gas is used. For further study, I recommend that somebody can conduct study on drying bagasse by using solar energy instead of flue gas.
- Here the analytical and ANSYS Fluent analysis is done. To conduct experiment is so expensive, so doing the analysis using another analysis software like Math lab and so on are recommend for future.
- Future research is needed to develop an optimum bagasse dryer through deep research work on the theory and modelling of bagasse drying process.

REFERENCE

[1] Adriano V. Ensinas, Silvia A. Nebra, Miguel A. Lozano, and Luis M. Serra, "Analysis of process steam demand reduction and electricity generation in sugar and ethanol production from sugarcane," *Elsevier Ltd*, Aug. 2007.

[2] Roni Maryana, Dian Ma'rifatun, A. Wheni I., Satriyo K.W., and W. Angga Rizal, "Alkaline Pretreatment on Sugarcane Bagasse for Bioethanol Production," *Elsevier Sci. Ltd*, 2014.

[3] Ali K. Abdel-Rahman, "Utilization of By-Products and Waste Materials in the Sugar Industry," Assiut, Egypt, 02-May-2015.

[4] Elbager M.A. Edreisa and Hong Yaob, "Kinetic thermal behaviour and evaluation of physical structure of sugar cane bagasse char during non-isothermal steam gasification," *Journals of Materials Research and Technology*, Mar. 2016.

[5] J.O. Agunsoye and , V.S. Aigbodion, "Bagasse filled recycled polyethylene bio-composites: Morphological and mechanical properties study," *Elsevier BV*, Sep. 2013.

[6] Toolseeram Ramjeawon, "Life cycle assessment of electricity generation from bagasse in Mauritius," *Elsevier Sci. Ltd*, Nov. 2007.

[7] Juan H. Sosa-Arnao and Sílvia A. Nebra, "Bagasse Dryer Role in the Energy Recovery of Water Tube Boilers," *Taylor Francis*, Mar. 2009.

[8] Juan H. Sosa-Arnao, Fabiano Marquezi de Oliveira, Jefferson L. G. Corrêa, Maria A.Silva, and Silvia A. Nebra, "SUGAR CANE BAGASSE DRYING," *Proceedings of the 14th International Drying Symposium (IDS 2004)*, Aug. 2004.

[9] Myrian Aparecida S. Schettino and José Nilson F. Holanda, "Characterization of sugarcane bagasse ash waste for Its Use in Ceramic Floor Tile," *Elsevier Ltd*, 2013.

[10] E. Hugot, *Handbook of Cane Sugar Engineering*, 3rd,completely revised,edition. Amesterdam, Netherlands: ELSEVIER SCIENCE PUBLISHING COMPANY INC., 1986.

[11] Peter Rein, *Cane Sugar Engineering*. Germany, Berlin: Elbe Druckerei Wittenberg, 2007.

[12] Sankalp Shrivastav and Ibrahim Hussain, "Design of Bagasse Dryer to Recover Energy of Water Tube Boiler in a Sugar Factory," *Int. J. Sci. Res. IJSR*, vol. 2, no. 8, August 2013, pp. 356–358.

[13] A. N. Wanjari, B. N. Thorat, C. G. J. Baker, and A. S. Mujumdar, "Design and Modeling of Plug Flow Fluid Bed Dryers," *Taylor Francis Group LLC*, pp. 147–157, Feb. 2007.

[14] Wade A. Amos, "Report on Biomass Drying Technology," Nov. 1998.

[15] Geethanjali S. Yarnal and Vinod S. Puranik, "Energy Management Study in Sugar Industries by Various Bagasse Drying Methods," vol. 29, No. 3, Dec. 2009.

[16] V. V. Patil, A.M. Patil, and, P. D. Kulkarni, "DESIGN AND DEVELOPMENT OF BAGASSE DRYER FOR MODERN JAGGERY HOUSE," *IJARSE*, vol. 2, Sep. 2013.

[17] Jorge Barrosoa, Fe ´lix Barreras, Hippolyte Amavedac, and Antonio Lozano, "On the optimization of boiler efficiency using bagasse as fuel," *Elsevier Sci. Ltd*, Mar. 2003.

[18] Ali Kamel Abdel-Rahman, A.A. Tawfik, M.R. Bayoumi, and M.G. Morsy, "Bagasse Drying: Advantages and Merits (Performance of a Fluidized-Bed Bagasse Dryer)," *Researchgate*, Dec. 2015.

[19] Ali K. Abdel-Rahman, "Utilization of By-Products and Waste Materials in the Sugar Industry," May 2015.

[20] Ed Randel, Jim Schack, and Ananta Islam, "Fluid bed-dryers: Static versus Vibrating," 2013.

[21] Al-Zafer A. Tawfik, Ali K. Abdel-Rahman, and Mohamed R. Bayoumi, "Performance of Pneumatic Bagasse Dryers," *Researchgate*, Dec. 2004.

[22] Wen-Ching Yang, *Handbook of Fluidization and Fluid-Particle Systems*. United States of America: Marcel Dekker, Inc., 2003.

[23] Maria Laura Passos, Marcos Antonio S. Barrozo, and Arun S. Mujumdar, *Fluidization Engineering*, 2nd Edition. Laval – Canada, 2014.

[24] OKORONKWO C.A, NWUFO, O.C, NWAIGWE K.N, OGUEKE N.V, and ANYANWU E.E, "Experimental Evaluation of A Fluidized Bed Dryer Performance," *The International Journal Of Engineering And Science (IJES)*, vol. 2, no. 6, pp. 45–53, 2013.

[25] V. V. Patil, A.M. Patil, and P. D. Kulkarni, "DESIGN AND DEVELOPMENT OF BAGASSE DRYER FOR MODERN JAGGERY HOUSE," *Int. J. Adv. Res. Sci. Eng.*, vol. no.3, 01 September 2014, pp. 599–605.

[26] Omoniyi, T.E., Olorunnisola A.O, "Experimental Characterisation of Bagasse Biomass Material for Energy Production," *Int. J. Eng. Technol.*, vol. 4, no. 10, NaN, 2014, pp. 582–589.

[27] L.A.B Cortez and E.O. Gomez, "A Method for Exergy Analysis of Sugarcane Bagasse Boilers," *Brazilian Journal of Chemical Engineering*, vol. 15 No. 1, Dec. 1997.

[28] R J Panchal, S M Shinde, and S J Panchal, "Effect of Bagasse Moisture on Boiler Performance," *INTERNATIONAL RESEARCH JOURNAL OF MULTIDISCIPLINARY STUDIES (IRJMS)*, vol. 2, no. 1, Mar. 2016.

[29] R.S. KHURMI and J.K. GUPTA, *A TEXTBOOK OF MACHINE DESIGN*, 14th ed. EURASIA PUBLISHING HOUSE (PVT.) LTD. RAM NAGAR, NEW DELHI-110 055, 2005.

[30] S M Yahya, *Turbines Compressors & Fans*. New Delhi.

[31] Sankalp Shrivastav and Ibrahim Hussain, "Design of Bagasse Dryer to Recover Energy of Water Tube Boiler in a Sugar Factory," *International Journal of Science and Research (IJSR)*, vol. 2, no. 8, Aug. 2013.

[32] Yunus A. Cengel, *Thermodynamics An Engineering Approach*, Fifth. .

[33] James Carvill, *Mechanical Engineer's Data Handbook*. Greate Britain: Elsevier Science Ltd., 1993.

[34] YUNUS A. CENGEL, *HEAT TRANSFER*. .

[35] R.K. RAJPUT, *Heat and Mass Transfer*, Second. INDIA, 2003.

[36] THEODORE L. BERGMAN, ADRIENNE S. LAVINE, FRANK P. INCROPERA, and DAVID P. DEWITT, *Fundamentals of Heat and Mass Transfer*, Seventh Edition. United States of America, 2008.

[37] T. Kuppan, *Heat Exchanger Design Handbook*. United States of America: MARCEI, DEKKER, INC.

[38] Oluleye, A.E. and Ogungbemi, and A .A. and Anyaeche, "Design and Fabrication of a Low Cost Fluidized Bed Reactor," vol. 3, 2012.

[39] Syahrul HUSAIN, Akihiko HORIBE, and Naoto HARUKI, "Heat and Mass Transfer Analysis of Fluidized Bed Grain Drying," *Hideo INABA Al*, vol. 4, Jan. 2007.

[40] Desmond E Winterbone, *Advanced Thermodynamics for Engineers*. Greate Britain, 1997.

[41] Christopher Tremblay and Dongmei Zhou, "*A Study of Efficient Drying Parameters for Bed Dryers,"* Proc. 2nd Int. Conf. Fluid Flow Heat Mass Transf., May 2015.

[42] J.SUDHAKAR and , P.VIJAY, "Control of Moisture Content in Bagasse by Using Bagasse Dryer," *International Journal of Engineering Trends and Technology (IJETT)*, vol. 4, no. 5, May 2013.

[43] Jau-Jang Lu & Wei-Hsin Chen, *" Investigation on the ignition and burnout temperatures of bamboo and sugarcane bagasse by thermogravimetric analysis"* 2015 Elsevier Ltd.

[44] ANSYS FLUENT Tutorial Guide, October 2012

APPENDIX

7.1 Appendix A: Effectiveness Relations for Heat Exchangers

Taken from reference [34], HEAT TRANSFER,YUNUS A. CENGEL, pp. 694

Table A-1: Effectiveness Relations for Heat Exchangers

Effectiveness relations for heat exchangers: NTU = UA_s/C_{min} and $c = C_{min}/C_{max} = (\dot{m}C_p)_{min}/(\dot{m}C_p)_{max}$ (Kays and London, Ref. 5.)

Heat exchanger type	Effectiveness relation
1 *Double pipe:*	
Parallel-flow	$\varepsilon = \dfrac{1 - \exp[-\text{NTU}(1+c)]}{1+c}$
Counter-flow	$\varepsilon = \dfrac{1 - \exp[-\text{NTU}(1-c)]}{1 - c\exp[-\text{NTU}(1-c)]}$
2 *Shell and tube:*	
One-shell pass 2, 4, . . . tube passes	$\varepsilon = 2\left\{1 + c + \sqrt{1+c^2}\,\dfrac{1+\exp[-\text{NTU}\sqrt{1+c^2}]}{1-\exp[-\text{NTU}\sqrt{1+c^2}]}\right\}^{-1}$
3 *Cross-flow (single-pass)*	
Both fluids unmixed	$\varepsilon = 1 - \exp\left\{\dfrac{\text{NTU}^{0.22}}{c}[\exp(-c\ \text{NTU}^{0.78}) - 1]\right\}$
C_{max} mixed, C_{min} unmixed	$\varepsilon = \dfrac{1}{c}(1 - \exp\{1 - c[1 - \exp(-\text{NTU})]\})$
C_{min} mixed, C_{max} unmixed	$\varepsilon = 1 - \exp\left\{-\dfrac{1}{c}[1 - \exp(-c\ \text{NTU})]\right\}$
4 *All heat exchangers with* $c = 0$	$\varepsilon = 1 - \exp(-\text{NTU})$

7.2 Appendix B: NTU Relations for Heat Exchangers

Taken from reference [34], HEAT TRANSFER,YUNUS A. CENGEL, pp. 697

Table B-2: NTU Relations for Heat Exchangers

NTU relations for heat exchangers NTU = UA_s/C_{min} and $c = C_{min}/C_{max} = (\dot{m}C_p)_{min}/(\dot{m}C_p)_{max}$ (Kays and London, Ref. 5.)

Heat exchanger type	NTU relation
1 *Double-pipe:* Parallel-flow	$\text{NTU} = -\frac{\ln[1-\varepsilon(1+c)]}{1+c}$
Counter-flow	$\text{NTU} = \frac{1}{c-1}\ln\left(\frac{\varepsilon-1}{\varepsilon c-1}\right)$
2 *Shell and tube:* One-shell pass 2, 4, . . . tube passes	$\text{NTU} = -\frac{1}{\sqrt{1+c^2}}\ln\left(\frac{2/\varepsilon-1-c-\sqrt{1+c^2}}{2/\varepsilon-1-c+\sqrt{1+c^2}}\right)$
3 *Cross-flow (single-pass)* C_{max} mixed, C_{min} unmixed	$\text{NTU} = -\ln\left[1+\frac{\ln(1-\varepsilon c)}{c}\right]$
C_{min} mixed, C_{max} unmixed	$\text{NTU} = -\frac{\ln[c\ln(1-\varepsilon)+1]}{c}$
4 *All heat exchangers with* $c = 0$	$\text{NTU} = -\ln(1-\varepsilon)$

7.3 Appendix C: Flue gas properties Calculator

Fluegas Properties Calculator

Flue Gas Properties Calculator

Fluegas Composition, mole %		
Nitrogen	=	60.7
Oxygen	=	4.72
Carbon Dioxide	=	17.45
Water	=	16.93
Argon	=	0
Sulphur Dioxide	=	0
Carbon Monoxide	=	0
Temperature, F	=	486
Enthalpy, Btu/lb	=	Calc

Calculate

RESULTS

Gas Molecular Weight	29.2460
Density, lb/ft3	0.0423
Enthalpy, Btu/lb	112.5126
Temperature, °F	486.0000
Specific Heat, Btu/lb-F	0.2739
Thermal Cond., Btu/hr-ft-F	0.0228
Viscosity, Cp	0.0258

7.4 Appendix D: Flue Gas Properties

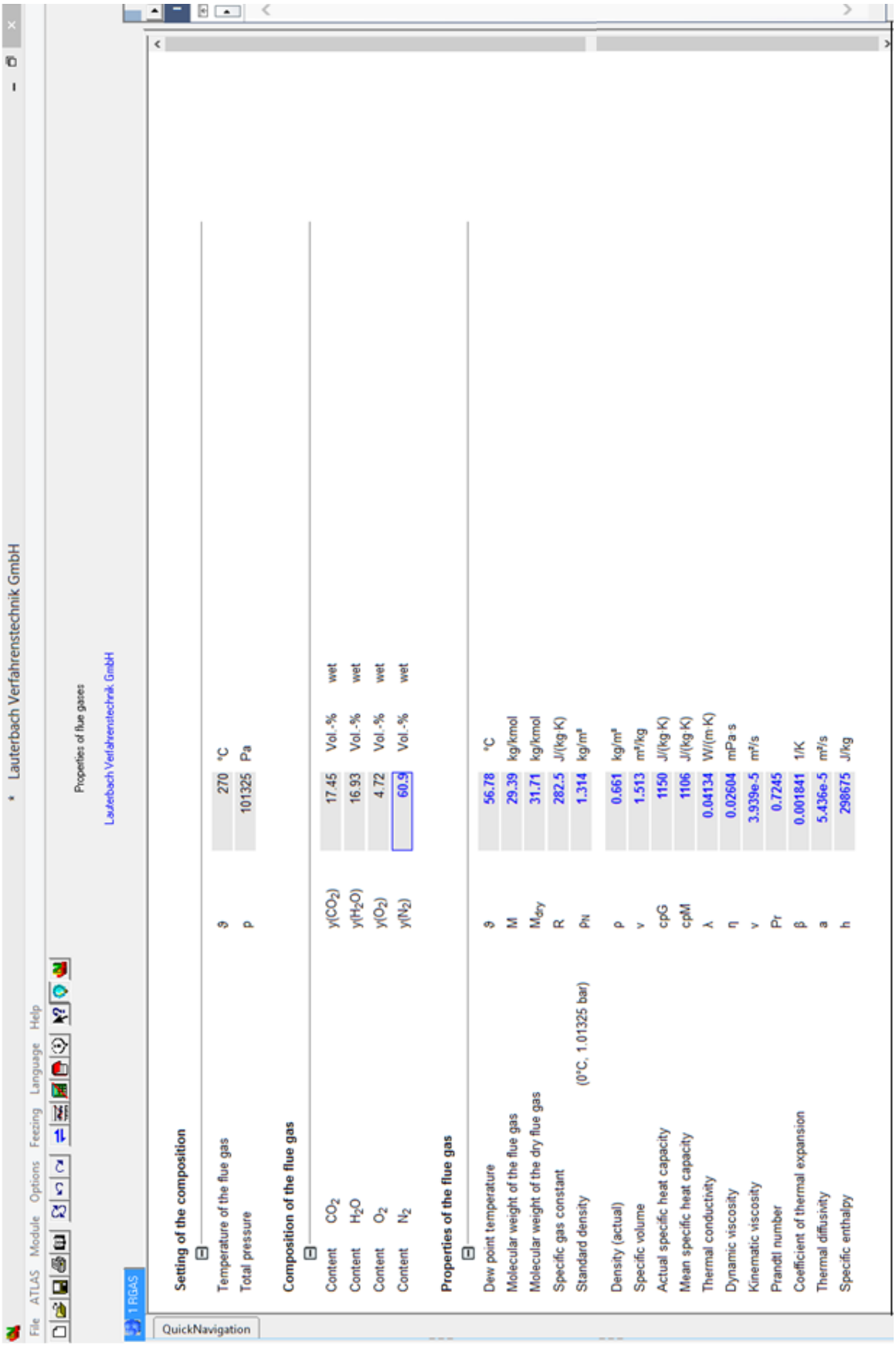

7.5 Appendix E: Geometry and Mesh Report

Geometry

Subject:	FBD
Author:	Belachew G.
Prepared For:	MSc Thesis
Date:	2018-11-11

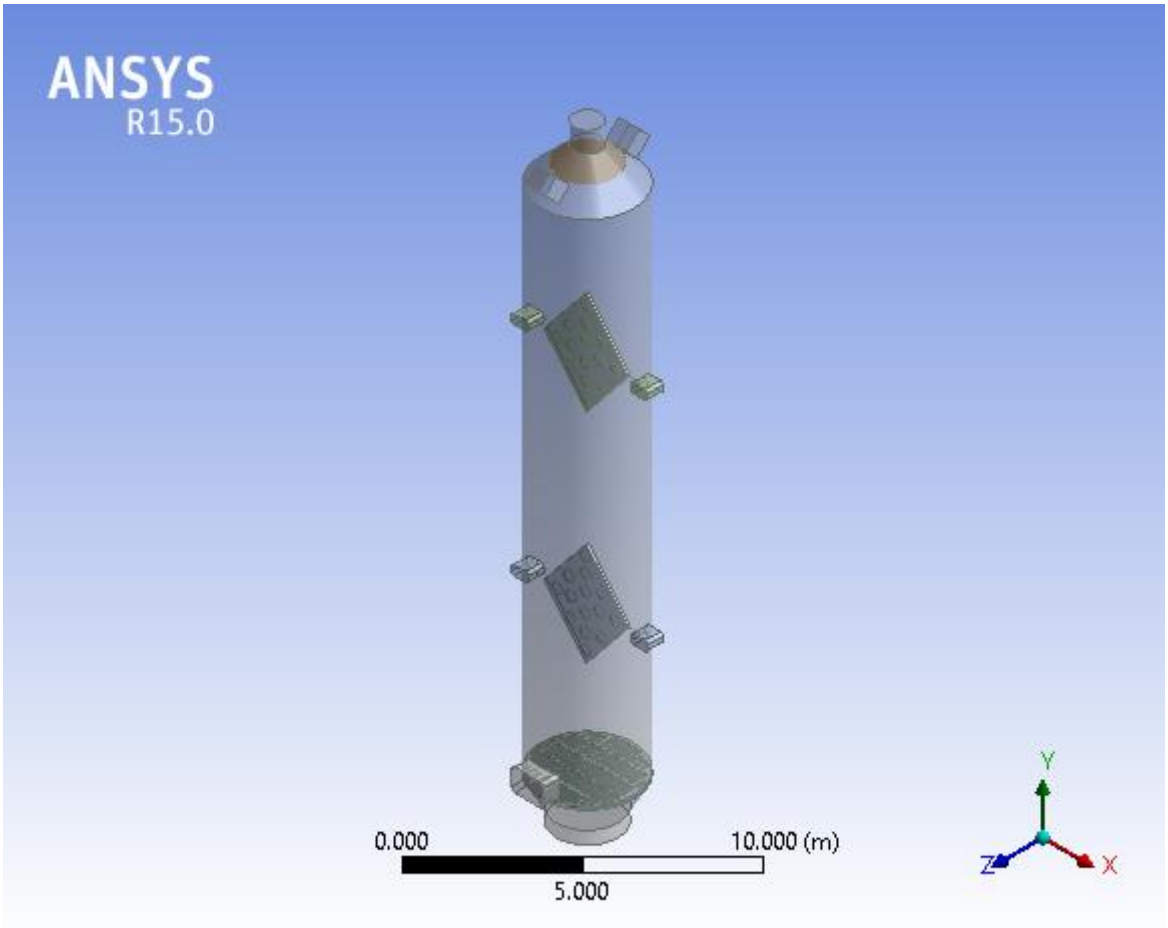

Mesh

Subject:	FBD
Author:	Belachew G.
Prepared For:	MSc Thesis
Date	Sunday, 11 November, 2018

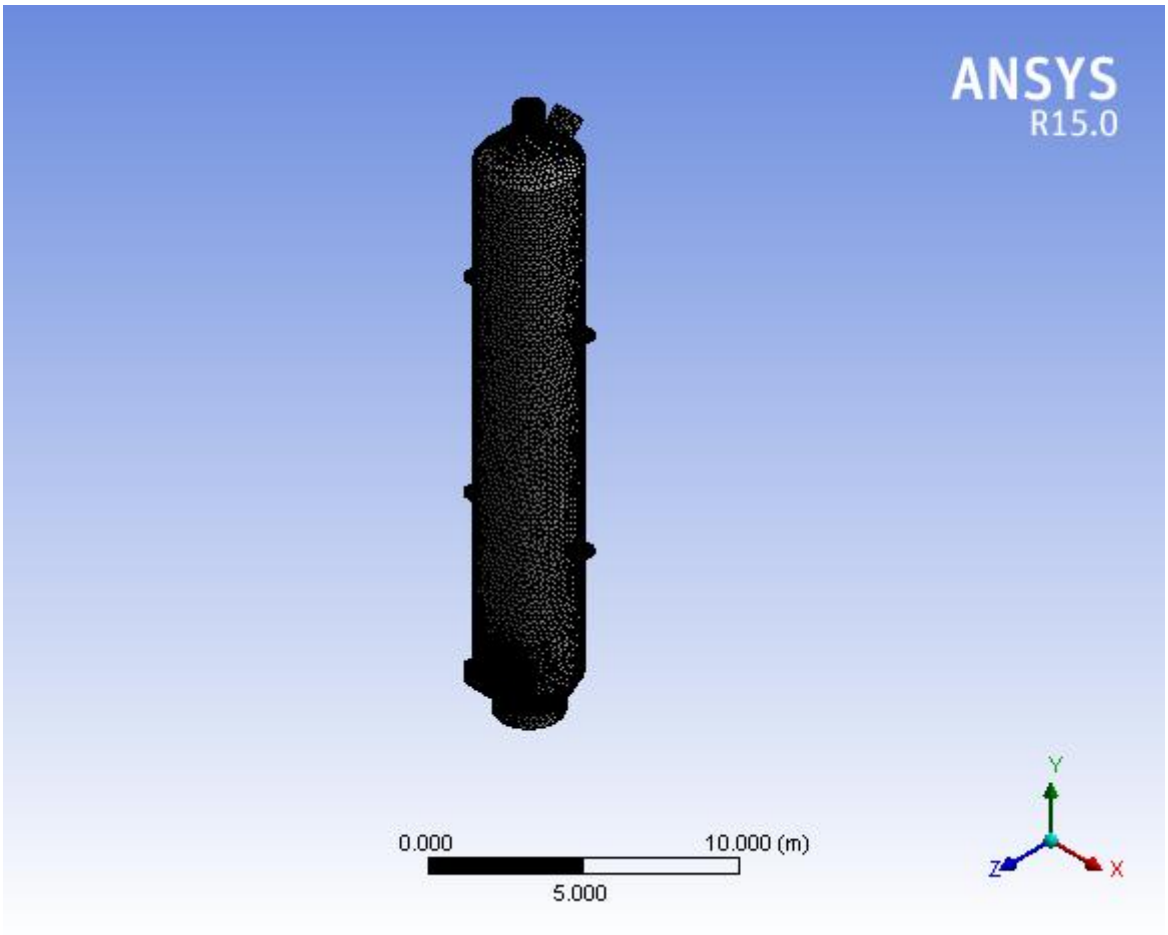

Project

First Saved	Friday, 9 November, 2018
Last Saved	Sunday, 11 November, 2018
Product Version	15.0 Release
Save Project Before Solution	No
Save Project After Solution	No

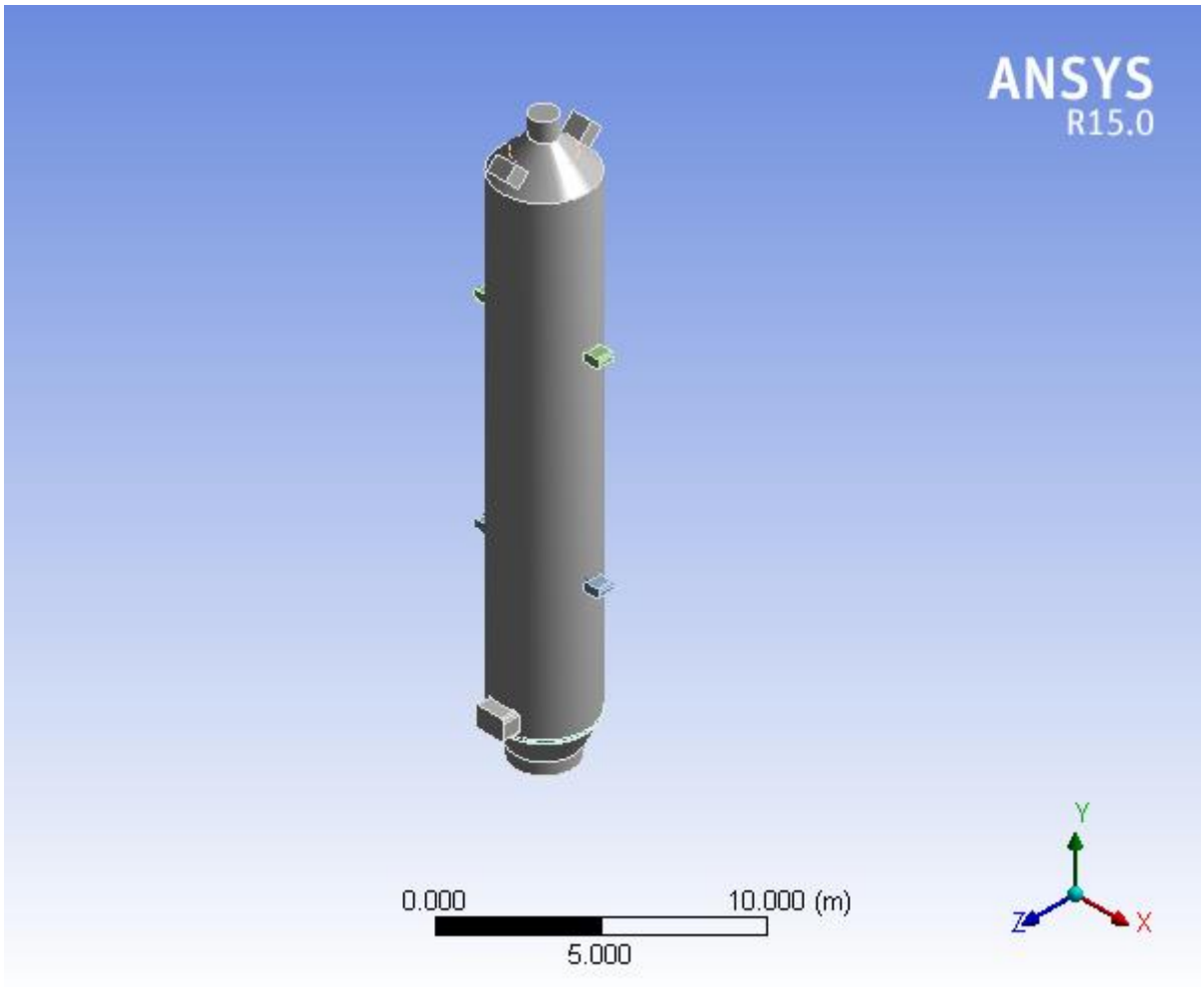

Contents

Units

TABLE 1

Unit System	Metric (m, kg, N, s, V, A) Degrees rad/s Celsius
Angle	Degrees
Rotational Velocity	rad/s
Temperature	Celsius

Model (B3)

Geometry

TABLE 2
Model (B3) > Geometry

Object Name	*Geometry*
State	Fully Defined
Definition	
Source	C:\Users\pc\Desktop\NEW FBD_files\dp0\Geom\DM\Geom.agdb
Type	DesignModeler
Length Unit	Meters
Bounding Box	
Length X	5.3398 m
Length Y	23.7 m
Length Z	4.3577 m
Properties	
Volume	224.2 m³
Scale Factor Value	1.
Statistics	
Bodies	5
Active Bodies	5
Nodes	394815
Elements	1144785
Mesh Metric	None
Basic Geometry Options	
Parameters	Yes
Parameter Key	DS
Attributes	No
Named Selections	No
Material Properties	No
Advanced Geometry Options	
Use Associativity	Yes
Coordinate Systems	No
Reader Mode Saves Updated File	No
Use Instances	Yes
Smart CAD Update	No
Compare Parts On Update	No
Attach File Via Temp File	Yes
Temporary Directory	C:\Users\pc\AppData\Local\Temp
Analysis Type	3-D
Decompose Disjoint Geometry	Yes

Enclosure and Symmetry Processing	No

TABLE 3
Model (B3) > Geometry > Parts

Object Name	*Solid*	*Solid*	*Solid*	*Solid*	*Solid*
State	Meshed				
Graphics Properties					
Visible	Yes				
Transparency	1				
Definition					
Suppressed	No				
Coordinate System	Default Coordinate System				
Reference Frame	Lagrangian				
Material					
Fluid/Solid	Defined By Geometry (Solid)				
Bounding Box					
Length X	3.6 m	5.3398 m		2.1 m	3.58 m
Length Y	23.7 m	4. m		2.e-002 m	0.1 m
Length Z	4.3577 m	0.6 m		2.1 m	3.58 m
Properties					
Volume	221.6 m³	1.0393 m³		3.9637e-002 m³	0.4785 m³
Centroid X	-6.5676e-005 m	-3.8528e-004 m		2.0362e-002 m	-8.7839e-003 m
Centroid Y	-5.1826e-002 m	-4.1369 m	4.3631 m	10.8 m	-9.8 m
Centroid Z	5.5874e-003 m	6.3181e-003 m		8.4783e-003 m	1.466e-002 m
Statistics					
Nodes	49944	71590		88536	113155
Elements	269588	367457		56325	83958
Mesh Metric	None				

Coordinate Systems

TABLE 4
Model (B3) > Coordinate Systems > Coordinate System

Object Name	*Global Coordinate System*
State	Fully Defined
Definition	
Type	Cartesian
Coordinate System ID	0.
Origin	
Origin X	0. m
Origin Y	0. m
Origin Z	0. m
Directional Vectors	
X Axis Data	[1. 0. 0.]
Y Axis Data	[0. 1. 0.]
Z Axis Data	[0. 0. 1.]

Connections

TABLE 5
Model (B3) > Connections

Object Name	*Connections*
State	Fully Defined
Auto Detection	
Generate Automatic Connection On Refresh	Yes

Transparency	
Enabled	Yes

TABLE 6
Model (B3) > Connections > Contacts

Object Name	*Contacts*
State	Fully Defined
Definition	
Connection Type	Contact
Scope	
Scoping Method	Geometry Selection
Geometry	All Bodies
Auto Detection	
Tolerance Type	Slider
Tolerance Slider	0.
Tolerance Value	6.1705e-002 m
Use Range	No
Face/Face	Yes
Face/Edge	No
Edge/Edge	No
Priority	Include All
Group By	Bodies
Search Across	Bodies

TABLE 7
Model (B3) > Connections > Contacts > Contact Regions

Object Name	*Contact Region*
State	Fully Defined
Scope	
Scoping Method	Geometry Selection
Contact	1 Face
Target	3 Faces
Contact Bodies	Solid
Target Bodies	Solid

Mesh

TABLE 8
Model (B3) > Mesh

Object Name	*Mesh*
State	Solved
Defaults	
Physics Preference	CFD
Solver Preference	Fluent
Relevance	100
Sizing	
Use Advanced Size Function	On: Curvature
Relevance Center	Fine
Initial Size Seed	Active Assembly
Smoothing	High
Transition	Slow
Span Angle Center	Fine
Curvature Normal Angle	Default (12.0 °)
Min Size	Default (2.4682e-003 m)

Max Face Size	Default (0.246820 m)
Max Size	Default (0.493640 m)
Growth Rate	Default (1.10)
Minimum Edge Length	2.e-002 m
Inflation	
Use Automatic Inflation	None
Inflation Option	Smooth Transition
Transition Ratio	0.272
Maximum Layers	5
Growth Rate	1.2
Inflation Algorithm	Pre
View Advanced Options	No
Assembly Meshing	
Method	None
Patch Conforming Options	
Triangle Surface Mesher	Program Controlled
Patch Independent Options	
Topology Checking	Yes
Advanced	
Number of CPUs for Parallel Part Meshing	Program Controlled
Shape Checking	CFD
Element Midside Nodes	Dropped
Straight Sided Elements	
Number of Retries	0
Extra Retries For Assembly	Yes
Rigid Body Behavior	Dimensionally Reduced
Mesh Morphing	Disabled
Defeaturing	
Pinch Tolerance	Default (2.2214e-003 m)
Generate Pinch on Refresh	No
Automatic Mesh Based Defeaturing	On
Defeaturing Tolerance	Default (1.2341e-003 m)
Statistics	
Nodes	394815
Elements	1144785
Mesh Metric	None

Named Selections

TABLE 9
Model (B3) > Named Selections > Named Selections

Object Name	*FLUE GAS INLET*	*BAGASSE INLET*	*BAGASSE OUTLET*	*FLUEGAS & VAPOUR OUTLET*
State	Fully Defined			
Scope				
Scoping Method	Geometry Selection			
Geometry	1 Face	2 Faces	1 Face	
Definition				
Send to Solver	Yes			
Visible	Yes			
Program Controlled Inflation	Exclude			
Statistics				
Type	Manual			

Total Selection	1 Face	2 Faces	1 Face
Suppressed	0		
Used by Mesh Worksheet	No		

7.6 Appendix F: ANSYS Fluent Input Summary Report

Models Input Summary

```
Fluent
Version: 3d, dp, pbns, ske, transient (3d, double precision, pressure-
based, standard k-epsilon, transient)
Release: 15.0.0
Title:

Models
------

   Model                         Settings
   ------------------------------------------------------------------
   Space                         3D
   Time                          Unsteady, 1st-Order Implicit
   Viscous                       Standard k-epsilon turbulence model
   Wall Treatment                Standard Wall Functions
   Heat Transfer                 Enabled
   Solidification and Melting    Disabled
   Radiation                     None
   Species                       Disabled
   Coupled Dispersed Phase       Disabled
   NOx Pollutants                Disabled
   SOx Pollutants                Disabled
   Soot                          Disabled
   Mercury Pollutants            Disabled
```

Boundary Conditions Input Summary

```
Fluent
Version: 3d, dp, pbns, ske, transient (3d, double precision, pressure-
based, standard k-epsilon, transient)
Release: 15.0.0
Title:

Boundary Conditions
-------------------
   Zones
      name            id   type
      ---------------------------------
      bagasse_inlet   6    mass-flow-inlet
      wall-solid      1    wall
      fluegas_inlet   7    velocity-inlet
      outlet          8    pressure-outlet

   Setup Conditions

      bagasse_inlet
```

Condition	Value
Reference Frame	0
Mass Flow Specification Method	0
Mass Flow Rate (kg/s)	15.23
Mass Flux (kg/m2-s)	1
Average Mass Flux (kg/m2-s)	1
Upstream Torque Integral (n-m)	1
Upstream Total Enthalpy Integral (w/m2)	1
Total Temperature (k)	308
Supersonic/Initial Gauge Pressure (pascal)	0
Direction Specification Method	1
Coordinate System	0
X-Component of Flow Direction	1
Y-Component of Flow Direction	0
Z-Component of Flow Direction	0
X-Component of Flow Direction	1
Y-Component of Flow Direction	0
Z-Velocity (m/s)	0
X-Component of Axis Direction	1
Y-Component of Axis Direction	0
Z-Component of Axis Direction	0
X-Coordinate of Axis Origin (m)	0
Y-Coordinate of Axis Origin (m)	0
Z-Coordinate of Axis Origin (m)	0
Turbulent Specification Method	2
Turbulent Kinetic Energy (m2/s2)	1
Turbulent Dissipation Rate (m2/s3)	1
Turbulent Intensity (%)	5
Turbulent Length Scale (m)	1
Hydraulic Diameter (m)	1
Turbulent Viscosity Ratio	10
is zone used in mixing-plane model?	no

wall-solid

Condition	Value
Wall Thickness (m)	0.05
Heat Generation Rate (w/m3)	0
Material Name	steel
Thermal BC Type	0
Temperature (k)	300
Heat Flux (w/m2)	0
Convective Heat Transfer Coefficient (w/m2-k)	0
Free Stream Temperature (k)	300
Enable shell conduction?	no
Wall Motion	0
Shear Boundary Condition	0
Define wall motion relative to adjacent cell zone?	yes
Apply a rotational velocity to this wall?	no
Velocity Magnitude (m/s)	0
X-Component of Wall Translation	1
Y-Component of Wall Translation	0
Z-Component of Wall Translation	0
Define wall velocity components?	no
X-Component of Wall Translation (m/s)	0
Y-Component of Wall Translation (m/s)	0
Z-Component of Wall Translation (m/s)	0

External Emissivity	1
External Radiation Temperature (k)	300
Wall Roughness Height (m)	0
Wall Roughness Constant	0.5
Rotation Speed (rad/s)	0
X-Position of Rotation-Axis Origin (m)	0
Y-Position of Rotation-Axis Origin (m)	0
Z-Position of Rotation-Axis Origin (m)	0
X-Component of Rotation-Axis Direction	0
Y-Component of Rotation-Axis Direction	0
Z-Component of Rotation-Axis Direction	1
X-component of shear stress (pascal)	0
Y-component of shear stress (pascal)	0
Z-component of shear stress (pascal)	0
Fslip constant	0
Eslip constant	0
Surface tension gradient (n/m-k)	0
Specularity Coefficient	0
Convective Augmentation Factor	1
Enable Thermal Stabilization?	no
Scale Factor	0
Stabilization Method	1

fluegas_inlet

Condition	Value
Velocity Specification Method	2
Reference Frame	0
Velocity Magnitude (m/s)	7.75
Supersonic/Initial Gauge Pressure (pascal)	0
Coordinate System	0
X-Velocity (m/s)	0
Y-Velocity (m/s)	0
Z-Velocity (m/s)	0
X-Component of Flow Direction	1
Y-Component of Flow Direction	0
Z-Component of Flow Direction	0
X-Component of Axis Direction	1
Y-Component of Axis Direction	0
Z-Component of Axis Direction	0
X-Coordinate of Axis Origin (m)	0
Y-Coordinate of Axis Origin (m)	0
Z-Coordinate of Axis Origin (m)	0
Angular velocity (rad/s)	0
Temperature (k)	543
Turbulent Specification Method	2
Turbulent Kinetic Energy (m2/s2)	1
Turbulent Dissipation Rate (m2/s3)	1
Turbulent Intensity (%)	5
Turbulent Length Scale (m)	1
Hydraulic Diameter (m)	1
Turbulent Viscosity Ratio	10
is zone used in mixing-plane model?	no

outlet

Condition	Value

Gauge Pressure (pascal)	0
Backflow Total Temperature (k)	300
Backflow Direction Specification Method	1
Coordinate System	0
X-Component of Flow Direction	1
Y-Component of Flow Direction	0
Z-Component of Flow Direction	0
X-Component of Axis Direction	1
Y-Component of Axis Direction	0
Z-Component of Axis Direction	0
X-Coordinate of Axis Origin (m)	0
Y-Coordinate of Axis Origin (m)	0
Z-Coordinate of Axis Origin (m)	0
Turbulent Specification Method	2
Backflow Turbulent Kinetic Energy (m2/s2)	1
Backflow Turbulent Dissipation Rate (m2/s3)	1
Backflow Turbulent Intensity (%)	5
Backflow Turbulent Length Scale (m)	1
Backflow Hydraulic Diameter (m)	1
Backflow Turbulent Viscosity Ratio	10
Is zone used in mixing-plane model?	no
Radial Equilibrium Pressure Distribution	no
Average Pressure Specification?	no
	0
Specify targeted mass flow rate	no
Targeted mass flow (kg/s)	1
Upper Limit of Absolute Pressure Value (pascal)	5000000
Lower Limit of Absolute Pressure Value (pascal)	1

Cell Zone Conditions Input Summary

```
Fluent
Version: 3d, dp, pbns, ske, transient (3d, double precision, pressure-
based, standard k-epsilon, transient)
Release: 15.0.0
Title:

Cell Zone Conditions
--------------------

   Zones

      name           id   type
      -------------------------
      fluid-domain   3    fluid

   Setup Conditions

      fluid-domain

         Condition                                                    Value
         ------------------------------------------------------------------
-------------------------------------------------------------------
       Material Name                                              flue-gas
       Specify source terms?                                         no
       Source Terms                                            ((mass) (x-
momentum) (y-momentum) (z-momentum) (k) (epsilon) (energy))
       Specify fixed values?                                         no
       Local Coordinate System for Fixed Velocities                  no
```

```
       Fixed Values                                                ((x-
velocity (inactive . #f) (constant . 0) (profile  )) (y-velocity (inactive
. #f) (constant . 0) (profile  )) (z-velocity (inactive . #f) (constant .
0) (profile  )) (k (inactive . #f) (constant . 0) (profile  )) (epsilon
(inactive . #f) (constant . 0) (profile  )) (temperature (inactive . #f)
(constant . 0) (profile  )))
       Frame Motion?                                              no
       Relative To Cell Zone                                      -1
         Reference Frame Rotation Speed (rad/s)                     0
         Reference Frame X-Velocity Of Zone (m/s)                   0
         Reference Frame Y-Velocity Of Zone (m/s)                   0
         Reference Frame Z-Velocity Of Zone (m/s)                   0
         Reference Frame X-Origin of Rotation-Axis (m)              0
         Reference Frame Y-Origin of Rotation-Axis (m)              0
         Reference Frame Z-Origin of Rotation-Axis (m)              0
         Reference Frame X-Component of Rotation-Axis               0
         Reference Frame Y-Component of Rotation-Axis               0
         Reference Frame Z-Component of Rotation-Axis               1
         Reference Frame User Defined Zone Motion Function          none
         Mesh Motion?                                               no
         Relative To Cell Zone                                      -1
         Moving Mesh Rotation Speed (rad/s)                         0
         Moving Mesh X-Velocity Of Zone (m/s)                       0
         Moving Mesh Y-Velocity Of Zone (m/s)                       0
         Moving Mesh Z-Velocity Of Zone (m/s)                       0
         Moving Mesh X-Origin of Rotation-Axis (m)                  0
         Moving Mesh Y-Origin of Rotation-Axis (m)                  0
         Moving Mesh Z-Origin of Rotation-Axis (m)                  0
         Moving Mesh X-Component of Rotation-Axis                   0
         Moving Mesh Y-Component of Rotation-Axis                   0
         Moving Mesh Z-Component of Rotation-Axis                   1
         Moving Mesh User Defined Zone Motion Function              none
         Deactivated Thread                                         no
         LES zone?                                                  no
         Laminar zone?                                              no
         Set Turbulent Viscosity to zero within laminar zone?       yes
         Embedded Subgrid-Scale Model                               0
         Momentum Spatial Discretization                            0
         Cwale                                                      0.325
         Cs                                                         0.1
         Porous zone?                                               no
         Conical porous zone?                                       no
         X-Component of Direction-1 Vector                          1
         Y-Component of Direction-1 Vector                          0
         Z-Component of Direction-1 Vector                          0
         X-Component of Direction-2 Vector                          0
         Y-Component of Direction-2 Vector                          1
         Z-Component of Direction-2 Vector                          0
         X-Component of Cone Axis Vector                            1
         Y-Component of Cone Axis Vector                            0
         Z-Component of Cone Axis Vector                            0
         X-Coordinate of Point on Cone Axis (m)                     1
         Y-Coordinate of Point on Cone Axis (m)                     0
         Z-Coordinate of Point on Cone Axis (m)                     0
         Half Angle of Cone Relative to its Axis (deg)              0
         Relative Velocity Resistance Formulation?                  yes
         Direction-1 Viscous Resistance (1/m2)                      0
         Direction-2 Viscous Resistance (1/m2)                      0
         Direction-3 Viscous Resistance (1/m2)                      0
```

```
Choose alternative formulation for inertial resistance?   no
Direction-1 Inertial Resistance (1/m)                     0
Direction-2 Inertial Resistance (1/m)                     0
Direction-3 Inertial Resistance (1/m)                     0
C0 Coefficient for Power-Law                              0
C1 Coefficient for Power-Law                              0
Porosity                                                  1
Equilibrium Thermal Model (if no, Non-Equilibrium)?       yes
Non-Equilibrium Thermal Model?                            no
Solid Material Name                                  aluminum
Interfacial Area Density (1/m)                            1
Heat Transfer Coefficient (w/m2-k)                        1
```

Material Properties Input Summary

```
Version: 3d, dp, pbns, ske, transient (3d, double precision, pressure-
based, standard k-epsilon, transient)
Release: 15.0.0
Title:

Material Properties
-------------------

   Material: steel (solid)

      Property                Units    Method     Value(s)
      ------------------------------------------------------
      Density                 kg/m3    constant   8030
      Cp (Specific Heat)      j/kg-k   constant   502.48
      Thermal Conductivity    w/m-k    constant   16.27

   Material: bagasse (fluid)

      Property                          Units      Method     Value(s)
      ------------------------------------------------------------------
      Density                           kg/m3      constant   250
      Cp (Specific Heat)                j/kg-k     constant   460
      Thermal Conductivity              w/m-k      constant   0.60000002
      Viscosity                         kg/m-s     constant   0.001003
      Molecular Weight                  kg/kgmol   constant   18.0152
      Thermal Expansion Coefficient     1/k        constant   0
      Speed of Sound                    m/s        none       #f

   Material: flue-gas (fluid)

      Property                          Units      Method     Value(s)
      ------------------------------------------------------------------
      Density                           kg/m3      constant   0.67799997
      Cp (Specific Heat)                j/kg-k     constant   230
      Thermal Conductivity              w/m-k      constant   0.0242
      Viscosity                       kg/m-s     constant   1.7894001e-05
      Molecular Weight                  kg/kgmol   constant   28.966
      Thermal Expansion Coefficient     1/k        constant   0
      Speed of Sound                    m/s        none       #f

   Material: aluminum (solid)

      Property                Units    Method     Value(s)
      ------------------------------------------------------
```

```
      Density                kg/m3    constant   2719
      Cp (Specific Heat)     j/kg-k   constant   871
      Thermal Conductivity   w/m-k    constant   202.4
```

Solver Settings

```
Fluent
Version: 3d, dp, pbns, ske, transient (3d, double precision, pressure-
based, standard k-epsilon, transient)
Release: 15.0.0
Title:

Solver Settings
---------------

   Equations

      Equation     Solved
      -------------------
      Flow         yes
      Turbulence   yes
      Energy       yes

   Numerics

      Numeric                           Enabled
      ----------------------------------------
      Absolute Velocity Formulation     yes

   Unsteady Calculation Parameters


      ---------------------------------
      Time Step (s)                     1
      Max. Iterations Per Time Step     5

   Relaxation

      Variable                      Relaxation Factor
      ---------------------------------------------
      Pressure                      0.3
      Density                       1
      Body Forces                   1
      Momentum                      0.7
      Turbulent Kinetic Energy      0.8
      Turbulent Dissipation Rate    0.8
      Turbulent Viscosity           1
      Energy                        1

   Linear Solver

                                    Solver     Termination   Residual
Reduction
      Variable                      Type       Criterion     Tolerance
      ------------------------------------------------------------------
      Pressure                      V-Cycle    0.1
      X-Momentum                    Flexible   0.1           0.7
      Y-Momentum                    Flexible   0.1           0.7
```

Z-Momentum	Flexible	0.1	0.7
Turbulent Kinetic Energy	Flexible	0.1	0.7
Turbulent Dissipation Rate	Flexible	0.1	0.7
Energy	F-Cycle	0.1	

Pressure-Velocity Coupling

Parameter	Value
Type	SIMPLE

Discretization Scheme

Variable	Scheme
Pressure	Second Order
Momentum	Second Order Upwind
Turbulent Kinetic Energy	First Order Upwind
Turbulent Dissipation Rate	First Order Upwind
Energy	Second Order Upwind

Solution Limits

Quantity	Limit
Minimum Absolute Pressure	1
Maximum Absolute Pressure	5e+10
Minimum Temperature	1
Maximum Temperature	5000
Minimum Turb. Kinetic Energy	1e-14
Minimum Turb. Dissipation Rate	1e-20
Maximum Turb. Viscosity Ratio	100000